

# THE PROCEEDINGS OF THE PHYSICAL SOCIETY

## Section A

VOL. 65, PART 9

1 September 1952

No. 393A

### On the Theory of the Angular and Lateral Spread of the Nucleon Component of the Cosmic Radiation

BY H. S. GREEN AND H. MESSEL

University of Adelaide, South Australia

*MS. received 13th December 1951*

**ABSTRACT.** The three-dimensional development of the nucleon component of extensive air showers is investigated. A vectorial diffusion equation is derived for the phase-space distribution of the nucleons, and solved as far as required to determine the mean square angular deviation, and the mean square distance from the shower axis. Account is taken of the variation of density in the atmosphere, and numerical results are obtained for all altitudes. These are exhibited graphically. The lateral spread of the nucleon cascade in lead is also determined, and the results tabulated. A full discussion is given of the significance of the numerical values obtained.

#### § 1. INTRODUCTION

UNTIL the last few years it was commonly supposed that the primary component of cosmic radiation consisted mainly of electrons. On this hypothesis, the development of extensive air showers was explained in terms of a cascade of high energy electrons and gamma-rays. The theory of the longitudinal and lateral development of such cascades was given by Heisenberg (1946) and Molière (1942) among others. Most subsequent work (Nordheim and Roberg 1949, Nordheim 1941) has also been based on the assumption that extensive air showers were initiated by electrons. Only recently it has been shown experimentally (Critchfield *et al.* 1950) that the proportion of electrons, if any, in the primary cosmic radiation is less than  $\frac{1}{2}\%$ , and that actually protons and alpha-particles predominate in number. These nucleons, through their collisions with the nuclei of the air, are instrumental in the production of a nucleon cascade (Messel and Ritson 1950, Jánosy and Messel 1951, Messel 1951 a, b). Besides protons and neutrons, charged and neutral mesons ( $\pi$ -mesons and mesons of greater mass) result from the nucleon collisions, among which the neutral  $\pi$ -mesons decay to produce gamma-rays (Carlson *et al.* 1950).

It is now generally accepted that these gamma-rays, a mere by-product of the nucleon cascade, are mainly responsible for the soft component of extensive air showers. This circumstance removes the physical basis of previous theories of the development of the soft component, a correct treatment of which would take into account its continuous evolution from the nucleon cascade.



The inadequacy of the earlier theories is particularly evident if one considers the lateral spread of extensive air showers. The spread of the soft component will in fact be determined primarily by the spread of the nucleon and meson components. Strangely enough the first experiments (Cocconi *et al.* 1949, Greisen *et al.* 1950) appeared to support the theory of Molière, and indicated that the spread of the penetrating component was practically the same as for the soft component. Succeeding experiments from another source (Eidus, Alyмова *et al.* 1950, Vernov *et al.* 1950, Eidus, Blinova *et al.* 1950), however, showed that the extent of air showers was much greater than predicted by Molière, and could not be explained by any mechanism hitherto proposed.

The purpose of this paper is to show that the above discrepancy can be resolved by the theory of the lateral spread of the nucleon component of cosmic radiation. As a preliminary to this work it was necessary to know the mean square angle of scatter of the nucleons involved in nucleon-nucleon and nucleon-nucleus collisions. We have already found (Green and Messel 1951 a, b) that the mean square angle of scatter of particles resulting from the nucleon-nucleon collision should be  $(U + U')/UU'$  where  $U$  and  $U'$  are the energies of the incident and scattered particles measured in proton masses. We found also (Messel and Green 1952) that the corresponding mean square angle for a nucleon-nucleus collision was proportional to  $1/U$ . These results are rather insensitive to the particular form of cross section for nuclear collisions adopted, and are a natural consequence of the properties of relativistic transformations.

Our considerations relate only to particles with energies greater than several  $10^3$  mev. At these energies, the angular deflection of a particle resulting from a nuclear collision is small; we therefore systematically neglect the average value of  $(1 - \cos \theta)^2$ , which varies as the mean fourth power of the deflection  $\theta$ . This is the only approximation employed. In the atmosphere, the density of the air varies with height in a manner which depends on the temperature distribution. In evaluating our results we have considered an isothermal atmosphere as the most faithful simple representation of the physical reality. The result differs widely from what would be obtained under the assumption of constant density. Previous work on the lateral spread of the soft component in the atmosphere assumed a constant density, and is open to criticism on this account alone.

Results are obtained for absorbers of both constant and variable density, applicable to lead slabs, for example, and the atmosphere respectively. The mean square angular deviation from the shower axis, and the mean square distance from the shower axis are evaluated from various initial conditions. Information is thus obtained bearing on the energy spectrum of the primary component of the cosmic radiation. This and other experimental implications are discussed in the final section.

## § 2. THREE-DIMENSIONAL DIFFUSION EQUATION

In this section a diffusion equation will be derived for the phase-space distribution function  $f$ , which measures the probability\*  $f(\mathbf{p}, \mathbf{r}, z) d\mathbf{p} d\mathbf{r}$  of finding a nucleon with momentum in the range  $\mathbf{p}, d\mathbf{p}$ , at height  $z$ , and with a horizontal displacement  $\mathbf{r}, d\mathbf{r}$ , from the axis of the shower. The height  $z$ , and the two components of the vector  $\mathbf{r}$  are measured in centimetres; the three components of the momentum  $\mathbf{p}$  in units of  $M\mathbf{c}$ , where  $M$  is the proton mass and  $\mathbf{c}$  the velocity

\* The differential element  $d\mathbf{p}$  stands for  $d\mathbf{p}/2\pi p^2$ , i.e.  $d p_1 d p_2 d p_3 / 2\pi p^2$ .



of light. At the ultra-relativistic energies which we consider, the magnitude  $p$  of the momentum is indistinguishable from the energy  $U$ , measured in units of  $Mc^2$ .

Let  $\nu(\mathbf{p}', \mathbf{p}) d\mathbf{p}$  be the differential probability of finding a nucleon with momentum  $\mathbf{p}$ ,  $d\mathbf{p}$  among the nucleons which result from the collision with a nucleus of a nucleon of momentum  $\mathbf{p}'$ . This will not be required explicitly for our present purpose, though it has been determined in our previous work (Messel and Green 1952).

Let  $\delta(z)$  be the density of the medium in which the cascade develops; then the probability that a nucleon will collide with a nucleus of the medium in traversing a layer of thickness  $dz$  is  $k\delta(z)dz/C$  where  $C$  is the cosine of the angle between its direction of motion and the vertical, and  $k$  is a constant whose value is  $1/75 \text{ cm}^2/\text{g}$  in air, or  $1/160 \text{ cm}^2/\text{g}$  in lead.

Consider a nucleon with momentum  $\mathbf{p}$  arriving at height  $z$ . The probability that it has traversed the layer of depth  $\zeta - z$  immediately above, without collision, is

$$\exp[-\{\theta(z) - \theta(\zeta)\}/C], \text{ where } \theta(z) = k \int_z^\infty \delta(z') dz'. \quad \dots\dots(1)$$

The probability that it resulted from a collision between depths  $\zeta$  and  $\zeta + d\zeta$  is  $-\theta'(\zeta)d\zeta/C$ .

The probability that its immediate ancestor had momentum  $\mathbf{p}'$ ,  $d\mathbf{p}'$  is  $f(\mathbf{p}', \mathbf{p}, \zeta) d\mathbf{p}' d\mathbf{p}$ , where  $\mathbf{p}$ ,  $d\mathbf{p}$  was its displacement from the shower axis. The probability that it generated a nucleon with momentum  $\mathbf{p}$ ,  $d\mathbf{p}$  is  $\nu(\mathbf{p}', \mathbf{p}) d\mathbf{p}$ . Hence

$$f(\mathbf{p}, \mathbf{r}, z) = - \int_z^\infty \int f(\mathbf{p}', \mathbf{p}, \zeta) \nu(\mathbf{p}', \mathbf{p}) \exp[-\{\theta(z) - \theta(\zeta)\}/C] \theta'(\zeta) d\zeta / C d\mathbf{p}' + f(\mathbf{p}, \mathbf{p}_\infty, \infty) \exp[-\theta(z)/C] \quad \dots\dots(2)$$

where the components of  $\mathbf{p}$  are connected with those of  $\mathbf{r}$  by

$$p_1 = r_1 - p_1(\zeta - z)/p_3, \quad p_2 = r_2 - p_2(\zeta - z)/p_3 \quad \dots\dots(3)$$

and  $\mathbf{p}_\infty$  is the value of  $\mathbf{p}$  for  $\zeta = \infty$ .

By differentiating (2) with respect to  $z$ ,  $r_1$  and  $r_2$ , one obtains the differential equation\*

$$\frac{C}{\theta'(z)} \left\{ \frac{\partial f(\mathbf{p})}{\partial z} - \frac{p_1}{p_3} \frac{\partial f(\mathbf{p})}{\partial r_1} - \frac{p_2}{p_3} \frac{\partial f(\mathbf{p})}{\partial r_2} \right\} + f(\mathbf{p}) = \int f(\mathbf{p}') \nu(\mathbf{p}', \mathbf{p}) d\mathbf{p}'. \quad \dots\dots(4)$$

Since  $C$ , the cosine of the angle made by  $\mathbf{p}$  with the vertical, may be written  $p_3/p$ , one obtains, on making the substitution  $z = -r_3$ , the vector equation\*

$$-\frac{1}{\theta'(-r_3)} \frac{\mathbf{p}}{p} \frac{\partial f(\mathbf{p})}{\partial \mathbf{r}} + f(\mathbf{p}) = \int f(\mathbf{p}') \nu(\mathbf{p}', \mathbf{p}) d\mathbf{p}'. \quad \dots\dots(5)$$

It is customary to measure the vertical distance in  $\text{g}/\text{cm}^2$ , which may be effected by taking  $\theta(z)$  instead of  $z$  as the variable. Then the eqn. (4) becomes

$$C \frac{\partial f}{\partial \theta} - \frac{1}{\theta'} \left( \frac{p_1}{p} \frac{\partial f}{\partial r_1} + \frac{p_2}{p} \frac{\partial f}{\partial r_2} \right) + f = \int f(\mathbf{p}') \nu(\mathbf{p}', \mathbf{p}) d\mathbf{p}' \quad \dots\dots(6)$$

where  $\theta'$  continues to represent the function  $\theta'(z)$ , expressed as a function of  $\theta$ . In an isothermal atmosphere,

$$\theta(z) = (kp_0/g) \exp(-g\delta_0 z/p_0), \quad \theta' = -g\delta_0 \theta/p_0 \quad \dots\dots(7)$$

\* The variables on which  $f(\mathbf{p}, \mathbf{r}, z)$  depend are dropped wherever no confusion is likely to arise.

where  $p_0$  and  $\delta_0$  represent the pressure and density at sea level, and  $\mathbf{g}$  is the acceleration due to gravity. For a medium of constant density  $\delta$ , on the other hand,

$$\theta' = -k\delta \quad \dots\dots(8)$$

which is constant; the unit of length may then be chosen so that  $k\delta = 1$ .

### § 3. EQUATIONS FOR THE ANGULAR AND LATERAL SPREAD

To obtain the equations satisfied by the mean values of the quantities  $r_1^m r_2^n$ , it is convenient to follow Borsellino (1950), by considering the two-dimensional Fourier transforms of  $f$  with respect to  $r_1$  and  $r_2$ :

$$g(\mathbf{p}, \boldsymbol{\lambda}, \theta) = \int \int f(\mathbf{p}, \mathbf{r}, \theta) \exp(-i\boldsymbol{\lambda} \cdot \mathbf{r}) dr_1 dr_2. \quad \dots\dots(9)$$

Then one has 
$$g = \sum_{m,n} g_{mn}(\mathbf{p}, \theta) \lambda_1^m \lambda_2^n / (m! n!), \quad \dots\dots(10)$$

where 
$$g_{mn} = \int \int (-ir_1)^m (-ir_2)^n f(\mathbf{p}, \mathbf{r}, \theta) dr_1 dr_2. \quad \dots\dots(11)$$

The equation satisfied by  $g$  is obtained from (6):

$$C \frac{\partial g}{\partial \theta} - \frac{i\boldsymbol{\lambda} \cdot \mathbf{p}}{\theta' p} g + g = \int g(\mathbf{p}') \nu(\mathbf{p}', \mathbf{p}) d\bar{\mathbf{p}}'. \quad \dots\dots(12)$$

By differentiating (12)  $m$  times with respect to  $\lambda_1$ , and  $n$  times with respect to  $\lambda_2$ , then setting  $\lambda_1 = \lambda_2 = 0$ , one obtains a set of equations for the  $g_{mn}$ . For example, if

$$g_{00} = x, \quad -ig_{10} = u_1, \quad -ig_{01} = u_2, \quad -(g_{20} + g_{02}) = z \quad \dots\dots(13)$$

one has

$$C \frac{\partial x(\mathbf{p})}{\partial \theta} + x(\mathbf{p}) = \int x(\mathbf{p}') \nu(\mathbf{p}', \mathbf{p}) d\bar{\mathbf{p}}'. \quad \dots\dots(14)$$

$$\left. \begin{aligned} C \frac{\partial u_1(\mathbf{p})}{\partial \theta} - \frac{p_1}{\theta' p} x(\mathbf{p}) + u_1(\mathbf{p}) &= \int u_1(\mathbf{p}') \nu(\mathbf{p}', \mathbf{p}) d\bar{\mathbf{p}}' \\ C \frac{\partial u_2(\mathbf{p})}{\partial \theta} - \frac{p_2}{\theta' p} x(\mathbf{p}) + u_2(\mathbf{p}) &= \int u_2(\mathbf{p}') \nu(\mathbf{p}', \mathbf{p}) d\bar{\mathbf{p}}' \end{aligned} \right\} \quad \dots\dots(15)$$

$$C \frac{\partial z(\mathbf{p})}{\partial \theta} - \frac{2\mathbf{p}}{\theta' p} \cdot \mathbf{u}(\mathbf{p}) + z(\mathbf{p}) = \int z(\mathbf{p}') \nu(\mathbf{p}', \mathbf{p}) d\bar{\mathbf{p}}'. \quad \dots\dots(16)$$

Writing  $u_1 = p_1 y/p$  and  $u_2 = p_2 y/p$ , the last equation becomes

$$C \frac{\partial z(\mathbf{p})}{\partial \theta} - \frac{2S^2}{\theta'} y(\mathbf{p}) + z(\mathbf{p}) = \int z(\mathbf{p}') \nu(\mathbf{p}', \mathbf{p}) d\bar{\mathbf{p}}', \quad \dots\dots(17)$$

where

$$S^2 = (p_1^2 + p_2^2)/p^2 = 1 - C^2. \quad \dots\dots(18)$$

Multiplying the two equations (15) by  $p_1/p$  and  $p_2/p$  respectively, and adding, one has

$$S^2 \left\{ C \frac{\partial y(\mathbf{p})}{\partial \theta} - \frac{1}{\theta'} x(\mathbf{p}) + y(\mathbf{p}) \right\} = \int \frac{(p_1 p_1' + p_2 p_2')}{p p'} y(\mathbf{p}') \nu(\mathbf{p}', \mathbf{p}) d\bar{\mathbf{p}}'. \quad \dots\dots(19)$$

The equations (14), (17) and (19) will now be written in polar coordinates; the following notations will be used. The cosine of the angle between the vectors  $\mathbf{p}$  and  $\mathbf{p}'$  will be denoted by  $c$ , and its sine by  $s$ ; the angle between the plane containing both  $\mathbf{p}$  and  $\mathbf{p}'$ , and that containing both  $\mathbf{p}$  and the vertical, will be denoted

by  $\phi$ . Then

$$\int d\bar{\mathbf{p}}' = \int_p^\infty dp' \int_{-1}^1 dc \int_0^{2\pi} d\phi / 2\pi$$



and the cosine of the angle between  $\mathbf{p}'$  and the vertical is  $C' = Cc + Ss \cos \phi$ ; also  $(p_1 p_1' + p_2 p_2')/p p' = (\mathbf{p} \cdot \mathbf{p}' - p_3 p_3')/p p' = c - C C' = S(Sc - Cs \cos \phi)$ . Hence

$$C \frac{\partial x(U, C)}{\partial \theta} + x(U, C) = \int_U^\infty \int_{-1}^1 \int_0^{2\pi} x(U', Cc + Ss \cos \phi) \nu(U', U, c) dU' dc d\phi / 2\pi \quad \dots\dots (20)$$

$$S^2 \left\{ C \frac{\partial y(U, C)}{\partial \theta} - \frac{x(U, C)}{\theta'} + y(U, C) \right\} = \int_U^\infty \int_{-1}^1 \int_0^{2\pi} S(Sc - Cs \cos \phi) \times y(U', Cc + Ss \cos \phi) \nu(U', U, c) dU' dc d\phi / 2\pi \quad \dots\dots (21)$$

$$C \frac{\partial z(U, C)}{\partial \theta} - \frac{2S^2}{\theta'} y(U, C) + z(U, C) = \int_U^\infty \int_{-1}^1 \int_0^{2\pi} z(U', Cc + Ss \cos \phi) \nu(U', U, c) dU' dc d\phi / 2\pi \quad \dots\dots (22)$$

where  $p$  and  $p'$  have been replaced by  $U$  and  $U'$ .

The physical quantities of primary interest are the mean square angular deviation and the mean square distance of the particles from the shower axis. They are given by

$$\omega^2(U, \theta) = \left\{ \int_{-1}^1 x(U, C, \theta) S^2 dC \right\} \left\{ \int_{-1}^1 x(U, C, \theta) dC \right\}^{-1} \quad \dots\dots (23)$$

$$\text{and} \quad l^2(U, \theta) = \left\{ \int_{-1}^1 z(U, C, \theta) dC \right\} \left\{ \int_{-1}^1 x(U, C, \theta) dC \right\}^{-1}. \quad \dots\dots (24)$$

In order to determine these, it is not necessary to solve the equations (20) to (22) completely; one requires only certain coefficients in the expansions of  $x(U, C)$  and  $z(U, C)$  in Legendre polynomials. One therefore writes

$$\left. \begin{aligned} x(U, C) &= \sum_{K=0}^{\infty} (K + \frac{1}{2}) x_K(U) P_K(C), & y(U, C) &= \sum_{K=0}^{\infty} (K + \frac{1}{2}) y_K(U) P_K(C), \\ z(U, C) &= \sum_{K=0}^{\infty} (K + \frac{1}{2}) z_K(U) P_K(C) \end{aligned} \right\} \dots\dots (25)$$

$$\text{then} \quad \omega^2(U) = \frac{2}{3} \{x_0(U) - x_2(U)\} / x_0(U) \quad \dots\dots (26)$$

$$\text{and} \quad l^2(U) = z_0(U) / x_0(U). \quad \dots\dots (27)$$

The coefficients required are determined in the following section.

#### § 4. DETERMINATION OF THE LEGENDRE COEFFICIENTS

When the expansions (25) are substituted in the integrals of (20)–(22) the latter simplify. Use is made of the addition theorem for Legendre polynomials:

$$\int_0^{2\pi} P_K(Cc + Ss \cos \phi) d\phi / 2\pi = P_K(C) P_K(c)$$

$$\begin{aligned} \text{also} \quad \int_0^{2\pi} P_K(Cc + Ss \cos \phi) \cos \phi d\phi / 2\pi &= P_K'(C) P_K'(c) / K(K+1) \\ &= \frac{Ss}{K(K+1)} \frac{dP_K(C)}{dC} \frac{dP_K(c)}{dc}. \end{aligned}$$

$$\text{If} \quad \nu_K(U', U) = \int_{-1}^1 \nu(U', U, c) P_K(c) dc \quad \dots\dots (28)$$

$$\begin{aligned} \text{one has} \quad \int_{-1}^1 \int_0^{2\pi} x(U', Cc + Ss \cos \phi) \nu(U', U, c) dc d\phi / 2\pi \\ = \sum_{K=0}^{\infty} (K + \frac{1}{2}) x_K(U') \nu_K(U', U) P_K(C) \quad \dots\dots (29) \end{aligned}$$

therefore, multiplying (20) by  $P_K(C)$ , and integrating with respect to  $C$  from  $-1$  to  $1$ , one obtains

$$\begin{aligned} \frac{\partial}{\partial \theta} \left\{ \frac{K+1}{2K+1} x_{K+1}(U) + \frac{K}{2K+1} x_{K-1}(U) \right\} + x_K(U) \\ = \int_U^\infty x_K(U') \nu_K(U', U) dU'. \quad \dots\dots (30) \end{aligned}$$

Again, one has by a straightforward but tedious calculation

$$\begin{aligned} \int_{-1}^1 dC \int_{-1}^1 \int_0^{2\pi} S(Sc - Cs \cos \phi) y(U', Cc + Ss \cos \phi) \nu(U', U, c) dc d\phi / 2\pi \\ = \frac{2}{3} \{y_0(U') - y_2(U')\} \nu_1(U', U); \quad \dots\dots (31) \end{aligned}$$

hence, writing

$$b(U) = \int_{-1}^1 y(U, C) S^2 dC = \frac{2}{3} \{y_0(U) - y_2(U)\} \quad \dots\dots (32)$$

one obtains by integrating (21) with respect to  $C$

$$\begin{aligned} \frac{\partial}{\partial \theta} \int_{-1}^1 (C-1) S^2 y(U, C) dC + \frac{\partial b(U)}{\partial \theta} - \frac{2}{3\theta} \{x_0(U) - x_2(U)\} + b(U) \\ = \int_U^\infty b(U') \nu_1(U', U) dU'. \quad \dots\dots (33) \end{aligned}$$

Now, this equation is exact, but the integral of the first term contains a factor  $(1-C)^2$ , the average value of which is negligible, since it varies as the mean fourth power of the deflection from the shower axis. Hence, using (26), (33) becomes

$$\frac{\partial b(U)}{\partial \theta} - x_0(U) \omega^2(U) / \theta' + b(U) = \int_U^\infty b(U') \nu_1(U', U) dU'. \quad \dots\dots (34)$$

Similarly one obtains, on integrating (22) with respect to  $C$  from  $-1$  to  $1$ ,

$$\frac{\partial z_1(U)}{\partial \theta} - 2 \frac{(bU)}{\theta'} + z_0(U) = \int_U^\infty z_0(U') \nu_0(U', U) dU'. \quad \dots\dots (35)$$

Now it may be seen from (22) that  $z(U, C)$  is proportional to  $S^2$ ; hence

$$z_1(U) - z_0(U) = \int_{-1}^1 z(U, C) (C-1) dC$$

may be neglected; i.e. one may substitute  $z_0(U)$  for  $z_1(U)$  in (35).

We shall first determine the mean square angular deviation, from (30). Following the approximation of neglecting the mean value of  $(1-C)^2$ , we shall neglect

$$\int_{-1}^1 x(U, C) (1-C)^2 dC = \frac{2}{3} x_2 + \frac{4}{3} x_0 - 2x_1$$

by setting

$$x_1 = \frac{1}{3} x_2 + \frac{2}{3} x_0. \quad \dots\dots (36)$$

From (30) one then obtains by substituting  $k=0$  and  $k=1$ , and subtracting the results,

$$\begin{aligned} \frac{\partial}{\partial \theta} \{x_0(U) - x_2(U)\} + \{x_0(U) - x_2(U)\} = \int_U^\infty \{x_0(U') - x_2(U')\} \nu_0(U', U) dU' \\ + \int_U^\infty x_0(U') \{\nu_0(U', U) - \nu_2(U', U)\} dU'. \quad \dots\dots (37) \end{aligned}$$

The coefficient

$$x_0(U) = \int_{-1}^1 x(U, C) dC = \int_{-1}^1 \int \int f dr_1 dr_2 dC$$



is simply the average number of nucleons at depth  $\theta$  in the medium, and is known to be

$$x_0(U, \theta) = \frac{1}{2\pi i} \frac{1}{U_0} \int_{s_0-i\infty}^{s_0+i\infty} (U/U_0)^{-(s+1)} \exp \{-h(s)\theta\} ds \quad \dots\dots (38)$$

where 
$$h(s) = 1 - \int_0^\infty \left(\frac{U}{U'}\right)^s U' \nu_0(U', U) d\left(\frac{U}{U'}\right) \quad \dots\dots (39)$$

if the shower is supposed to be generated by a primary nucleon of energy  $U_0$ . The equation (37) can then be solved by means of a single Mellin transform; the result is

$$\frac{2}{3}\{x_0(U, \theta) - x_2(U, \theta)\} = \frac{1}{2\pi i} \frac{1}{U_0^2} \int_{s_0-i\infty}^{s_0+i\infty} \left(\frac{U}{U_0}\right)^{-(s+1)} j(s) [\exp \{-h(s-1)\theta\} - \exp \{-h(s)\theta\}] ds \quad \dots\dots (40)$$

where

$$\{h(s) - h(s-1)\}j(s) = \frac{2}{3} \int_0^\infty \left(\frac{U}{U'}\right)^s U'^2 \{\nu_0(U', U) - \nu_2(U', U)\} d\left(\frac{U}{U'}\right). \quad \dots\dots (41)$$

We have here used the result of our previous paper (Messel and Green 1952), that  $U'^2\{\nu_0(U', U) - \nu_2(U', U)\}$  is a function of  $U/U'$  only. We state here, for convenience the explicit values of  $\nu_0(U', U)$  and  $\nu_0(U', U) - \nu_2(U', U)$ :

$$\nu_0(U', U) = \frac{1}{2\pi i} \frac{1}{U'} \int_{s_0-i\infty}^{s_0+i\infty} \left(\frac{U}{U'}\right)^{-(s+1)} \{1 - f[D_A \alpha(s)]\} ds \quad \dots\dots (42)$$

and

$$\begin{aligned} \frac{2}{3}\{\nu_0(U', U) - \nu_2(U', U)\} \\ = \frac{1}{2\pi i} \frac{1}{U'^2} \int_{s_0-i\infty}^{s_0+i\infty} \left(\frac{U}{U'}\right)^{-(s+1)} \left\{ \frac{2 - \alpha(s) - \alpha(s-1)}{\alpha(s) - \alpha(s-1)} \right\} \{f[D_A \alpha(s)] - f[D_A \alpha(s-1)]\} ds \end{aligned} \quad \dots\dots (43)$$

where 
$$f(\lambda) = 1 - 2\{1 - (1 + \lambda) e^{-\lambda}\}/\lambda^2 \quad \dots\dots (44)$$

$$\alpha(s) = 1 - 2 \int_0^\infty \int_0^\infty \epsilon^s w(\epsilon, \epsilon_1) d\epsilon d\epsilon_1 \quad \dots\dots (45)$$

in which  $D_A$  is the average number of collisions suffered by a nucleon in a diametrical passage through a nucleus of atomic number  $A$ ; and  $w(\epsilon_1, \epsilon_2) d\epsilon_1 d\epsilon_2$  is the probability that, in an inelastic nucleon-nucleon collision, the scattered nucleons have energies in the ratios  $\epsilon_1, \epsilon_2$  to that of the incident nucleon. From (39) and (42) it follows that

$$h(s) = f[D_A \alpha(s)]; \quad \dots\dots (46)$$

also, from (41) and (43) one has

$$j(s) = \{2 - \alpha(s) - \alpha(s-1)\} \{\alpha(s) - \alpha(s-1)\}^{-1}. \quad \dots\dots (47)$$

The mean square angular deviation from the shower axis, according to (26), is obtained immediately by taking the quotient of (40) and (38). The result, it may be observed, is independent of the variation in density of the medium, which is entirely taken account of by the variation of  $\theta$  with  $z$ ; the denominator  $\theta'$  does not appear in the result.

The mean square distance from the shower axis is determined by  $z_0(U, \theta)$ ; however, eqn. (35) can only be solved when the solution of (34) is known. This equation is readily solved by Mellin transforms; one has

$$b(U, \theta) = \frac{1}{2\pi i} \int_{s_0-i\infty}^{s_0+i\infty} U^{-(s+1)} \exp \{-h(s)\theta\} \int_0^\theta \frac{a(s, \lambda)}{\theta'(\lambda)} \exp \{h(s)\lambda\} d\lambda ds \quad \dots\dots (48)$$

$$\begin{aligned} \text{where} \quad a(s, \theta) &= \frac{2}{3} \int_0^\infty U^s \{x_0(U, \theta) - x_2(U, \theta)\} dU \\ &= U_0^{s-1} j(s) [\exp \{-h(s-1)\theta\} - \exp \{-h(s)\theta\}] \end{aligned} \quad \dots\dots (49)$$

according to (40).

The determination of  $z_0(U, \theta)$  from (35) is now precisely similar:

$$z_0(U, \theta) = \frac{1}{2\pi i} \int_{s_0-i\infty}^{s_0+i\infty} U^{-(s+1)} 2 \exp \{-h(s)\theta\} \int_0^\theta \frac{b(s, \lambda)}{\theta'(\lambda)} \exp \{h(s)\lambda\} d\lambda ds \quad \dots\dots (50)$$

where

$$b(s, \theta) = U_0^{s-1} \exp \{-h(s)\theta\} \int_0^\theta \frac{j(s)}{\theta'(\lambda)} [\exp \{h(s)\lambda - h(s-1)\lambda\} - 1] d\lambda \quad \dots\dots (51)$$

is the Mellin transform of  $b(U, \theta)$ .

## § 5. EXPLICIT RESULTS

We now proceed to summarize results for the various situations of physical interest: in an isothermal atmosphere, and a medium of constant density, for a single incident primary particle of energy  $U_0$  and a primary power law spectrum with exponent  $\gamma$ , and for differential and integral spectra. Small letters will relate to differential spectra, and the corresponding capitals to integral spectra. The suffix *i* will characterize the value for a single incident primary nucleon; the suffix *p*, that for the incident power law spectrum. Primed symbols will indicate values correct only for a medium of constant density, e.g. lead.

The average number of particles per unit energy range at depth  $\theta$ , measured in units of the interaction mean free path, has been denoted so far by  $x_0(U, \theta)$ ; we shall now revert to the customary notation by replacing this quantity by  $n(U, \theta)$ . Thus one has the boundary conditions

$$\begin{aligned} n_i(U, \theta=0) &= \delta(U - U_0) & N_i(U, \theta=0) &= 1, \quad U < U_0 \\ n_p(U, \theta=0) &= \begin{cases} \gamma U_c^\gamma / U^{\gamma+1}, & U > U_c \\ 0, & U < U_c \end{cases} \\ N_p(U, \theta=0) &= \begin{cases} U_c^\gamma / U^\gamma, & U > U_c \\ 1, & U < U_c \end{cases} \end{aligned} \quad \dots\dots (52)$$

where  $U_c$  is the geomagnetic cut-off energy, measured in proton mass units. From previous work (Messel 1951 a, b), it is known that

$$\begin{aligned} n_i(U, \theta) &= \frac{1}{2\pi i} \frac{1}{U_0} \int_{s_0-i\infty}^{s_0+i\infty} \left(\frac{U}{U_0}\right)^{-(s+1)} \exp \{-h(s)\theta\} ds \\ N_i(U, \theta) &= \frac{1}{2\pi i} \int_{s_0-i\infty}^{s_0+i\infty} \left(\frac{U}{U_0}\right)^{-s} \exp \{-h(s)\theta\} ds/s \\ n_p(U, \theta) &= \frac{1}{2\pi i} \frac{1}{U_c} \int_{s_0-i\infty}^{s_0+i\infty} \left(\frac{U}{U_c}\right)^{-(s+1)} \exp \{-h(s)\theta\} \frac{\gamma ds}{(\gamma-s)} \\ N_p(U, \theta) &= \frac{1}{2\pi i} \int_{s_0-i\infty}^{s_0+i\infty} \left(\frac{U}{U_c}\right)^{-s} \exp \{-h(s)\theta\} \frac{\gamma ds}{s(\gamma-s)} \end{aligned} \quad \dots\dots (53)$$

where  $h(s)$  is given by (46), (44) and (45).

For  $U > U_c$ , the last two integrals may be evaluated immediately

$$\begin{aligned} n_p(U, \theta) &= \gamma (U_c/U)^{\gamma+1} \exp \{-h(\gamma)\theta\} U_c \\ N_p(U, \theta) &= (U_c/U)^\gamma \exp \{-h(\gamma)\theta\}. \end{aligned} \quad \dots\dots (54)$$



From (40) one has for the mean square angle

$$\begin{aligned}\omega_1^2(U, \theta) &= \frac{1}{n_i(U, \theta)} \frac{1}{2\pi i} \frac{1}{U_0^2} \int_{s_0-i\infty}^{s_0+i\infty} \left(\frac{U}{U_0}\right)^{-(s+1)} j(s) [\exp\{-h(s-1)\theta\} \\ &\quad - \exp\{-h(s)\theta\}] ds \\ \Omega_1^2(U, \theta) &= \frac{1}{N_i(U, \theta)} \frac{1}{2\pi i} \frac{1}{U_0} \int_{s_0-i\infty}^{s_0+i\infty} \left(\frac{U}{U_0}\right)^{-s} j(s) [\exp\{-h(s-1)\theta\} \\ &\quad - \exp\{-h(s)\theta\}] \frac{ds}{s} \\ w_p^2(U, \theta) &= \frac{1}{n_p(U, \theta)} \frac{1}{2\pi i} \frac{1}{U_c^2} \int_{s_0-i\infty}^{s_0+i\infty} \left(\frac{U}{U_c}\right)^{-(s+1)} j(s) [\exp\{-h(s-1)\theta\} \\ &\quad - \exp\{-h(s)\theta\}] \frac{\gamma ds}{\gamma - s + 1} \\ \Omega_p^2(U, \theta) &= \frac{1}{N_p(U, \theta)} \frac{1}{2\pi i} \frac{1}{U_c} \int_{s_0-i\infty}^{s_0+i\infty} \left(\frac{U}{U_c}\right)^{-s} j(s) [\exp\{-h(s-1)\theta\} \\ &\quad - \exp\{-h(s)\theta\}] \frac{\gamma ds}{s(\gamma - s + 1)} \dots\dots\dots(55)\end{aligned}$$

where  $s_0 < \gamma + 1$ , and  $j(s)$  is given by (47) and (45).

For  $U > U_c$ , the last two integrals become

$$\begin{aligned}\omega_p^2(U, \theta) &= \frac{1}{UU_c} j(\gamma + 1) [1 - \exp\{h(\gamma)\theta - h(\gamma + 1)\theta\}] \text{ (radians)}^2 \\ \Omega_p^2(U, \theta) &= \frac{\gamma}{U(\gamma + 1)} j(\gamma + 1) [1 - \exp\{h(\gamma)\theta - h(\gamma + 1)\theta\}] \text{ (radians)}^2. \dots\dots(56)\end{aligned}$$

To evaluate these results, we have taken  $\gamma = 1.1$ , and

$$\begin{aligned}w(\epsilon_1, \epsilon_2) &= 120\epsilon_1\epsilon_2(1 - \epsilon_1 - \epsilon_2) \\ \alpha(s) &= 1 - 240\{(s+2)(s+3)(s+4)(s+5)\}^{-1} \dots\dots(57)\end{aligned}$$

which were found (Messel 1951 a, b) to give best agreement with experimental data for the average numbers. With these values, eqns. (56) simplify to

$$\begin{aligned}\omega_p^2(U, \theta) &= 2.55 (UU_c)^{-1} (1 - e^{-0.2\theta}) \\ \Omega_p^2(U, \theta) &= 1.34 U^{-1} (1 - e^{-0.2\theta}). \dots\dots(58)\end{aligned}$$

The results for the mean square distance from the shower axis, derived from (50), are as follows:

For media of constant density

$$\begin{aligned}l_1^2(U, \theta) &= \frac{1}{n_i(U, \theta)} \frac{1}{2\pi i} \frac{2}{U_0^2} \int_{s_0-i\infty}^{s_0+i\infty} \left(\frac{U}{U_0}\right)^{-(s+1)} j(s) J'(s, \theta) ds \\ L_1^2(U, \theta) &= \frac{1}{N_i(U, \theta)} \frac{1}{2\pi i} \frac{2}{U_0} \int_{s_0-i\infty}^{s_0+i\infty} \left(\frac{U}{U_0}\right)^{-s} j(s) J'(s, \theta) ds/s \dots\dots(59)\end{aligned}$$

$$\begin{aligned}\text{where } J'(s, \theta) &= \frac{\exp\{-h(s-1)\theta\} - \exp\{-h(s)\theta\}}{\{h(s) - h(s-1)\}^2} \\ &\quad - \frac{\theta \exp\{-h(s)\theta\}}{\{h(s) - h(s-1)\}} - \frac{1}{2}\theta^2 \exp\{-h(s)\theta\}. \dots\dots(60)\end{aligned}$$

For the power-law spectrum

$$\begin{aligned}l_p^2(U, \theta) &= \frac{1}{n_p(U, \theta)} \frac{1}{2\pi i} \frac{2}{U_c^2} \int_{s_0-i\infty}^{s_0+i\infty} \left(\frac{U}{U_c}\right)^{-(s+1)} j(s) J'(s, \theta) \gamma ds / (\gamma - s + 1) \\ L_p^2(U, \theta) &= \frac{1}{N_p(U, \theta)} \frac{1}{2\pi i} \frac{2}{U_c} \int_{s_0-i\infty}^{s_0+i\infty} \left(\frac{U}{U_c}\right)^{-s} j(s) J'(s, \theta) \gamma ds / s(\gamma - s + 1). \dots\dots(61)\end{aligned}$$

For  $U > U_0$ , (61) reduces to

$$l_p'^2(U, \theta) = 2(UU_0)^{-1} j(\gamma+1) J'(\gamma+1, \theta)$$

$$L_p'^2(U, \theta) = \frac{2\gamma j(\gamma+1)}{U(\gamma+1)} J'(\gamma+1, \theta). \quad \dots\dots (62)$$

In lead,  $D_A = 8.9$ , and  $\theta$  is measured in units of  $160 \text{ g/cm}^2$ ; then

$$l_p'^2(U, \theta) = 1.02(UU_0)^{-1} e^{-0.1\theta} \{e^{0.1\theta} - 1 - 0.1\theta - \frac{1}{2}(0.1\theta)^2\} \times 10^5 \text{ cm}^2.$$

$$L_p'^2(U, \theta) = 5.3 U^{-1} e^{-0.1\theta} \{e^{0.1\theta} - 1 - 0.1\theta - \frac{1}{2}(0.1\theta)^2\} \times 10^4 \text{ cm}^2. \quad \dots\dots (63)$$

The following results are for an isothermal atmosphere with surface density  $\delta_0$  and surface pressure  $p_0$ :

$$l_p^2(U, \theta) = (p_0/\delta_0 g)^2 \frac{1}{n_p(U, \theta)} \frac{1}{2\pi i} \frac{2}{U_c^2} \int_{s_0-i\infty}^{s_0+i\infty} \left(\frac{U}{U_c}\right)^{-(s+1)} j(s) J(s, \theta) \frac{\gamma ds}{\gamma-s+1}$$

$$L_p^2(U, \theta) = (p_0/\delta_0 g)^2 \frac{1}{N_p(U, \theta)} \frac{1}{2\pi i} \frac{2}{U_c} \int_{s_0-i\infty}^{s_0+i\infty} \left(\frac{U}{U_c}\right)^{-s} j(s) J(s, \theta) \frac{\gamma ds}{s(\gamma-s+1)} \quad \dots (64)$$

where  $J(s, \theta) = \exp \left\{ -h(s)\theta \right\} \left[ \frac{\{g(s)\theta\}}{1^2 \cdot 1!} + \frac{\{g(s)\theta\}^2}{2^2 \cdot 2!} + \dots \right]$

$$g(s) = h(s) - h(s-1). \quad \dots\dots (65)$$

For  $U > U_0$ , and  $\gamma = 1.1$  as before, one has

$$l_p^2(U, \theta) = 309 (UU_0)^{-1} e^{-0.2\theta} \left\{ 0.2\theta + \frac{(0.2\theta)^2}{2^2 \cdot 2!} + \frac{(0.2\theta)^3}{3^2 \cdot 3!} + \dots \right\} \text{ km}^2$$

$$L_p^2(U, \theta) = 162 U^{-1} e^{-0.2\theta} \left\{ 0.2\theta + \frac{(0.2\theta)^2}{2^2 \cdot 2!} + \frac{(0.2\theta)^3}{3^2 \cdot 3!} + \dots \right\} \text{ km}^2 \quad \dots\dots (66)$$

for an isothermal atmosphere of  $0^\circ \text{C}$ .

The root mean square angular deviation in the atmosphere, for an integral spectrum, obtained from (58), is exhibited in fig. 1. The root mean square lateral spread from the shower axis for an isothermal atmosphere of  $0^\circ \text{C}$  is shown in fig. 2.

In the table below, we give the root mean square lateral spread in centimetres for an integral spectrum with power law 1.1 in lead.

Depth (cm)	Energy in Proton Mass Units *		
	$U \geq 5$	$U \geq 10$	$U \geq 30$
1.41	0.04	0.03	0.02
2.82	0.12	0.08	0.05
7.05	0.46	0.32	0.19
14.1	1.26	0.89	0.52
28.2	3.42	2.42	
42.3	6.18	4.37	
56.4	9.16	6.48	
84.6	15.63		

\* Proton mass unit  $\approx 10^3 \text{ mev}$ .

## § 6. DISCUSSION

The mean square angular deviation from the vertical, shown in fig. 1, is inversely proportional to the minimum energy of the particles considered. Assuming the primaries are incident in the vertical direction, the deviation increases rapidly down to the first  $250 \text{ g/cm}^2$  of air encountered, but thereafter tends to an almost constant value. This is in accordance with observation



(Lord and Schien 1950). Actually the primaries are inclined to the vertical, their distribution about the vertical having been determined (Van Allen and Gangnes 1950). If, however, this initial distribution is inserted as a boundary condition to the equation which determines the mean square angular deviation, the result for large depths is not affected, as the initial value appears multiplied by a factor  $\exp(-0.2\theta)$ .

In determining the mean square distance from the shower axis, assumed to be vertical, we have not taken account of the angular deviation from the vertical of the primary particles. If this were done, one would obtain misleadingly large values owing to the large lateral distances travelled by particles which are initially almost horizontal. On the other hand, if one wishes to know the lateral spread of showers initiated by particles inclined to the vertical, this is easily obtained by taking a shower axis inclined to the vertical at the same angle.

The mean square distance from the shower axis, exhibited in fig. 2, is also inversely proportional to the minimum energy of the particles considered. Leaving aside for the moment the magnitude of the results, it will be seen that there is a rapid increase down to an atmospheric depth of about  $400 \text{ g/cm}^2$ . This is solely a result of the fact that the density is so small, which enables a particle, once deflected at a high altitude, to travel large distances in a lateral direction without collision.

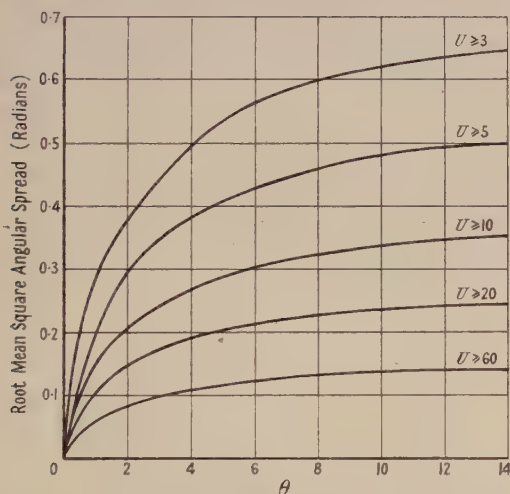


Fig. 1. Root mean square angular deviation of nucleons with energies greater than  $U$  plotted against the depth  $\theta$  measured in interaction mean free paths. The curves are for an incident integral primary power law spectrum with exponent 1.1.

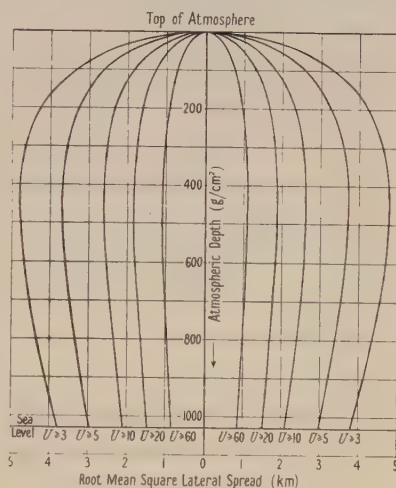


Fig. 2. Root mean square lateral spread of nucleons with energies greater than  $U$  plotted against atmospheric depth. The middle line corresponds to the axis of the shower. The curves are for an incident integral primary power law spectrum with exponent 1.1.

Following the first collision, a particle may easily travel a distance of several kilometres from the shower axis before making the next impact. Thereafter the density increases and the collisions become correspondingly more frequent. It can be seen from this that there will be large fluctuations in the distance travelled by a particle from the shower axis, particularly in the first few hundred grams of material traversed. This will need to be taken into account in interpreting the experimental data.

Below  $400 \text{ g/cm}^2$  the mean square distance from the shower axis decreases, owing to the loss of particles from the energy range considered. The mean lateral extent of showers is therefore greatest at about 8000 metres. For an equivalent atmosphere of constant density, no such maximum extent would occur. From the table it will be seen that, in lead also, no maximum spread is attained in the first few metres; a maximum exists, but it occurs much deeper than in a medium of variable density. It is therefore most important to take the variation of density with height into account in considering the development of a cascade in the atmosphere. This, however, was not done in previous work on the lateral spread of the soft component of the cosmic radiation.

The actual values for the mean square distance from the shower axis are unexpectedly large. This does not necessarily imply that individual showers are diffused over a wide area. The relation between the mean square distance from the shower axis and what one would normally regard as the radius of the shower depends critically on the behaviour of the radial distribution at large distances. In the present instance, it is necessary to interpret the large value found for the mean square distance as due to a long 'tail'. In a qualitative way it is easy to see how such a 'tail' may arise from the fluctuations, noted above, in which a particle can travel many kilometres away from the shower axis. It has already been pointed out by Messel (1951 c) that the number distribution has also a long 'tail', for a precisely similar reason: the ability of particles to traverse long distances in the upper atmosphere, with large fluctuations in the collision mean free path. To discuss this phenomenon from the quantitative point of view, it will be necessary to determine the radial distribution function relating to particles in a shower; this we hope to do shortly.\*

The present results for the atmosphere have been evaluated using an integral power law spectrum for the primary particles with the exponent 1.1, which is now most generally accepted. We have also worked out results for the exponent 1.7, and find values at sea level which are still much larger than those given here.

Experimentally, the lateral spread of extensive air showers has been investigated recently by Cocconi *et al.* (1949), and Greisen *et al.* (1950), up to a distance of 100 metres from the core; and by the Russian school (Eidus, Alymova *et al.* 1950, Vernov *et al.* 1950, Eidus, Blinova *et al.* 1950) up to distances of the order of a kilometre. Cocconi *et al.* and Greisen *et al.* found densely populated cores to the showers, with the soft component decreasing more rapidly than the nucleon component towards the periphery. The Russian school found a core, consisting of both the soft and hard components, of mean radius 100 metres; outside this core is a region, of the order of 1 km in radius, in which the nucleon component predominates. In this region the particle density decreases as  $r^{-2.6}$  with the distance from the core, a behaviour which, if continued, would give an infinite mean spread. Since we find a finite value, there is presumably a 'cut-off' at a distance of many kilometres. We wish to stress at this point that our results do *not* indicate high density showers (detectable by ordinary counter arrangements) diffused over wide areas. Assuming our interpretation of a long tail then what would be observed, experimentally, are showers of high density diffused over distances of several hundreds of metres from the shower axis, and surrounded by a very wide area in which the particle

\* This has now been done. The results will appear in the *Physical Review*.



density is comparatively small and difficult to detect experimentally. It is, however, desirable to carry out experiments over the wide areas of low density which would provide satisfactory data for a quantitative comparison with the theory.

The reason why Molière's theory, based on a physical picture which is now generally admitted to be erroneous, gave apparent agreement with the experiments of Cocconi *et al.* (1949) was the fact that it is actually correct for the central region to which these experiments were limited.

We infer that the centre of a shower consists of a core, composed of descendants of the particles of very high energy produced early in the nucleon cascade. Among these particles there will exist neutral mesons, which through their decay into  $\gamma$ -rays, generate the soft component, which predominates in the core. The particles in the outer region are the descendants of particles with somewhat lower energies, among which the  $\pi$ -mesons are not sufficiently energetic to generate electrons and photons in the same proportion as found in the core.

These conclusions, which were already drawn from the result of our calculation of the mean square angular deflection in nucleon-nucleon collisions (Green and Messel 1951 b), have been confirmed experimentally by McCusker and Millar (1951) who found that the proportion of the penetrating to the soft component increased with distance from the core. It is reasonable to suppose that a satisfactory quantitative discussion of the soft component can be based on the foregoing considerations.

## REFERENCES

- BORSELLINO, A., 1950, *Nuovo Cim.*, **7** (No. 4), 700.  
 CARLSON, A. G., HOOPER, J. E., and KING, D. T., 1950, *Phil. Mag.*, **41**, 701.  
 COCCONI, G., COCCONI-TONGIORGI, V., and GRIESEN, K., 1949, *Phys. Rev.*, **76**, 1020.  
 CRITCHFIELD, C. L., NEY, E. P., and OLEKSA, S., 1950, *Phys. Rev.*, **79**, 402.  
 EIDUS, L. KH., ALYMOVA, M. M., and VIDENSKII, V. G., 1950, *Dokl. Akad. Nauk., S.S.S.R.*, **75**, 669.  
 EIDUS, L. KH., BLINOVA, N. M., VIDENSKII, V. G., and SUVOROV, L., 1950, *Dokl. Akad. Nauk., S.S.S.R.*, **74**, 477.  
 GREEN, H. S., and MESSEL, H., 1951 a, *Phys. Rev.*, **83**, 842; 1951 b, *Proc. Phys. Soc. A*, **64**, 1083.  
 GRIESEN, K., WALKER, W. D., and WALKER, S. P., 1950, *Phys. Rev.*, **80**, 535.  
 HEISENBERG, W., 1946, *Cosmic Radiation* (New York: Dover Publications).  
 JÁNOSSY, L., and MESSEL, H., 1951, *Proc. R. Irish Acad. A*, **54**, 245.  
 LORD, L., and SCHIEN, M., 1950, *Phys. Rev.*, **77**, 19.  
 MCCUSKER, C. B. A., and MILLAR, D. D., 1951, *Proc. Phys. Soc. A*, **64**, 915.  
 MESSEL, H., 1951 a, Commun. Dublin Inst. for Advanced Studies, A, No. 7; 1951 b, *Proc. Phys. Soc. A*, **64**, 726; 1951 c, *Ibid.*, **64**, 807.  
 MESSEL, H., and GREEN, H. S., 1952, *Proc. Phys. Soc. A*, **65**, 245.  
 MESSEL, H., and RITSON, D. M., 1950, *Proc. Phys. Soc. A*, **63**, 1359.  
 MOLIÈRE, G., 1942, *Naturwissenschaften*, **30**, 87.  
 NORDHEIM, L. W., 1941, *Phys. Rev.*, **59**, 929 (A).  
 NORDHEIM, L. W., and ROBERG, S., 1949, *Phys. Rev.*, **75**, 444.  
 VAN ALLEN, J. A., and GANGNES, A. V., 1950, *Phys. Rev.*, **78**, 50.  
 VERNOV, S. N., GRIGOROV, N. L., and CHARAKHCHYAN, A. N. 1950, *Izv. Akad. Nauk., S.S.S.R., Ser. Fiz.*, **14**, 51.

# The Altitude Variation of Penetrating Showers

By A. L. HODSON

The Physical Laboratories, University of Manchester

*Communicated by P. M. S. Blackett; MS. received 6th November 1951, and in amended form 21st April 1952*

**ABSTRACT.** The altitude variations of local penetrating showers and of extensive penetrating showers have been studied between sea level and 33 500 ft.

The attenuation length in air of the radiation producing local penetrating showers is found to be  $(129 \pm 2)$  g/cm<sup>2</sup>. This value has been corrected for the effect of deviations of the radiation from vertical incidence on the apparatus. Local penetrating showers observed under a transition layer of lead 10 cm thick are about 750 times more frequent at 33 500 ft. and 500 times more frequent at 30 000 ft. than at sea level.

## § 1. INTRODUCTION

BROADBENT and Jánosy (1947) showed that showers at sea level containing penetrating particles are of two types: 'local penetrating showers' produced in the materials of the apparatus by single incident particles and 'extensive air showers' containing penetrating particles or radiation capable of producing them. Most of the local penetrating showers are produced by fast nucleons, and the altitude variation of these showers is a measure of the attenuation of fast nucleons in air. The events which discharge a penetrating shower detector in extensive air showers are not necessarily of this type, and it is necessary to separate the two types of showers if we are to measure the attenuation of nucleons. Tinlot (1948 b) and George and Jason (1950) attempted this separation at mountain altitudes, but in the existing measurements at higher altitudes (Wataghin 1947, Tinlot 1948 a, Walsh and Piccioni 1950) no separation was made.

## § 2. EXPERIMENTAL ARRANGEMENTS

The penetrating shower detector used in our second series\* of measurements is shown in fig. 1. The events recorded were sevenfold coincidences between the trays of counters T (split into three interlaced counter groups), M (split into two) and B (split into two). Each shower recorded therefore contained at least three particles, of which at least two could penetrate 22 cm of lead. This detector is similar to that used by Broadbent and Jánosy but smaller.

An unshielded counter tray  $E_B$  of total sensitive area 1190 cm<sup>2</sup>, was placed 78 cm from the centre of tray T. Sevenfold coincidences (denoted by P) and sevenfold coincidences accompanied by a discharge in  $E_B$  (denoted by P,  $E_B$ ) were recorded simultaneously. The events in which a sevenfold P coincidence was not accompanied by a discharge in  $E_B$  are denoted by P- $E_B$ .

Broadbent and Jánosy (1947) found that a 10 cm layer of lead placed over the P set produces a large increase in the rate of local penetrating showers,

\* In 1947 two flights were made in which sixfold coincidences between T, M, B were recorded with and without discharges in  $E_B$ . The results were similar to those obtained with the sevenfold set, and the mean apparent attenuation length deduced was 117 g/cm<sup>2</sup>. These results were communicated by Professor P. M. S. Blackett to the Cracow Conference, 1947.



but little change in that of extensive penetrating showers. In our experiments two blocks of lead were mounted on horizontal rails so that they could be moved from fairly remote positions to positions directly above T. During flights the blocks were moved from one position to the other every four minutes. The

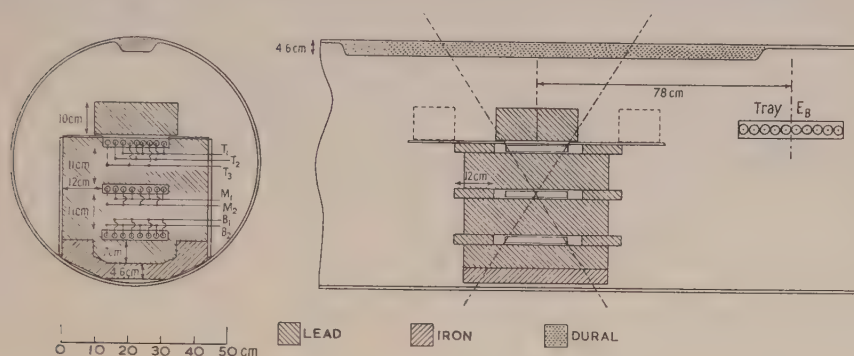


Fig. 1. The penetrating shower detector.

difference due to the lead, in the rate of P events unaccompanied by discharges in  $E_B$ , is expected to be due almost entirely to local penetrating showers. The apparatus was placed inside a duralumin case (a bomb case) and carried in the bomb bay of an R.A.F. Mosquito aeroplane.

### § 3. EXPERIMENTAL RESULTS

Three flights were made in February 1948: the aircraft climbed as rapidly as possible and flew at constant altitude on an E-W line, the average geomagnetic latitude being  $56^\circ$  N.

The sea-level rates used for comparison were corrected for casual coincidences and for triple-knock-on events (Jánossy 1942). It was found that the altitude increase of (P,  $E_B$ ) events was about the same as that of all sevenfold coincidences, and since it seemed unlikely that local and extensive penetrating showers should show the same altitude variation, a cause was sought. It seemed possible that penetrating showers produced in the aircraft structure, and especially in the fuselage petrol tanks above the bomb bay, might discharge the tray  $E_B$  as well as the sevenfold set. Four more flights were therefore made in November 1949 with additional unshielded counter trays in the rear compartment of the aircraft, remote from the P set and separated from the outer air only by a thin layer of plywood.

Two of these trays  $E_I$ ,  $E_{II}$  each contained three counters each of active area  $119 \text{ cm}^2$  and one half-size counter of  $60 \text{ cm}^2$ . Tray  $E_{III}$  contained seven large and three half-size counters. In order to obtain information about extensive penetrating showers the discharges of all these counters were recorded separately in a neon lamp hodoscope, whenever they were coincident with a master pulse from the sevenfold P set.

In the flights of this third series there was no petrol in the tanks above the bomb bay. The results were in good agreement with those of the second series. The large altitude increase of (P,  $E_B$ ) events was confirmed, and a similar increase was found for the showers which discharged the distant trays  $E_I$ ,  $E_{II}$ ,  $E_{III}$  as well as the P set. The results of the two series are combined in table 1, and the data

Table 1. Mean Hourly Counting Rates obtained with the Sevenfold Coincidence Set

Altitude (ft.)	Sevenfold coincidences (P)	Coincidences (P, E <sub>B</sub> )	Coincidences (P, E <sub>R</sub> )	Coincidences (P, E <sub>I II III</sub> )	Extensive penetrating showers (P, E)	Local penetrating showers (P-E)	Transition difference of local showers
Sea level	0.094 ± 0.006 (225)	0.024 ± 0.004 (50)	0.017 ± 0.003 (28)	0.008 ± 0.002 (13)	0.026 ± 0.004	0.067 ± 0.006	
23 000 ft.	23.9 ± 2.9 (69)	6.2 ± 1.5 (18)	6.2 ± 2.2 (8)	3.1 ± 1.6 (4)	6.8 ± 1.6	17.1 ± 2.4	
27 000 ft.	54.3 ± 5.3 (104)	13.5 ± 2.7 (26)	8.9 ± 4.0 (5)	8.9 ± 4.0 (5)	14.3 ± 2.9	39.9 ± 4.6	
30 000 ft.	58.2 ± 7.0 (69)	11.7 ± 3.2 (14)	5.7 ± 2.2 (7)	1.7 ± 1.2 (2)	13.2 ± 3.4	45.0 ± 6.1	
33 500 ft.	81.2 ± 6.5 (154)	11.3 ± 2.5 (22)	5.8 ± 3.5 (3)	1 count in 0.49 h	12.2 ± 2.7	68.9 ± 6.0	
Sea level	0.214 ± 0.009 (655)	0.043 ± 0.005 (91)	0.023 ± 0.003 (45)	0.009 ± 0.002 (18)	0.050 ± 0.005	0.164 ± 0.008	0.097 ± 0.010
23 000 ft.	36.8 ± 3.5 (111)	5.9 ± 1.4 (18)	1 count in 1.42 h	No count in 1.42 h	6.3 ± 1.5	30.5 ± 3.2	13.4 ± 4.0
27 000 ft.	70.8 ± 6.3 (128)	10.4 ± 2.4 (19)	1 count in 0.42 h	1 count in 0.42 h	11.2 ± 2.6	59.7 ± 5.7	19.7 ± 7.3
30 000 ft.	111.0 ± 9.7 (131)	15.0 ± 3.6 (18)	8.1 ± 2.7 (10)	1 count in 1.18 h	16.3 ± 3.8	94.7 ± 8.9	49.6 ± 10.8
33 500 ft.	142.8 ± 8.9 (258)	16.2 ± 3.0 (30)	1 count in 0.48 h	No count in 0.48 h	17.1 ± 3.3	125.7 ± 8.3	56.8 ± 10.2

Upper set of results  $\Sigma=0$ ; lower set of results  $\Sigma=10$  cm Pb.(P, E<sub>R</sub>) denotes coincidences between the P set and one or more of the trays E<sub>I</sub>, E<sub>II</sub>, E<sub>III</sub>.(P, E<sub>I II III</sub>) denotes coincidences between the P set and all three trays E<sub>I</sub>, E<sub>II</sub>, E<sub>III</sub>.(P, E) denotes showers discharging the P set and one or more of the unshielded trays E<sub>B</sub>, E<sub>J</sub>, E<sub>II</sub>, E<sub>III</sub>.

(P-E) denotes showers discharging the P set but no unshielded tray.



on local penetrating showers are discussed below. The results on extensive showers will be treated elsewhere.

In fig. 2 the hourly rates of events, P, P-E and the transition difference (P-E with 10 cm lead)-(P-E with no lead) are plotted logarithmically against the atmospheric depth. In each case the variation is well represented by an

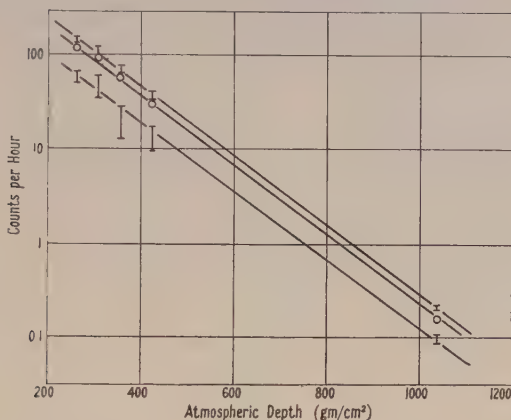


Fig. 2.  
Top curve : P events  
Middle curve : P-E events } 10 cm lead.  
Bottom curve : Transition difference.

exponential law. The best-fit attenuation lengths for the various events, calculated by least squares, are shown in table 2.

Since the events (P, E) are a small and nearly constant fraction of all P events, the fraction of the P events due to extensive penetrating showers which fail to discharge the unshielded trays may also be taken as constant over the altitude range with which we are concerned. The altitude variation of events P-E may thus be taken as representing closely that of single fast nucleons.

Table 2. Apparent Attenuation Lengths (in g/cm² of air)

Altitude range	$\Sigma=0$		$\Sigma=10$ cm Pb		Transition difference
	P	P-E	P	P-E	
33 500 ft.-sea level	$112.0 \pm 1.5$	$110.4 \pm 1.8$	$118.0 \pm 1.1$	$115.8 \pm 1.2$	$120.5 \pm 3.2$

A correction should be applied to the result because we do not measure the attenuation of a parallel beam of nucleons. We assume cosmic-ray particles are incident isotropically on the top of the atmosphere and that fast secondary nucleons preserve the direction of the primary. The intensity of fast nucleons at depth  $x$  in the atmosphere at an angle  $\theta$  to the vertical is given by  $I(x, \theta) = I(x \sec \theta, 0) = A \exp(-\mu x / \cos \theta)$  assuming exponential absorption. If the detector has an angular variation of sensitivity  $P(\theta)$  for penetrating showers formed by an incident particle making an angle  $\theta$  with the vertical, the rate of local penetrating showers recorded at a depth  $x$  is

$$R(x) = \int_0^{\pi/2} \exp\left(\frac{-\mu x}{\cos \theta}\right) P(\theta) \sin \theta d\theta.$$

Since it is not possible to calculate  $P(\theta)$  for a given detector it was determined experimentally in a sea-level experiment. The bomb case containing the P set was rotated about its horizontal axis and the counting rate was determined for  $30^\circ$  and  $50^\circ$  rotation. Since any fast nucleons at sea level must be incident nearly vertically,  $P(\theta)$  is determined directly in this way. The angular sensitivity of the P set is approximately represented by  $P(\theta) = \cos \theta$  for the set without the movable lead blocks and by  $P(\theta) = \cos^2 \theta$  for the set with the blocks.

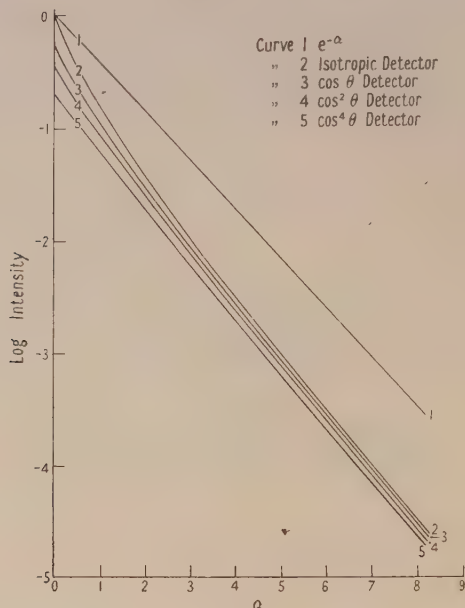


Fig. 3. Altitude response curves for various detectors.

The angular variation of the difference (lead in—lead out) is well represented by  $P(\theta) = \cos^4 \theta$ . It is reasonable on geometrical grounds that the angular dependence should be greater for the showers produced in the 10 cm lead blocks than for other showers. We now evaluate  $R(\theta)$  for the three cases.

(i) No lead blocks,  $P(\theta) = \cos \theta$ .

Writing

$$\frac{\mu x}{\cos \theta} = \frac{a}{\cos \theta} = z$$

$$\begin{aligned} R(x) \propto R(a) &= \frac{1}{2} e^{-a} (1 - a) - \frac{1}{2} a^2 \int_0^a \frac{e^{-z}}{z} dz \\ &= \frac{1}{2} e^{-a} (1 - a) - \frac{1}{2} a^2 \text{Ei}(-a), \end{aligned}$$

where  $\text{Ei}(a)$  is the exponential integral.

(ii)  $\Sigma = 10$  cm lead (blocks in place),  $P(\theta) = \cos^2 \theta$ .

$$R(a) = \frac{1}{6} e^{-a} (2 - a + a^2) + \frac{1}{6} a^3 \text{Ei}(-a).$$

(iii) The transition difference  $P(\theta) = \cos^4 \theta$ .

$$R(a) = e^{-a} \left( \frac{1}{5} - \frac{1}{20} a + \frac{a^2}{60} - \frac{a^3}{120} + \frac{a^4}{120} \right) + \frac{a^5}{120} \text{Ei}(-a).$$

The values of  $R(a)$  are plotted logarithmically against  $a$  in fig. 3, together with  $R(a)$  for a detector of uniform angular sensitivity. The P set thus follows



curves 3-5 instead of curve 1, the exponential for a parallel beam of particles. (Over the range of depths ( $a=2.5$  to 8) with which we are here concerned curves 3-5 are nearly exponential.) The 'apparent' attenuation lengths deduced from the experimental curves are clearly shorter than the 'true' attenuation length for a parallel beam. Over the range considered the corrections to be applied are +16% for an isotropic detector, +14% for a ' $\cos\theta$ ' detector, +12% for a ' $\cos^2\theta$ ' detector and +10% for a ' $\cos^4\theta$ ' detector.

On making the appropriate corrections we find the following values for the true attenuation length:

$$\lambda = 126 \pm 2 \text{ g/cm}^2 \text{ from P-E with no lead blocks.}$$

$$\lambda = 130 \pm 1.3 \text{ g/cm}^2 \text{ from P-E with 10 cm lead.}$$

$$\lambda = 132 \pm 3.5 \text{ g/cm}^2 \text{ from the transition difference.}$$

It will be observed that with the correction for inclined primaries the three values of  $\lambda$  are in much better agreement than the uncorrected values.

The most probable value for the attenuation length of fast nucleons in air is  $129 \pm 2 \text{ g/cm}^2$  where the estimated error allows for statistical fluctuations and the uncertainty of  $P(\theta)$ .

#### § 4. COMPARISON WITH THE RESULTS OF OTHER WORKERS

While preparations were being made for the third series of flights, Tinlot (1948 a, b) reported measurements of penetrating showers at aeroplane altitudes, mountain altitudes and sea level. At first sight it might appear that our final result for the attenuation length of fast nucleons in air ( $129 \pm 2 \text{ g/cm}^2$ ) is significantly higher than the frequently quoted value obtained by Tinlot ( $118 \pm 2 \text{ g/cm}^2$ ). In deriving the latter value no distinction was made between extensive penetrating showers and local penetrating showers, and no correction was made for inclined primaries. Although it is necessary in principle to separate the two types of penetrating shower, it turns out that the rate of extensive penetrating showers is so small, and varies with altitude in such a way, that the lack of separation is not very serious (see table 2). The difference between the two results is mainly due to the correction for inclined primaries. Since Tinlot's detector was geometrically very similar to the one used here with  $\Sigma=10 \text{ cm}$  of lead, his result may be compared with the apparent attenuation length applicable to coincidences P for  $\Sigma=10 \text{ cm Pb}$  (table 2), i.e.  $118.0 \pm 1.1 \text{ g/cm}^2$ . The agreement here is very satisfactory.

From measurements with a large sevenfold coincidence set at sea level and at the Jungfraujoch (3457 m) George and Jason (1950) deduce an apparent attenuation length for the primaries of local penetrating showers  $\lambda=114 \pm 10 \text{ g/cm}^2$ .

Using a much less selective type of detector, Walsh and Piccioni (1950) found an apparent attenuation length of  $112 \pm 2 \text{ g/cm}^2$ . By assuming that their detector was not direction sensitive they concluded that the true attenuation length was  $\lambda=140 \text{ g/cm}^2$ . The correction which they make for the effect of inclined primaries seems rather high. However, although not stated explicitly, it may be that Walsh and Piccioni derived their value only from measurements made above 25000 ft., since at low altitudes many knock-on events produced by single mesons were recorded. A higher correction would then be applicable.

## ACKNOWLEDGMENTS

The author wishes to thank Professor P. M. S. Blackett for his interest in this work and for providing the necessary facilities. He is indebted to Dr. H. J. J. Braddick for his continued interest and for assistance at various times. Thanks are due to the Air Ministry for permission to make these flights. The author is especially grateful to Group-Captain J. C. MacDonald, then Officer Commanding, Coningsby R.A.F. Station, and to the officers, air crews and ground staff of 109 and 139 Squadrons for their keen co-operation.

## REFERENCES

- BROADBENT, D., and JÁNOSSY, L., 1947, *Proc. Roy. Soc. A*, **190**, 497.  
 GEORGE, E. P., and JASON, A. C., 1950, *Proc. Phys. Soc. A*, **63**, 1081.  
 JÁNOSSY, L., 1942, *Proc. Roy. Soc. A*, **179**, 361.  
 TINLOT, J., 1948 a, *Phys. Rev.*, **73**, 1476; 1948 b, *Ibid.*, **74**, 1197.  
 WALSH, T. G., and PICCIONI, O., 1950, *Phys. Rev.*, **80**, 619.  
 WATAGHIN, G., 1947, *Phys. Rev.*, **71**, 453.

## The Calculation of Scattering Amplitudes \*

By G. J. KYNCH

Department of Mathematical Physics, University of Birmingham†

*MS. received 26th May 1952*

**ABSTRACT.** In two earlier papers a differential equation was given for the asymptotic phases required in the two-body scattering problem. The method implied a resolution of the wave function into eigenfunctions of the orbital or total angular momentum as the potential was central or non-central. This feature can be avoided and in this paper a integro-differential equation is given for the total scattering amplitude corresponding to a given incident wave. It can be applied to any scattering or ionization problem, single or multiple, where no particles are bound after scattering which were not bound before. The method is applicable to the Schrödinger or Dirac equations.

If used with time-dependent equations the usual time-dependent perturbation theory results, owing to the apparent necessity of adhering to a definite time distinction between initial and final states. The same is true for the quantized field equations in the Heisenberg representation.

### § 1. INTRODUCTION

THE importance of scattering problems in atomic and nuclear physics has led to a wide selection of theoretical methods of handling them. The general problem is to find the probability or cross section that a system of particles which starts in a state A should end in a state B after a reaction or collision process. The state A is completely described by the states of the individual parts and their directions of motion and energies. The same information is needed to describe the state B.

The wave equation gives us rather more information than this; it leads to the scattering amplitude  $f(A:B)$  for the process, and while this gives the cross section, which is proportional to  $|f|^2$ , the amplitude  $f$  also contains the relative

\* This paper forms a continuation of two papers entitled "The Two-Body Scattering Problem with Non-Central Forces", published in *Proc. Phys. Soc. A*, 1952, pp. 83, 94.

† Now at University College of Wales, Aberystwyth.



phases of the waves. This is as it should be, since this extra information is needed to obtain predictions on more complicated experiments on polarization, double scattering, and so on. In fact, the scattering amplitude  $f(A:B)$ , given for all  $A$  and  $B$ , can be in principle determined by scattering experiments and is the most that can be learned from them. This was first clearly stated by Heisenberg, who introduced his now-famous  $S$ -matrix theory, this matrix being simply related to  $f$  in the matrix formulation of quantum mechanics.

One very useful method of calculating the scattering amplitude is a perturbation theory based on an expansion in powers of an interaction constant, especially when the first-order term by itself is adequate. However, this is not true for the collisions between nuclei or nuclear particles, where the first-order term or Born approximation, as it is usually called, is not accurate enough even at high energies. The inclusion of several terms of higher order is then necessary to improve the accuracy sufficiently. In polarization experiments, for example, Born approximation often leads to the answer that there is no effect at all. In problems of nuclear solutions it is more usual to make an expansion in terms of angular momenta and obtain an exact solution. This method is quite efficient if only a few eigenvalues of the angular momentum are needed. It is probably seen at its best in the theory of nuclear reaction, where, coupled with the idea of the compound nucleus, an immense range of results have been successfully interpreted. In the two-body problem it is cumbersome when tensor forces are introduced, and the three-body problem is even worse.

In these circumstances it seemed worth while to attempt a generalization of a method recently published (Kynch 1952 a, b, to be referred to as I and II) for the two-body problem. A very brief account of this method illustrates some features of the more general method now being given and the reasons why it was chosen. We expressed the wave function for a given total angular momentum as a matrix  $\psi = Yua, r$  where  $u = u_1 + u_2 S$ ;  $Y$  is an angular function,  $u_1$  and  $u_2$  are free wave functions,  $a(r)$  is an amplitude and  $S(r)$  is the phase-matrix whose limit as  $r \rightarrow \infty$  is effectively the  $f(A:B)$  of the problem. A suitable definition of  $a(r)$  leads to an equation for  $S$ :

$$S(R) = \int_0^R u(r) V(r) u(r) dr.$$

This is an exact equation and  $S$  occurs in the integrand. Now this equation bears a strong resemblance to Born approximation and reduces to it if  $S$  is neglected on the right-hand side; also it does not contain the amplitude factor  $a(r)$ , and can be derived without introducing that factor at all. The important feature of the equation, however, for its generalization turns out to be the fact that  $S(R)$  and  $u(R)$  have a physical meaning. Since  $S(\infty)$  is the phase-matrix for the actual potential, then  $S(R)$  is the phase-matrix for the same potential cut-off outside a sphere of radius  $R$ , and  $u(R)$  is with constant  $S$  the free wave function outside this sphere. By an examination of Dirac's method (1932) of deriving Born approximation as a perturbation theory we were led to a suitable equation which can be applied not only to individual angular momentum but to a scattering problem as a whole.

Using the stationary state method we use an extension of Born approximation to calculate the change in the scattering amplitude  $f(A:B)$  due to a small change  $dV$  in an existing potential  $V$ . Except for constants this is

$$df(A:B) = \int \psi(-B) dV \psi(A) d\tau,$$

where  $\psi(A)$  is the *total* wave function of that state of the system with interaction  $V$  where its constituents are incidents in state  $A$ , and can emerge after scattering in various ways, including  $B$ . Let  $\psi(-B)$  be the *total* wave function describing the system incident in the state  $(-B)$ , i.e. the same as  $B$  but with the direction of motion of the various parts reversed, and scattered in various ways, one of them being  $(-A)$ . Notice that, except for the incident waves,  $\psi(A)$  and  $\psi(-B)$  contain only outgoing waves. Thus  $\psi(-B)$  and  $\psi^*(B)$  are not the same, as  $\psi^*(B)$  contains the incident wave plus incoming waves (cf. § 2).

This equation is not by itself sufficient to give a practical method of calculation. It is combined with a method of assembling the potential, piece by piece, so that at every stage  $\psi(A)$  and  $\psi(-B)$  are calculated from the asymptotic forms using the wave equation either with no potential or with a simple potential. This means that, apart from the incident wave and these simple solutions, we derive equations which only contain the scattering amplitudes  $f(A: B)$ .

In view of the generality of the problem it is not to be expected that the resulting equations are simple, or that their solution is easy, but we can show by suitable examples that our equation does lead to considerable simplifications.

At this stage in fact we try to establish three advantages of the method. First we are able to derive new results, e.g. equations for the total scattering amplitude in the two-body problem. Second, when we discuss such problems as the scattering of electrons by atoms, we see that we have a simple extension of methods used previously (Mott and Massey 1949), which helps to make clear the approximations made. The reason for this lies in the third advantage of our procedure, that the functions  $\psi(A)$  and  $\psi(-B)$  are determined directly from the asymptotic forms and the scattering amplitudes. If any process is neglected on physical grounds, for instance that it makes little difference to the cross section, then a term of a known form is neglected, so that the error can be estimated directly.

At the moment the field of application does not include all bound state problems. Where the grouping of the incoming particles into atoms or nuclei is different from that of the outgoing particles, it can be used only to discuss the effect of any additional interactions which come into play.

Equation (1) is very similar to equations given by Schwinger (1951). In fact, if we apply our method to time-dependent equations we obtain just his equations (2.14) and (2.129). For this reason we have not discussed the quantized fields equations at all in this paper, although most of the results for example on the  $S$ -matrix can be derived very quickly in the Heisenberg representation. In § 5, non-relativistic time-dependent perturbation theory is mentioned briefly.

## § 2. THE SCATTERING OF A PARTICLE

### (i) *Generalization of Born Approximation*

The general method to be adopted is illustrated by the scattering of a particle by a centre of force. The wave equation is written

$$(\nabla^2 + k^2)\psi = V\psi, \quad \dots\dots(2.1)$$

where  $k^2$  is the energy and  $V$  the potential, in suitable units. In the method of stationary states, to obtain the Born approximation we write  $\psi(k_2) = \exp(ik_1 \cdot r) + \psi_1(k_1)$  where  $\exp(ik_1 \cdot r)$  represents an incoming plane wave, and solve the resulting equation for  $\psi_1$  with the condition that it only contains



outgoing waves, i.e. for large values of  $r$  it can be written

$$\psi_1 \sim f(k_1: r) \frac{\exp(ikr)}{r}, \quad \dots\dots(2.2)$$

It should be borne in mind that in this and later formulae the function  $f$  depends only on the *direction*  $k_1$  of the incident wave and the *direction* of  $r$ , but not on their magnitudes. To first order in the potential we obtain the Born approximation

$$f(k_1: k_2) = -\frac{1}{4\pi} \int \exp(-ik_2 \cdot r) V(r) \exp(ik_1 \cdot r) dv. \quad \dots\dots(2.3)$$

Let us now construct an analogous formula when there is a small change in the potential. Let  $\psi(k_1)$  be the correct wave function for an incoming plane wave  $\exp(ik_1 \cdot r)$  with a potential  $V$ , and  $\psi(-k_2)$  be the correct solution with the same potential and an incoming wave  $\exp(-ik_2 \cdot r)$

$$\left. \begin{aligned} \psi(k_1) &\sim \exp(ik_1 r) + f(k_1: r) \frac{\exp(ikr)}{r}, \\ \psi(-k_2) &\sim \exp(-ik_2 \cdot r) + f(-k_2: r) \frac{\exp(ikr)}{r}. \end{aligned} \right\} \quad \dots\dots(2.4)$$

First, since  $\psi(k_1)$  and  $\psi(-k_2)$  satisfy the same wave equation, we notice that, in a sphere of radius  $R$

$$\begin{aligned} 0 &= \int [\nabla^2 \psi(-k_2) \psi(k_1) - \psi(-k_2) \nabla^2 \psi(k_1)] dv \\ &= \int \left( \frac{\partial \psi(-k_2)}{\partial r} \psi(k_1) - \psi(-k_2) \frac{\partial \psi(k_1)}{\partial r} \right)_{r=R} R^2 d\Omega. \end{aligned}$$

We proceed in the same way as Dirac (1932), using the asymptotic form (2.4) for large value of  $R$ . In the limit  $R \rightarrow \infty$  we find that

$$f(k_1: k_2) = f(-k_2: -k_1). \quad \dots\dots(2.5)$$

In fact the non-zero terms arising from  $f(k_1: r)$  are of the form

$$\begin{aligned} \lim_{R \rightarrow \infty} \int f(k_1: r) \left\{ \frac{\partial}{\partial r} (\exp(-ik_2 \cdot r) \frac{\exp(ikr)}{r}) - \exp(-ik_2 \cdot r) \frac{\partial}{\partial r} \left( \frac{\exp(ikr)}{r} \right) \right\}_{r=R} R^2 d\Omega \\ = 4\pi f(k_1: k_2). \quad \dots\dots(2.6) \end{aligned}$$

It is now easy to prove that an increase  $dV(r)$  in the potential results in an increase in the scattering amplitude

$$df(k_1: k_2) = -\frac{1}{4\pi} \int \psi(-k_2) dV \psi(k_1) dv. \quad \dots\dots(2.7)$$

Let  $\psi' = \psi + d\psi$  be the correct solution for the potential  $V' = V + dV$ . Then the wave equations give

$$\begin{aligned} \int_R \psi'(-k_2) dV \psi(k_1) dv &= \int [\nabla^2 \psi'(-k_2) \psi(k_1) - \psi'(-k_2) \nabla^2 \psi(k_1)] dv \\ &= \int [\nabla^2 d\psi(-k_2) \psi(k_1) - d\psi(-k_2) \nabla^2 \psi(k_1)] dv. \end{aligned}$$

Since asymptotically  $d\psi(-k_2) = df(-k_2: r) \exp(ikr)/r$  we derive

$$\int \psi'(-k_2) dV \psi(k_1) dv = -4\pi df(-k_2: -k_1) = -4\pi df(k_1: k_2).$$

In the limit as  $dV \rightarrow 0$  this goes into eqn. (2.7).

## (ii) The Method of Assembled Potentials

We now establish a method which enables the calculation of  $f(k_1: k_2)$  for any potential  $V(r)$ . This is done by choosing  $V$  and  $dV$  in our equations so that the

integral only extends over a very small region in space, and in that region  $\psi(k_1)$  and  $\psi(-k_2)$  are determined by the simple equation  $(\nabla^2 + k^2)\psi = 0$ .

Let  $\sigma$  and  $\sigma'$  be two closed surfaces such that  $\sigma'$  encloses  $\sigma$  and let us assume that

$$\begin{aligned} V &= V(r) \text{ inside } \sigma, & V &= 0 \text{ outside } \sigma, \\ V + dV &= V(r) \text{ inside } \sigma', & V + dV &= 0 \text{ outside } \sigma'. \end{aligned}$$

Moreover let  $\psi_\sigma$  be the solution for the potential  $V$  and  $\psi_{\sigma'}$  the solutions for the potential  $V + dV$  such that  $\psi_\sigma(k_1)$  has the form (2.4). Then eqn. (2.7) gives

$$-\frac{1}{4\pi} \{f_{\sigma'}(k_1 : k_2) - f_\sigma(k_1 : k_2)\} = \int_\sigma \psi_{\sigma'}(-k_2) dV \psi_\sigma(k_1) dv.$$

In the limit as  $\sigma' \rightarrow \sigma$  this gives a differential equation for  $f_\sigma$  where the right-hand side involves a surface integral, and the  $\psi_\sigma$  are only required on the surface of  $\sigma$ . But on the surface of  $\sigma$  and outside they are determined by the free-space wave equation and the asymptotic form. Thus the only unknown in the equation is  $f_\sigma$ .

In practice it seems to be most convenient to choose as the surface  $\sigma$  a set of spheres, since  $\psi_\sigma$  assumes a simple form. Thus if  $\sigma$  is a sphere of radius  $R$  and  $\sigma'$  a sphere of radius  $R + dR$  we find that eqn. (2.7) becomes, in the limit  $dR \rightarrow 0$ ,

$$-\frac{1}{4\pi R^2} \frac{df_R(k_1 : k_2)}{dR} = \int \{\psi_R(-k_2) V(r) \psi_R(k_1)\}_{r=R} d\Omega, \dots\dots (2.8)$$

the integral extending over all surface elements  $dS = R^2 d\Omega$ ,  $d\Omega = \sin \theta d\theta d\phi$  of the sphere.

This can be transformed into an explicit equation for  $f_R(k_1 : k_2)$  using the solutions of the wave equation in spherical harmonics.

A far neater form is obtained by using the integral representation of the solution of the wave equation

$$\psi_R(k_1) = \exp(ik_1 \cdot r) + \frac{k^2}{2\pi^2} \int_{-\infty}^{+\infty} dp \int d\Omega_p p^2 \exp(ip \cdot r) \frac{f(k_1 : p)}{k^2 - p^2} \dots\dots (2.9)$$

the integral over  $p$  being taken along the  $p$ -axis from  $-\infty$  to  $+\infty$  in the complex plane above the pole at  $p = -k$  and below the pole at  $p = +k$ .

The resulting equation for  $f_R$  is  $(dp^\dagger = p^2 dp d\Omega_p)$

$$\begin{aligned} -\frac{1}{4\pi R^2} \frac{df_R(k_1 : k_2)}{dR} &= V(k_1 : k_2) + \frac{k^2}{2\pi^2} \int \frac{f_R(k_1 : p) dp^\dagger V(p : k_2)}{k^2 - p^2} \\ &+ \frac{k^2}{2\pi^2} \int \frac{V(k_1 : p) dp^\dagger f_R(p : k_2)}{k^2 - p^2} \\ &+ \left(\frac{k^2}{2\pi^2}\right)^2 \int \frac{f_R(k_1 : p)}{k^2 - p^2} dp^\dagger V(p : p') dp'^\dagger \frac{f_R(p' : k_2)}{k^2 - p'^2}, \end{aligned} \dots\dots (2.10)$$

where  $V(p : p') = \int \exp(-ip' \cdot R) V(R) \exp(ip \cdot R) d\Omega_R$ .\*

Two points may be mentioned. First the  $V(p : p')$  are not the matrix-elements of  $V$  in a momentum representation; the equation cannot be used therefore with non-local potentials. The second point is that although the last integral is convergent it leads to angular  $\delta$ -functions if the integrations over  $p$  and  $p'$  are carried out before the integrations over angles, as it is usually more convenient to do.

This equation is immediately available for the two-body problem, and in fact any problem of the collision of two particles where only elastic scattering occurs. It can also be applied to multiple scattering problems.

\* See author's correction added in proof on p. 764.



(iii) *Inclusion of Spin and Exchange*

With non-central forces it is necessary to include spin in our equations. This is quite trivial. We write

$$\psi_m(k_1) \sim \exp(ik_1 \cdot r) \chi_m + \sum f_{mm'} k(1:r) \frac{\exp(ikr)}{r} \chi_{m'},$$

where  $\chi_m$  form a complete set of spin-functions, e.g. for n-p scattering it is convenient to choose for  $\chi_m$  the triplet and singlet functions. The eqn. (2.10) is now replaced by a set of equations for the elements  $f_{mm',R}$ . It is perhaps easier to arrange the  $\psi_m$  as a column matrix, so that  $f_{mm'}$  is also a matrix. This fits in better with our general exposition.

If the potential is of an exchange type, this character is taken into account in evaluating  $V(p:p')$ . It occurs nowhere else.

(iv) *A Lemma on Asymptotic Wave Functions*

Before we consider a more general system it is necessary to examine an essential step in the calculations which is not obvious for a general system although it may be so for a two-body system. This is the statement that the asymptotic form of the wave function determines its values elsewhere and, in particular, at those points where  $dV$  is not zero. This can be demonstrated with the aid of the following lemma:

*Lemma.* If  $\phi$  is such that in the region outside a sphere  $\sigma$  (i)  $(\nabla^2 + k^2)\phi = 0$  outside  $\sigma$ , (ii)  $\lim_{r \rightarrow \infty} (\partial\phi/\partial r - ik\phi) = 0$ , (iii)  $\phi$  has assigned value  $\phi_\sigma$  on the surfaces  $\sigma$ , not all zero, then, as  $r \rightarrow \infty$ ,  $\phi \rightarrow g(\theta, \phi)e^{ikr}/r$  where  $g$  is not zero. The proof of this lemma is simple. Outside the surfaces  $\sigma$  the solution  $\phi$  can be expressed as a series  $r\phi = e^{ikr} \sum_n g_n(\theta, \phi) r^{-n}$  where  $r$  is the polar distance from any point. Because of (i) the  $g_n$  satisfy the recurrence relation

$$2ik \sin^2 \theta (n+1) g_{n+1} = \left\{ \sin \theta \frac{\partial}{\partial \theta} \left( \sin \theta \frac{\partial}{\partial \theta} \right) + \frac{\partial^2}{\partial \phi^2} + n(n+1) \right\} g_n.$$

Thus, if  $g_0 = g = 0$ , then  $\phi = 0$ .

It follows from this proof that there cannot be two solutions of the equation  $(\nabla^2 + k^2)\psi = 0$  satisfying (i) and (ii) with the same asymptotic form, but having different values on the surfaces  $\sigma$ , because their difference would satisfy (i) and (ii) and have  $g = 0$ , so that their difference would be zero.

This result can be extended easily to more than three dimensions.

§ 3. A GENERAL SCATTERING PROBLEM

The calculation of the previous section can be extended at once to calculate the scattering amplitude for the process where  $n$  particles A, B, . . . N with momentum  $k_a, k_b, \dots k_n$  come together and are scattered by a potential  $V$  and emerge with momenta  $k'_a, k'_b, \dots k'_n$ . Since bound states are considered later we shall assume that none are possible. We neglect spin since its inclusion merely involves an extra suffix. The potential  $V$  includes interactions between the particles and external forces if they occur, i.e.

$$\{(\nabla_a^2 + \nabla_b^2 + \dots + \nabla_n^2) + K^2\} \psi = V \psi, \quad \dots (3.1)$$

where  $K^2 = k_a^2 + \dots + k_n^2$ .

The calculation is made in a  $3n$ -dimensional space. If we assemble the potential in the same way as before using a  $(3n-1)$ -dimensional surface  $\sigma$ , then our equation for  $f$  is

$$-df_\sigma(k:k') = C \int \psi_\sigma(-k') V \psi_\sigma(k) d\sigma, \quad \dots (3.2)$$

where  $f_\sigma(k:k') = f_\sigma(k_a, k_b, \dots, k_n; k'_a, \dots, k'_n)$ ;  $d\sigma$  represents a volume element between  $\sigma$  and  $\sigma'$ ,  $C$  is a constant depending on  $n$ ,  $K$  and the rest of the notation is obvious. Many-body potentials cause no difficulty in this formulation.

The proof that  $\psi_\sigma$  is determined on the surface  $\sigma$  by its asymptotic form

$$\psi_\sigma(k) \sim \exp\{i(k_a.r_a + \dots + k_n.r_n)\} + f_\sigma(k:R)e^{iKR}/R^{(3n-1)/2}, \quad \dots (3.3)$$

where  $R$  is the distance from the origin in the  $3n$ -dimensional space, follows at once from the lemma of the last section.

This method could be used, for example, in collisions between three nuclear particles under their mutual interactions. The centre of gravity would first be eliminated, leaving only two coordinates  $r_a$  and  $r_b$  chosen so that the kinetic energy term in the Hamiltonian is  $(\nabla_a^2 + \nabla_b^2)$ . The potential would be expressed in terms of  $R$  and suitable angular coordinates.

Although this procedure shows the validity of the method, one objection at least can be raised which suggests that calculations should be made in other ways. Since potentials usually arise from two-body interactions, the integrations in (3.2) are bound to introduce a number of delta-functions corresponding to one, two or more particles not being scattered at all. Thus we could better express the asymptotic form (3.3) in a form which recognizes this explicitly and uses the individual  $r_a, r_b$ , etc.

To make this clear we choose an even simpler example of particles A and B scattered by an external potential  $V = V_a(r_a) + V_b(r_b)$  with no interaction between them. It is clear that either A or B or both can be scattered, and that we write

$$\begin{aligned} \psi_\sigma(k) \sim & \exp\{i(k_a.r_a + k_b.r_b)\} + f_\sigma(k_a:r_a) \frac{\exp(ik_a.r_a)}{r_a} \exp(ik_b.r_b) \\ & + f'_\sigma(k_b.r_b) \frac{\exp(ik_b.r_b)}{r_b} \exp(ik_a.r_a) + f''_\sigma(k_a, k_b:r_a, r_b) \frac{\exp(ik_a.r_a)}{r_a} \frac{\exp(ik_b.r_b)}{r_b}. \end{aligned}$$

This is correct, of course, since the wave equation is separable and  $f''_\sigma = f'_\sigma f'_\sigma$ .\*

The three-body problem is not considered further in this section for the following reasons. In practice only two bodies collide so that we must consider the problem of bound states. It is true that  $S$ -matrix theory suggests that an analytical continuation of the results to complex relative momenta should give the required answers; the only reply to this is that the behaviour of the  $S$ -matrix during this process is still a matter at best of controversy and at worst of complete ignorance.

Three further generalizations are useful. The first concerns coulomb potentials. It is possible to include some potentials on the left-hand side of eqn. (3.1), such as a coulomb term. This requires the use of the corresponding coulomb solutions instead of the plane waves  $\exp(ik_1.r)$  and outgoing waves  $\exp(ikr)/r$  in the asymptotic form of  $\psi$  and the use of the wave equation with a coulomb term in the derivation of  $\psi$  on a hypersurface from the asymptotic form. It must be possible, and the analytical difficulties are not enormous. The second suggestion is that  $\psi$  can be obtained in an integral representation in terms of its asymptotic form, and although the completely general expression has not been found, many terms in the integral equation for the  $f_\sigma$  can certainly be expressed as in (2.10) and it seems likely that the rest can also.

Finally the occurrence of identical particles causes no difficulty. If two particles are identical the calculation proceeds as above, and at any stage the

\* Incidentally, this can be proved using only eqn. (3.1).



correct solution is obtained by making the solution antisymmetrical in the two particles, if they have spin  $\frac{1}{2}$ , or symmetrical otherwise.

#### § 4. BOUND STATES

As a further illustration we consider such problems as the scattering of an electron by a hydrogen atom. When the nuclear motion is ignored, this is in effect the scattering of two interacting particles A and B by a centre of force. The potential energy is  $V = V_a(r_a) + V_b(r_b) + V_{ab}(r_{ab})$  where  $r_a$  and  $r_b$  are distances from the centre or nucleus. The wave equation is, in suitable units

$$\nabla^2 \psi = (\nabla_a^2 + \nabla_b^2) \psi = (V - E) \psi. \quad \dots (4.1)$$

The two particles are assumed distinct, in agreement with the remarks made at the end of § 3.

In the absence of the interaction  $V_{ab}$  this equation is separable and has solutions of the form  $\phi_m(A) \chi_n(B)$  where the solutions  $\phi_m(A)$  are a complete set of regular normalized solutions of  $(\nabla^2 + E_m) \phi_m = V_a \phi_m$  and similarly  $\chi_n(B)$  are solutions of  $(\nabla^2 + E_n) \chi_n = V_b \chi_n$ . The total energy is  $E = E_m(A) + E_n(B)$ .† Some of these states are assumed to be bound states.

When there are bound states and sufficient energy one possible process is that B collides with A, which is assumed to be in a bound state  $\alpha$ , and A is ejected leaving B in a bound state  $\beta$ . In accordance with our general procedure we consider two solutions of eqn. (4.1) of the form

$$\begin{aligned} \psi(1) &= \exp(ik_b \cdot r_b) \phi_\alpha(A) + \psi^{sc}(1), \\ \psi(-2) &= \exp(-ik_a \cdot r_a) \chi_\beta(B) + \psi^{sc}(-2), \end{aligned} \quad \dots (4.2)$$

when the incident particle B comes in from the direction  $k_b$  and A is emitted in the direction  $k_a$ . The total energy is  $E = k_b^2 + E_\alpha = k_a^2 + E_\beta$ .

The scattering amplitude which interests us is contained in the asymptotic form

$$\int \psi^{sc}(1) \chi_\beta^*(B) dv_b \sim f(\alpha, k_b; k_a, \beta) \frac{\exp(ik_a r_a)}{r_a}. \quad \dots (4.3)$$

Since  $\psi(1)$  and  $\psi(-2)$  satisfy the same wave equation,

$$\int \{\nabla^2 \psi(-2) \psi(1) - \psi(-2) \nabla^2 \psi(1)\} dv_a dv_b = 0.$$

Let  $\psi'(1) = \psi(1) + d\psi(1)$  satisfy the wave equation with a potential  $V' = V + dV$ . Then, as in deriving eqn. (2.7),

$$\int \psi(-2) dV \psi(1) dv_a dv_b = \int \{\nabla^2 \psi(-2) d\psi(1) - \psi(-2) \nabla^2 d\psi(1)\} dv_a dv_b, \quad \dots (4.4)$$

neglecting products of first-order corrections.

Because of eqn. (4.3) we expand the wave functions in terms of the complete set of functions  $\chi_n(B)$  for particle B†

$$d\psi(1) = \sum dF_m \chi_m(B), \quad \psi(-2) = \sum G_n \chi_n^*(B),$$

where  $dF_m$  and  $G_n$  are functions of  $r_a$ . Using the wave equation satisfied by the  $\chi_n(B)$ , the right-hand side of (4.4) becomes

$$\sum_m \sum_n \int [dF_m \chi_m (\nabla_a^2 + V_b - E_n) G_n \chi_n^* - G_n \chi_n^* (\nabla_a^2 + V_b - E_m) dF_m \chi_m] dv_a dv_b.$$

† To avoid difficulties in the subsequent discussion due to the asymptotic form of the wave functions when  $V_a$  and  $V_b$  are coulomb potentials we assume that they are cut off outside a radius  $r$ . The rest of the potentials is added to the term  $V_{ab}$ . This separation of the potentials into parts can be related to the screening effect of one particle A when bound to the nucleus.

‡ The expansion of  $\psi(-2)$  in terms of  $\chi_n^*$  corresponds to the change of direction of motion of B in  $\psi(-2)$ , for an unbound state, compared with the emerging waves from  $\psi(1)$ , when  $\chi_n$  is complex. For bound states we can choose real  $\chi_n$ .

The orthogonal properties of the  $\chi_m$  reduce this to a single sum

$$\sum_n \int [dF_n(\nabla_a^2 G_n) - G_n(\nabla_a^2 dF_n)] dv_a,$$

which is essentially the same as eqn. (2.6) of the previous section. Using Green's theorem and the fact that all the  $dF_m$  and  $G_n$  represent outgoing waves except  $G_\beta$  which contains in addition the incoming wave  $\exp(-ik_a \cdot r_a)$ , it reduces to a single term in  $dF_\beta$ . Now

$$dF_\beta = \int d\psi^{sc}(1) \chi_\beta^*(B) dv_b \sim df(\alpha, k_b: r_a, \beta) \frac{\exp(ik_a \cdot r_a)}{r_a}. \quad \dots\dots (4.5)$$

Consequently after some simplification we obtain

$$4\pi df(\alpha, k_b: k_a, \beta) = - \int \psi(-2) dV \psi(1) dv_a dv_b. \quad \dots\dots (4.6)$$

By an expansion of  $d\psi(-2)$  and  $\psi(1)$  in terms of the  $\phi_n(A)$  we can show that

$$df(\alpha, k_b: k_a, \beta) = df(-k_a, \beta: \alpha, -k_b) \quad \dots\dots (4.7)$$

so that if the two  $f$ 's are equal when the interaction is first included then they remain equal subsequently.

It is quite clear that this procedure applies whatever the transition to be discussed.

These equations are now transformed so as to be suitable for calculations or approximations. As an illustration let us suppose that  $E$  is greater than the ground state energies  $E_\alpha(A)$  and  $E_\beta(B)$  of  $A$  and  $B$  but less than the first excited states. Then the asymptotic form of  $\psi(1)$  and  $\psi(-2)$  are

$$\left. \begin{aligned} \psi(1) &\sim \phi_\alpha(A) \left\{ \exp(ik_b \cdot r_b) + f_{\alpha\alpha}(k_b: r_b) \frac{\exp(ik_b r_b)}{r_b} \right\} + f_{\alpha\beta}(k_b: r_a) \frac{\exp(ik_a r_a)}{r_a} \chi_\beta(B), \\ \psi(-2) &\sim \chi_\beta(B) \left\{ \exp(-ik_a \cdot r_a) + f_{\beta\beta}(-k_a: r_a) \frac{\exp(ik_a r_a)}{r_a} \right\} \\ &\quad + f_{\beta\alpha}(-k_a: r_b) \frac{\exp(ik_b r_b)}{r_b} \phi_\alpha(A), \end{aligned} \right\} \quad \dots\dots (4.8)$$

the abbreviated notation being obvious. There are three equations for  $f_{\alpha\alpha}$ ,  $f_{\beta\beta}$  and  $f_{\alpha\beta}(k_b: k_a) = f_{\beta\alpha}(-k_a: -k_b)$ .

The prescription for building up the potential rests on the fact that  $f_{\alpha\beta} = f_{\beta\alpha} = 0$  when  $V = V_a + V_b$ ; we therefore start at this point, which is quite convenient, as the wave equation is separable, and  $f_{\alpha\alpha}$  and  $f_{\beta\beta}$  can be calculated. The potential due to the interaction of  $A$  and  $B$  is now built up so that at every stage the values of  $\psi(1)$  and  $\psi(-2)$  can be determined on a certain surface from the asymptotic form and the known solutions for the separable equation with the potential  $V_a + V_b$ .

When the energy of the incident particle  $B$  becomes sufficiently large to make possible the use of the excited states of  $A$  (or  $B$ ) then additional terms must be added to the wave functions, and additional equations appear for the new scattering amplitudes.

These calculations are very similar to those previously made for the scattering of electrons by atoms, and there is no difficulty as long as  $V_{ab}$  is a repulsive potential, or, when it is attractive, not so large that particles  $A$  and  $B$  can form bound states. When we increase it up to the magnitude where a bound state first appears, a singularity appears in the direction  $r_a = r_b$  which cannot now be ignored. Our



present method breaks down and a discussion is now necessary of the nature of this singularity along the lines suggested in the previous paragraph. Such difficulties arise whenever complex particles A and B collide to give particles C, D, . . . and the potential whose effect on the scattering is under consideration happens to be responsible for the binding of any of these particles.

## § 5. THE DIRAC EQUATION AND TIME-DEPENDENT EQUATIONS

Once the method has been established there is little point in giving details of all the applications. For example, the results given in I and II can all be derived directly by the present method after resolving into separate angular momenta, or alternatively by expanding the scattering amplitude  $f(k_1:k_2)$  of eqn. (2.10).

In this section, therefore, we give a few results on other wave equations.

### (i) Dirac Equation

In II we considered an electron in an external field, using equations resolved into angular momenta. We now establish a more general result. Given the Dirac equation (the notation used is that of II and § 2)

$$\{-i\rho_1(\boldsymbol{\sigma} \cdot \nabla) + \rho_3\kappa + E\}\psi = V\psi \quad \dots\dots(5.1)$$

and its conjugate complex for  $\psi^*$  with a slightly different potential we can easily obtain

$$\int_R \psi(k_2)^* dV \psi(k_1) dv = \frac{1}{2k^2} \int_{r=R} \psi(k_2)^* (\rho_3\kappa + E) \cdot [n(\overleftarrow{\nabla} - \overrightarrow{\nabla}) - i\boldsymbol{\sigma} \cdot \mathbf{n} \times (\overleftarrow{\nabla} + \overrightarrow{\nabla})] d\psi(k_1) r^2 d\Omega,$$

where  $\mathbf{n}$  is a unit radial vector in the solid angle  $d\Omega$  and the arrows over  $\nabla$  indicate which way they operate. The second term tends to zero as  $R \rightarrow \infty$ . If the wave functions have the asymptotic forms

$$\begin{aligned} \psi(k_1) &= u_1 \exp(ik_1 \cdot r) + f(k_1:r) \frac{\exp(ikr)}{r}, \\ \psi(k_2)^* &= u_2^* \exp(-ik_2 \cdot r) + f^*(-k_1:r) \frac{\exp(ikr)}{r}, \end{aligned}$$

where  $u$  and  $f$  are spinors, the first term reduces so that

$$\begin{aligned} -2\pi u_2^* (\rho_3\kappa + E) df(k_1:k_2) &= k^2 \int \psi(k_2)^* dV \psi(k_1) dv \\ &= -2\pi df^*(-k_2:-k_1)(\rho_3\kappa + E)u_1, \quad \dots\dots(5.2) \end{aligned}$$

which reduces easily to eqn. (2.6) in the non-relativistic limit. There is also an equation analogous to (2.10). By using the simplest forms for  $u_1$  and  $u_2^*$ , and  $\rho_3$  diagonal we obtain equations for the corresponding component of the amplitude  $f$ . Moreover, with the usual restrictions on the potentials it can easily be verified that the components of  $f$  are related, as suggested in II.

### (ii) Time-Dependent Equations

Time-dependent perturbation theory considers the development of the wave function with time, due to a given perturbation. This exactly corresponds to our procedure for building up potentials. In fact, starting from the Schrödinger equation

$$\left(\nabla^2 + im \frac{\partial}{\partial t}\right) \psi = V\psi, \quad \dots\dots(5.3)$$

and proceeding as in § 2, we arrive at the equation

$$\int \psi^*(2) dV \psi(1) d\tau = im \left[ \int \psi^*(2) \psi(1) dv \right]_{t=t_1}^{t=t_2}. \quad \dots\dots(5.4)$$

The integration is taken over a four-dimensional volume between times  $t_1$  and  $t_2$  and  $dV = V' - V$  say. If  $\psi(2) = \psi(1)$  and we expand in terms of the eigenfunctions of  $V$  then we obtain the usual time-dependent expansion in the form of an integral equation.

Alternatively, let  $\psi(1) = \phi_1$  at  $t = t_1$  describe the incident state, and  $\psi(2)^* = \phi_2^*$  describe one of the states in which the particle can emerge. Then we can easily verify that

$$a_{12} = \left[ \int \phi_2^* \psi(1) dv \right]_{t=t_2} = \left[ \int \psi(2)^* \phi_1 dv \right]_{t=t_1}. \quad \dots\dots(5.5)$$

The function  $\psi^*(2)$  develops in time reversed in the same way as  $\psi(1)$  does in time, cf. (5.3). Finally from eqn. (5.4)

$$im da_{12} = \int \psi(2)^* dV \psi(1) dv dt, \quad \dots\dots(5.6)$$

where  $a_{12}$  is the probability amplitude of a transition from state  $\phi_1$  to the state  $\phi_2$ .

#### REFERENCES

- DIRAC, P. A. M., 1932, *Quantum Mechanics* (Oxford : University Press).  
 HEISENBERG, W., 1943, *Z. Phys.*, **120**, 513.  
 KYNCH, G. J., 1952 a, *Proc. Phys. Soc. A*, **65**, 83; 1952 b, *Ibid.*, **65**, 94.  
 MOTT, N. F., and MASSEY, H. S. W., 1949, *The Theory of Atomic Collisions*, 2nd edn. (Oxford : University Press).  
 SCHWINGER, J., 1951, *Phys. Rev.*, **82**, 914.

## Statistical Fluctuations in Nuclear Evaporation

By K. J. LE COUTEUR

Department of Theoretical Physics, University of Liverpool

*Communicated by H. Fröhlich; MS. received 15th February 1952, and read in part before the Physical Society at Liverpool in July 1950*

**ABSTRACT.** Previous treatments of nuclear evaporation have dealt with average values, neglecting fluctuations. In the present paper the fluctuations are considered in detail. The distributions of the number of neutrons and of the total energy associated with evaporation stars of a given size and the size distribution of stars of given total energy, are evaluated explicitly.

Knowledge of the fluctuations is useful for interpretation of data concerning small stars, such as those produced by  $\pi$ -meson capture or by artificially accelerated particles. The fluctuations are not very important in the large stars and do not modify any of the results of the author's previous mean value calculations.

The analysis of the mean evaporation process has also been put into a simplified form, from which numerical results can easily be obtained. The method has been used to compare experimental data with various theoretical energy-temperature relationships; the Fermi gas law previously used by the author seems to be the most satisfactory connection between the high-energy star data and the observed level density at low energies.



## § 1. INTRODUCTION

DETAILED investigations of Harding, Lattimore and Perkins (1949), Fujimoto and Yamaguchi (1949, 1950) and Le Couteur (1950, referred to as I and II), have shown that a very large class of nuclear disintegration stars can be described by evaporation theory. The different treatments have recently been compared by Yamaguchi (1950) and reviewed by Rochester and Rosser (1951) and Camerini, Lock and Perkins (1952). Since the calculations of I were completed further independent experiments of Perkins, Bernardini and Rochat, described in the second review, have confirmed the accuracy of the expected ratios of proton, deuteron, triton and  $\alpha$ -particle emission. Also observations of Hodgson (1951, 1952) of the frequency of emission of heavy splinters, hammer tracks and beryllium nuclei are in good agreement with predictions of Le Couteur from the formulae of I.

The experimental material used in I referred mainly to stars in silver and bromine with an average size of about 10 prongs and the formulae of I must be a good representation of the nuclear temperature at the average excitation, about 200 mev, of such stars.

It is rarely possible to measure the energies of all the charged particles emitted from a particular star and the neutrons are not observed, therefore the total energy released must be deduced from the star size by a combination of theoretical and statistical arguments. According to fig. 21 of Camerini *et al.*, the scale of average total excitation energy established by fig. 2 of I for silver and bromine is in agreement with experiments. With stars of a given size there must, however, be associated a whole distribution of excitation energies about this average value.

In this paper the fluctuations of the evaporation process are considered in detail. The distribution of star sizes arising from evaporation of a given total energy and the distribution of total energy associated with evaporation stars of a given size are worked out explicitly. One might expect the fluctuations to increase the width of the energy spectrum of particles emitted from stars of a given size over that calculated by the mean value methods of I; the increase however turns out to be negligible. Some types of fluctuation were very briefly considered by Fujimoto and Yamaguchi (1950) but previous treatments of nuclear evaporation have dealt mainly with the mean emission process; this procedure is justified by the results of this paper which show that the fluctuations are quite small.

In many experiments nuclear disintegrations are produced by artificially accelerated particles or by cosmic rays and only the size distribution is observed. To interpret these experiments one needs to infer the associated energy distribution which can usually be related to the primary collision process (e.g. Bernardini, Cortoni and Manfredini 1950, Barton, George and Jason 1951). For the smaller stars such as are produced artificially or by  $\pi$ -meson capture, knowledge of the fluctuations is very desirable.

One would like to go further and analyse the experimental data to yield some information about the variation of nuclear temperature with energy. This requires consideration of the change of disintegration characteristics, such as energy spectra and relative particle frequencies, with the total energy or rather with the star size, and knowledge of the fluctuations is essential.

Consideration of the fluctuations entailed the development (§ 4) of a simplified

treatment of the mean evaporation process which turns out to be quite accurate and easy to use. In the final sections of this paper, this method is used to compare the experimental energy spectra from moderately large stars with the predictions of various temperature laws.

To fix the law of temperature variation one must cover the largest possible range of energies, therefore in parallel with this work the disintegrations produced by low excitation energies of about 20 mev are being studied by Miss Lang, in this department.

The combination of material may give a reasonable indication of the nuclear specific heat.

## § 2. FORMULATION OF THE FLUCTUATION PROBLEM

The fluctuation problem presents no formal difficulties. Let

$$p(A_b, Z_b, U_b; A_c, Z_c, U_c) dU_c = p(B: C) dU_c \quad \dots\dots(2.1)$$

be the probability that a nucleus  $b$  of mass  $A_b$  charge  $Z_b$  with excitation energy  $U_b$  (often denoted by  $B$  or  $b$ ,  $U_b$ ) disintegrates to leave a residual nucleus  $c$  with excitation energy in the range  $dU_c$ , by emission of a fragment of type  $x$  (neutron,  $\alpha$ -particle etc.) of mass  $A_x = A_b - A_c$ . If  $U_b$  is below the threshold  $\epsilon_b$  for nucleon emission from  $b$  the probability vanishes, if  $U_b$  is above  $\epsilon_b$  the nucleus must disintegrate somehow and

$$\Sigma_c \int_0^{U_b} p(B: C) dU_c = 1. \quad \dots\dots(2.2)$$

In the notation of I, the total probability of emission of  $x$  from  $B$  is

$$P_x = P(B: c) = \int p(B: C) dU_c \quad \text{and} \quad \Sigma_x P_x = 1. \quad \dots\dots(2.3)$$

The binding energy  $Q_{bc}$  of  $x$  in  $b$  is defined by I eqn. (50), and the kinetic energy of the emitted particle is

$$T_x = U_b - U_c - Q_{bc}. \quad \dots\dots(2.4)$$

The elementary probabilities, which may be derived from the theory of Weisskopf (1937), are given explicitly in I, §§ 3.2 and 3.3. The probability of emission of  $x$  from  $B$  is of the form I (56)

$$P_x = P(B: c) = \gamma_x \rho_c \tau_c^2 / \rho. \quad \dots\dots(2.5)$$

Here  $\gamma_x$ , defined by I(51), is a statistical factor proportional to the mass and number of spin states of  $x$ , and  $\rho_c$  and  $\tau_c$  are the level density and temperature of the residual nucleus  $c$  at excitation energy  $R_x = U_b - Q_{bc} - V_x'$ , where  $V_x'$  is the effective potential barrier for emission of  $x$  from  $b$ . The factor  $\rho$  is chosen to make  $\Sigma P_x = 1$ . The distribution of  $T_x$  and  $U_c$  is

$$\begin{aligned} P(T_x) dT_x &= \exp[-(T_x - V_x')/\tau_c] (T_x - V_x') dT_x / \tau_c^2 \\ &= \frac{1}{P_x} p(B: C) dU_c. \end{aligned} \quad \dots\dots(2.6)$$

With this distribution the mean value and variance\* of  $T_x$  are

$$\bar{T}_x = 2\tau_c + V_x' \quad \text{and} \quad \sigma^2(T_x) = \bar{T}_x^2 - (\bar{T}_x)^2 = 2\tau_c^2. \quad \dots\dots(2.7)$$

In the notation of I (66), (67) the mean excitation energy of the residual nuclei  $c$  formed from  $b$  is  $U_b - H_b$ , which is determined by (2.4) and (2.7) as

$$H_b = \Sigma P_x h_x = \Sigma_x P_x (Q_{bc} + V_x' + 2\tau_c). \quad \dots\dots(2.8)$$

\* Mean square deviation, always denoted by  $\sigma^2$ .



Now let  $\mathbf{P}(\mathbf{O}:f) = \mathbf{P}(A_o, Z_o, U_o: A_f, Z_f)$  be the probability that an excited nucleus  $\mathbf{O}$  finally reaches stability as  $f$  with residual excitation energy below the threshold  $\epsilon_f$  for emission from  $f$ . Conventionally  $\mathbf{P}(\mathbf{O}:f) = \delta(o, f)$  for  $U_o < \epsilon_o$ ; for energies above the threshold the probabilities are determined by the integral equation

$$\mathbf{P}(\mathbf{O}:f) = \sum_a \int_0^{u_o} p(\mathbf{O}:A) dU_a \mathbf{P}(A:f). \quad \dots\dots(2.9)$$

The iterative solution is

$$\begin{aligned} \mathbf{P}(\mathbf{O}:f) = & \int_0^{\epsilon_f} p(\mathbf{O}:F) dU_f + \sum_a \iint p(\mathbf{O}:A) dU_a p(A:F) dU_f \\ & + \sum_{a,b} \iiint p(\mathbf{O}:A) dU_a p(A:B) dU_b p(B:F) dU_f + \dots, \quad \dots\dots(2.10) \end{aligned}$$

with  $U_o > U_A > U_B \dots > U_f$  and  $\epsilon_f > U_f \geq 0$ . The successive terms represent contributions from processes in which one, two, three emissions take place. The number of terms is limited by the initial energy  $U_o$ , since each process requires a threshold energy. The normalization

$$\sum_f \mathbf{P}(\mathbf{O}:f) = 1 \quad \dots\dots(2.11)$$

follows immediately from (2.2).

The probability distribution of numbers of each type of emitted fragment may be described by the moment generating function

$$M(\mathbf{O}:X, Y \dots) \equiv \sum \mathbf{P}(\mathbf{O}:r, s, \dots) \exp(rX + sY + \dots), \quad \dots\dots(2.12)$$

where  $\mathbf{P}(\mathbf{O}:r, s, \dots)$  is the probability that  $r$  particles of type  $x$ ,  $s$  of type  $y$  etc. have been evaporated in the disintegration of the initial nucleus  $\mathbf{O}$  and  $X, Y \dots$  are parameters.  $M$  is determined by the integral equation

$$M(\mathbf{O}:X, Y \dots) = \sum_a \int p(\mathbf{O}:A) dU_a \exp(X_{oa}) M(A:X, Y \dots) \quad \dots\dots(2.13)$$

where by  $X_{oa}$  is understood the parameter associated with the particle  $(x, y \dots)$  emitted in the nuclear transition  $o \rightarrow a$ .

The method may be further generalized to yield the joint probability distribution of the kinetic energies of the emitted particles. Let  $X, Y, \dots$  represent arbitrary functions of the kinetic energies of the corresponding particles  $x, y, \dots$ , so that in (2.13)  $X_{oa}$  is a function of  $U_o - U_a - Q_{oa}$ , then  $M$  becomes a characteristic functional (Bartlett and Kendall 1951) defining the energy distribution. This is easily understood by consideration of the special case in which all parameters vanish except one which is constant in a certain kinetic energy interval and zero outside it; then  $M$  gives the distribution of the number of particles emitted in this energy range. The substitution in (2.13) of

$$X = \lambda T_x^n, \quad Y = 0 \text{ etc.} \quad \dots\dots(2.14)$$

leads to a moment generating function  $M(\mathbf{O}:\lambda)$  which defines the probability distribution of the sum of  $n$ th powers of the kinetic energies  $T_x$  of the particles of type  $x$  emitted in the disintegration of  $\mathbf{O}$ .

### § 3. A SIMPLIFIED PROBLEM WITH ENERGY FLUCTUATION ONLY

To clarify the content of the formalism, let us consider a simplified problem in which only one type of particle can be emitted so that the nuclei may be specified by mass and energy only. In this case (2.9) or (2.13) are alternative

ways of working out the total number of particles emitted. The generating function for the number of particles emitted into the kinetic energy range  $\alpha, \beta$  is determined by

$$M(O: X) = \int p(O: A) dU_a e^{X} M(A: X), \quad \dots\dots (3.1)$$

where  $X$  vanishes outside the range  $l = U_o - Q - \alpha > U_a > U_o - Q - \beta = m$ , determined by (2.4), in which it is constant. The mean  $\bar{r}(O)$  and mean square  $\bar{r}^2(O)$  of the number of particles emitted into this range by disintegration of  $O$  are determined from the coefficients of  $X$  and  $X^2$  as

$$\bar{r}(O) = \int_0^{U_o} p(O: A) dU_a \bar{r}(A) + \int_m^l p(O: A) dU_a, \quad \dots\dots (3.2)$$

$$\bar{r}^2(O) = \int_0^{U_o} p(O: A) dU_a \bar{r}^2(A) + \int_m^l p(O: A) dU_a \{1 + 2\bar{r}(A)\}. \quad \dots\dots (3.3)$$

The integral equations may be solved approximately by expanding everything about the point  $U = w$  say. Define

$$\left. \begin{aligned} \bar{U}_a &= \int_0^{U_o} p(O: A) U_a dU_a, & \mu_n &= \int_0^{U_o} p(O: A) (U_a - w)^n dU_a, \\ \nu_n &= \int_m^l p(O: A) (U_a - w)^n dU_a \end{aligned} \right\} \dots\dots (3.4)$$

and then (3.2) becomes

$$(U_o - \bar{U}_a) \frac{d\bar{r}}{dw} + \frac{1}{2}[(U_o - w)^2 - \mu_2] \frac{d^2\bar{r}}{dw^2} + \dots = \nu_0 \quad \dots\dots (3.5)$$

and (3.3) becomes

$$(U_o - \bar{U}_a) \frac{d\bar{r}^2}{dw} + \frac{1}{2}[(U_o - w)^2 - \mu_2] \frac{d^2\bar{r}^2}{dw^2} + \dots = \nu_0 + 2 \left( \nu_0 \bar{r} + \nu_1 \frac{d\bar{r}}{dw} + \dots \right), \quad \dots\dots (3.6)$$

where  $\bar{r}, \bar{r}^2$  and their derivatives are evaluated for  $U = w$ . To simplify matters, choose  $w$  to make the terms in  $d^2\bar{r}/dw^2$  vanish. This requires

$$(U_o - w)^2 = \mu_2 = (U_o - \bar{U}_a)^2 + \sigma^2(U_a) \quad \text{or} \quad w = \frac{1}{2}(U_o + \bar{U}_a) - \frac{1}{2}\sigma^2(U_a)/(U_o - \bar{U}_a), \quad \dots\dots (3.7)$$

where  $\sigma^2(U_a)$  is the variance of  $U_a$  given  $U_o$ . The equations are then

$$\frac{d\bar{r}}{dw} = \frac{\nu_0}{H_o}, \quad \frac{d}{dw} \{\bar{r}^2 - (\bar{r})^2\} = \left(1 + \frac{2\nu_1}{H_o}\right) \frac{d\bar{r}}{dw} + \frac{d^2\bar{r}}{dw^2} \frac{\nu_2}{H_o}, \quad \dots\dots (3.8)$$

where, as in (2.8),  $H_o = U_o - \bar{U}_a$ . For the mean and variance of the *total number*  $r$  of particles emitted, these equations reduce to

$$\frac{d\bar{r}}{dw}(w) = \frac{1}{H_o}, \quad \frac{d}{dw} \{\bar{r}^2 - (\bar{r})^2\} = \frac{d\bar{r}}{dw} \frac{\sigma^2(U_a)}{H_o^2} + \frac{d^2\bar{r}}{dw^2} \frac{\mu_2}{H_o}. \quad \dots\dots (3.9)$$

For integration it suffices to take  $w = U_o - \frac{1}{2}Q$ , which is precise at low excitation energies when the nuclear temperature is negligible so that  $U_a = U_o - Q$ ,  $\sigma^2 = 0$ . Thus one has, for  $U > 2Q$

$$r(U) = \int_{3Q/2}^{U+\frac{1}{2}Q} \frac{dU_o}{H_o} + \frac{1}{2} = \int_Q^{U+\frac{1}{2}Q} \frac{dU_o}{H_o}, \quad \dots\dots (3.10)$$

$$\sigma_U^2(r) = [\bar{r}^2 - (\bar{r})^2]_U = \frac{1}{8} + \int_{5Q/2}^{U+\frac{1}{2}Q} \frac{d\bar{r} \sigma^2(U_a)}{H_o^2} = \frac{1}{8} + \int_{5Q/2}^{U+\frac{1}{2}Q} \frac{dU_o \sigma^2(U_a)}{H_o^3}, \quad \dots (3.11)$$

and (3.8) gives an equation like (3.10) for the energy spectrum of the particles.

The constants of integration are settled by reference to the exact solution which is obviously  $r=0$  for  $U < Q$ ,  $r=1$  for  $2Q > U \geq Q$ . Therefore (3.10) was adjusted to give the mean value  $\bar{r}(Q) = \frac{1}{2}$ . Similarly the variance  $\bar{r}^2 - (\bar{r})^2$  vanishes if  $U < 2Q$  and must increase rapidly to  $\frac{1}{4}$  at the value of  $U$ , slightly above  $2Q$ , for which  $r=1$  and  $r=2$  are equally probable; therefore (3.11) was adjusted to give the mean value  $\frac{1}{8}$  at  $U = 2Q$ .

In fig. 1 these approximations are compared with the exact solutions derived by numerical integration of (3.2) and (3.3) for the Weisskopf spectrum (2.6), with  $\tau_0 = [\frac{1}{6}(U_b - Q)]^{1/2}$  and  $Q = 10$  mev. In the range  $U > 2Q$ , for which a solution is required, the approximation (3.10) is of remarkable accuracy. In (3.11) neglect of the negative term in  $d^2\bar{r}/dw^2$  leads to a negligible overestimate of the variance of  $r$  at high energies; at energies below  $3Q$  the solution is too simple to follow the bumps in the curve of variance. The accuracy of these approximations is also good in the less realistic case of constant temperature which can be solved in terms of incomplete  $\Gamma$ -functions.

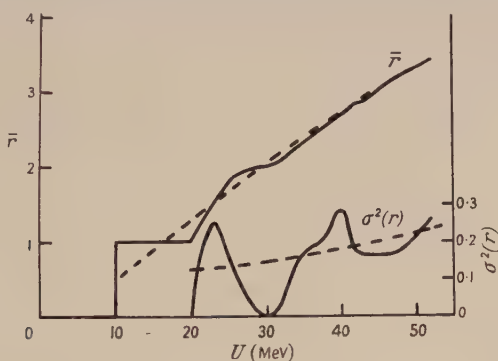


Fig. 1. Exact and approximate (broken curves) values of the mean  $\bar{r}$  and variance  $\sigma^2(r)$  of the number  $r$  of particles evaporated from a nucleus with initial excitation energy  $U$ . Binding energy  $Q = 10$  mev and nuclear temperature  $(U/6)^{1/2}$  mev are assumed.

Equation (3.10) for the mean emission is in agreement with the formulae used in the detailed mean value calculations of Le Couteur (I).

Equation (3.11) for the variance of  $r$  is easily understood. Emission of one particle leads to a spread  $\pm \sigma(U_a)$  in the residual excitation energy, which implies a spread  $\pm \sigma(U_a)/H_0$  in the number of further particles emitted; so the variance of  $r$  is made up of contributions  $\sigma^2/H_0^2$  from each particle emitted.

For the evaporation distribution (2.6), (2.7) the variance of  $r$  becomes

$$\sigma^2(r) = \frac{1}{8} + \int \frac{2\tau^2 d\bar{r}}{(Q + V' + 2\tau)^2} \ll \frac{1}{2}\bar{r},$$

because the temperature is usually much less than the binding energy  $Q$ . The variance of  $r$  is much less than that,  $\bar{r}$ , of a Poisson distribution with the same mean and for this reason the total number of particles emitted is a good indication of the total energy evaporated. The physical reason is that only the kinetic energy, but not the binding energy, removed by each particle is subject to fluctuation.

In experiments usually only the emission of charged particles is observed, but, since (§6) the neutron emission is fixed within very narrow limits by that



of the charged particles, the number of prongs remains a good indication of total energy.

This analysis is easily extended to the case where different types  $x, y, \dots$  of particles can be evaporated, if the emission probabilities are considered to be functions of excitation energy only. The mean and variance of the number  $n_x$  of particles of type  $x$  are given by

$$d\bar{n}_x/dw = P_x/H_0, \quad \dots\dots(3.12)$$

in agreement with I (68) and

$$d\sigma^2(n_x) = P_x(1 - P_x) d\bar{r} + P_x^2 d\bar{r}^2 \Sigma^2 / H^2 + 2P_x^2 d\bar{r}(1 - h_x/H), \quad \dots\dots(3.13)$$

where  $P_x$  and  $H$  are given by (2.5) and (2.8) and  $\Sigma^2$  is the variance of the residual energy after emission of any type of particle. Equation (3.13) shows that the variance of  $n_x$  is the sum of contributions from (i) a binomial fluctuation in the relative number of different types of particles emitted, (ii) a proportion of the fluctuation in the total number  $r$  of particles emitted, (iii) a small term depending on the difference between the mean energies removed by different particles.

The differential energy spectrum is given by similar modification of (3.8). Alternatively one can use the method of (2.14) for the moments of the spectrum, in particular for the Weisskopf distribution (2.6)

$$\left. \begin{aligned} \Sigma T_x &= \int (2\tau_c + V_x') P_x dU_b / H_b, \\ \Sigma T_x^2 &= \int [(2\tau_c + V_x')^2 + 2\tau_c^2] P_x dU_b / H_b. \end{aligned} \right\} \quad \dots\dots(3.14)$$

#### § 4. EXPLICIT SOLUTION OF THE SIMPLIFIED EVAPORATION PROBLEM

The formulae of § 3 can be integrated analytically if eqns. (3.10), (3.11) are combined with a simple energy temperature relationship. Consider the power law

$$U \propto \tau^\delta, \quad \dots\dots(4.1)$$

The Fermi-gas nuclear model corresponding to  $\delta=2$  was used in I and is approximately correct; here  $\delta=2$  or 3 will be considered.

If  $Q$  represents the sum of binding energy and potential barrier, (2.8) gives  $H_0 = Q + 2\tau(U_0 - Q)$  and (3.10) becomes

$$\bar{r}(U) = \int_Q^{U+\frac{1}{2}Q} \frac{dU_0}{Q + 2\tau(U_0 - Q)} = \int_0^{U-\frac{1}{2}Q} \frac{dU}{Q + 2\tau} = \frac{U - \frac{1}{2}Q}{\tau_m^\delta} \int_0^{\tau_m} \frac{d\tau^\delta}{Q + 2\tau}, \quad \dots\dots(4.2)$$

where  $\tau_m = \tau(U - \frac{1}{2}Q)$  is the maximum temperature involved. This may be expressed in terms of dimensionless parameters,

$$t = 2\tau/Q, \quad s = 2\tau_m/Q, \quad \dots\dots(4.3)$$

$$\text{as} \quad \bar{r}(U) = \frac{U - \frac{1}{2}Q}{Q} \int_0^s \frac{dt^\delta}{s^\delta(1+t)} = \frac{U - \frac{1}{2}Q}{Q} X, \quad \dots\dots(4.4)$$

$$\text{where} \quad X \simeq \left(1 - \frac{\delta}{\delta+1} s + \frac{\delta}{\delta+2} s^2 \dots\right) \quad \dots\dots(4.5)$$

may be expressed exactly in terms of  $\log s$  and is graphed in fig. 2. The average nuclear energy removed by each particle is  $Q/X$ , and so the average temperature is

$$\bar{\tau} = \frac{1}{2}Q(X^{-1} - 1) \simeq \begin{cases} \frac{2}{3}\tau_m - \frac{1}{9}\tau_m^2/Q & \text{for } \delta=2 \\ \frac{3}{4}\tau_m - \frac{3}{40}\tau_m^2/Q & \text{for } \delta=3 \end{cases} \quad \dots\dots(4.6)$$

which is also shown in fig. 2.

Similarly (3.11) gives the variance of  $r$  as

$$\sigma_{U^2}(r) = \frac{1}{8} + \int_0^{U-\frac{1}{2}Q} \frac{2\tau^2 dU}{(Q+2\tau)^3} = \frac{1}{8} + \frac{U-\frac{1}{2}Q}{Q} \frac{\tau_m^2}{Q^2} Y, \quad \dots\dots(4.7)$$

where

$$Y = \frac{2\delta}{\delta+2} \int_0^s \frac{dt^{\delta+2}}{s^{\delta+2}(1+t)^3} \simeq \frac{2\delta}{\delta+2} - \frac{6\delta}{\delta+3} s \dots\dots\dots(4.8)$$

is drawn in fig. 2. Also, from (3.14) the expected value of the sum of squares of the emitted kinetic energies is given by

$$\Sigma(T-V')^2 = 6 \int \frac{\tau^2 dU}{Q+2\tau} = \frac{U-\frac{1}{2}Q}{Q} \tau_m^2 \frac{6\delta}{\delta+2} \int_0^s \frac{dt^{\delta+2}}{s^{\delta+2}(1+t)^3} \dots\dots\dots(4.9)$$

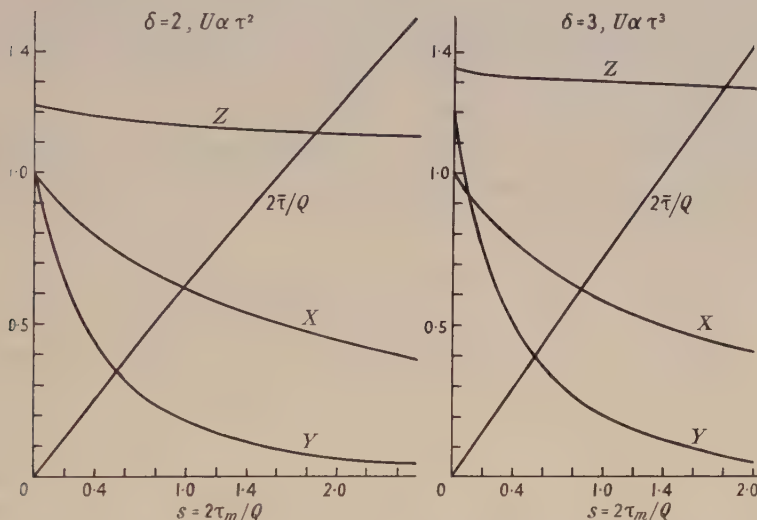


Fig. 2. Particles, with binding energy  $Q$  are evaporated from a nucleus with initial excitation energy  $U$  and temperature  $\tau_m = \tau(U - \frac{1}{2}Q)$ . The number emitted has mean  $\bar{r} = X(U - \frac{1}{2}Q)/Q$  and variance  $\sigma^2(r) = \frac{1}{8} + Y(U - \frac{1}{2}Q)\tau_m^2/Q^3$  and the variance of their kinetic energy spectrum is  $\sigma^2(T) = \tau_m^2 Z$ . The figure shows  $X$ ,  $Y$ ,  $Z$  and the average temperature  $\bar{\tau}$  as functions of the dimensionless parameter  $s = 2\tau_m/Q$ .

The variance of the kinetic energy is therefore

$$\sigma^2(T) = 6\bar{\tau}^2 - (2\bar{\tau})^2 = \tau_m^2 Z, \quad \dots\dots(4.10)$$

where

$$Z \simeq \left( \frac{11}{9} - \frac{28}{135} \frac{\tau_m}{Q} \right) \text{ for } \delta=2 \text{ and } Z \simeq \left( \frac{27}{20} - \frac{3}{20} \frac{\tau_m}{Q} \right) \text{ for } \delta=3 \dots\dots(4.11)$$

and is drawn in fig. 2.

The curves in fig. 2 are convenient for practical use. Strictly the constant of proportionality in (4.1) varies slowly with the nuclear mass and so changes during the evaporation. This can be allowed for adequately by using the average mass to evaluate  $\tau_m$ .

The results can be applied to stars where different types of particle are emitted if the mean  $H$  is approximated as in (4.2) with an appropriate  $Q$ . The results concerning energy spectra remain valid if in (3.14) the variation of  $P_x$  during the evaporation can be neglected. If these approximations are invalid, no question of principle arises, but use of the graphs must be replaced by numerical integration of the equations of § 2 and § 3, as was done in I.

The approximations give  $\sigma^2(T) = 11\bar{\tau}^2/4$  for  $\delta = 2$  and  $12\bar{\tau}^2/5$  for  $\delta = 3$ . Thus the width of the integral energy spectrum exceeds that of the Weisskopf distribution (2.6) corresponding to the same mean energy and temperature by a factor  $(11/8)^{1/2}$  for  $\delta = 2$  and  $(6/5)^{1/2}$  for  $\delta = 3$ : the broadening is greater for the square law than for the cube because the former leads to a more rapid cooling of the nucleus than does the latter. Therefore, as pointed out by Bagge (1941), experimental energy spectra should not be interpreted directly in terms of a Weisskopf distribution at constant temperature, though this has often been done.

The integral spectrum can be represented by the gamma distribution

$$P(T)dT = \exp[-(T - V')/\tau^*](T - V')^{l-1}dT/\Gamma(l)\tau^{*l}, \quad \dots\dots(4.12)$$

which has mean  $\bar{T} = V' + l\tau^*$  and variance  $l\tau^{*2}$ , if the values  $\tau^* = 11\tau_m/12$ ,  $l = 16/11$  for  $\delta = 2$  and  $\tau^* = 9\tau_m/10$ ,  $l = 5/3$  for  $\delta = 3$  are chosen to secure agreement with (4.6) and (4.10). The elementary Weisskopf spectrum (2.6) corresponds to  $l = 2$ .

If the total energy  $U$  is varied, the two temperature laws considered lead to significantly different variations of the mean energy  $\bar{T}$  and spectrum width  $\sigma(T)$ , the latter is approximately proportional to  $U^{1/\delta}$  or  $r^{1/\delta}$ . This is considered, in relation to the available evidence, in § 11.

#### 4.1. Variable Potential Barrier

There is strong evidence for a reduction of the potential barrier at high nuclear temperatures, as was assumed in I. This has an appreciable effect on the energy spectrum of the emitted particles as can be seen from the examples given in I, fig. 5. For simplicity suppose that  $V$  falls off linearly with temperature, so that for protons say

$$V' = V_f' - k\tau \quad \dots\dots(4.13)$$

and the parameters  $d, e$  of I are well represented by  $k = \frac{1}{3}$ . In this case the mean kinetic energy of the protons is

$$\bar{T} = V_f' + (2 - k)\bar{\tau}, \quad \dots\dots(4.14)$$

which can be evaluated easily from (4.6) or fig. 2. The change in  $V$  also slightly narrows the energy spectra. Analytically

$$(T - V_f')^2 = (2 - k)^2\tau^2 + 2\tau^2 = (6 - 4k + k^2)\tau^2$$

by (3.14) which may be calculated as (4.10) to yield

$$\begin{aligned} \sigma^2(T) &= (1 - \frac{2}{3}k + \frac{1}{6}k^2)\{\tau_m^2 Z + 4(\bar{\tau})^2\} - (2 - k)^2(\bar{\tau})^2 \\ &= \tau_m^2 Z - (\frac{2}{3}k - \frac{1}{6}k^2)\{\tau_m^2 Z - 2(\bar{\tau})^2\}, \quad \dots\dots(4.15) \end{aligned}$$

which is easily evaluated from fig. 2. Since  $k \gg \frac{1}{3}$  the reduction of  $\sigma^2(T)$  is small, being approximately

$$(\frac{2}{3}k - \frac{1}{6}k^2)\tau_m^2 \begin{cases} 0.33 & \text{for } \delta = 2, \\ 0.22 & \text{for } \delta = 3. \end{cases} \quad \dots\dots(4.16)$$

Comparison of this result with (4.14) shows that the width of the energy spectrum should be a better indication of nuclear temperature than is the mean energy, because  $V'$  is not accurately known.

#### § 5. NEUTRON-PROTON FLUCTUATIONS

In most experiments on nuclear evaporation the neutron emission is not observed and must be calculated as was done in § 3 of I. In I, § 3.3 it was explained



that the equations of emission I (65) contain controlling terms which tend to keep the neutron excess  $\Delta = N - Z$  of the evaporating nucleus close to the equilibrium value  $\Delta_e = N_e - Z_e$  of a stable nucleus of mass  $N + Z$ ; thus the disintegrating nucleus tends to follow the Heisenberg valley. This effect does not depend on the particular energy-temperature relationship assumed in I. Consider the more general case

$$U = A(1 + y\Delta^2/A^2)\tau^\delta \epsilon^{1-\delta}, \quad \dots\dots(5.1)$$

where  $y$  defined for  $\delta=2$  by I (38), is a small coefficient approximately equal to 1.5; then the entropy is

$$S = A \left(1 + \frac{y\Delta^2}{A^2}\right) \frac{\delta}{\delta-1} \left(\frac{\tau}{\epsilon}\right)^{\delta-1} = A^{1/\delta} \left(1 + \frac{y^2\Delta^2}{A^2}\right)^{1/\delta} \frac{\delta}{\delta-1} \left(\frac{U}{\epsilon}\right)^{(\delta-1)/\delta}, \quad \dots\dots(5.2)$$

$$\text{and} \quad \frac{\partial S}{\partial U} = \frac{1}{\tau}, \quad \left(\frac{\partial S}{\partial A}\right)_U = \frac{1}{\delta-1} \frac{U}{A\tau}, \quad \left(\frac{\partial S}{\partial \Delta}\right)_U = \frac{1}{\delta-1} \frac{2y\Delta}{A^2} \frac{U}{\tau}. \quad \dots\dots(5.3)$$

Now  $P_n/P_p = \exp\{S(A-1, \Delta-1, R_n) - S(A-1, \Delta+1, R_p)\}$  from (2.5) and the relative emission probabilities become, as in I, § 3.3,

$$\frac{P_n}{P_p} = \exp \left\{ \frac{1}{\tau} \left[ \frac{4\beta(\Delta - \Delta_e)}{A} + V_p' - (\delta-1)^{-1} \frac{4y\Delta R}{A^2} \right] \right\}, \quad \dots\dots(5.4a)$$

$$\frac{P_d}{P_p} = \exp \left\{ \frac{1}{\tau} \left[ -6.4 + \frac{1.6\beta(\Delta - \Delta_e)}{A} + V_p' - V_d' - (\delta-1)^{-1} \left(1 + \frac{2y\Delta}{A}\right) \frac{R}{A} \right] \right\}, \quad \dots\dots(5.4b)$$

$$\frac{P_t}{P_p} = \exp \left\{ \frac{1}{\tau} \left[ -8.8 + \frac{3.2\beta(\Delta - \Delta_e)}{A} + V_p' - V_t' - (\delta-1)^{-1} \left(2 + \frac{4y\Delta}{A}\right) \frac{R}{A} \right] \right\}, \quad \dots\dots(5.4c)$$

$$\frac{P_e}{P_p} = \exp \left\{ \frac{1}{\tau} \left[ -9.5 - \frac{0.8\beta(\Delta - \Delta_e)}{A} + V_p' - V_e' - (\delta-1)^{-1} \frac{2R}{A} \right] \right\}, \quad \dots\dots(5.4d)$$

$$\frac{P_\alpha}{P_p} = \exp \left\{ \frac{1}{\tau} \left[ 2.4 + \frac{0.8\beta(\Delta - \Delta_e)}{A} + V_p' - V_\alpha' - (\delta-1)^{-1} \left(3 + \frac{2y\Delta}{A}\right) \frac{R}{A} \right] \right\}. \quad \dots\dots(5.4e)$$

In each equation  $\tau$  is the mean of the temperatures and  $R$  the mean of the maximum excitation energies of the two alternative residual nuclei.  $\beta$ , defined by I (44), is about 23 mev. With  $\delta=2$  these equations are identical with I (65) in which  $\theta = \Delta/A$  and  $\tau = 2\sqrt{R/\lambda}$ . As shown in I, fig. 1, the term in  $\Delta - \Delta_e$  tend to make the final value of  $N - N_e$  insensitive to details of the energy-temperature dependence and to the initial conditions of the disintegration.

It will now be proved that fluctuations of the neutron excess from its calculated mean value are strongly damped by the controlling terms. Simple formulae will be derived for the final mean value (5.21) and variance (5.24) of  $(\Delta - \Delta_e)$ .

The calculation is much simplified by neglect of the fluctuation of the energy carried away by the different particles (which was considered in §§ 3 and 4); all particles are assumed to remove precisely the mean energy  $H$  defined by (2.8). Then eqn. (2.10) simplifies to

$$\mathbf{P}(\mathbf{O}:f) = \sum_{a, b, \dots} P(\mathbf{O}:a)P(\mathbf{A}:b) \dots P(\mathbf{E}:f) \quad \dots\dots(5.5)$$

with  $U_a = U_0 - H_0$ ,  $U_b = U_a - H_a$ , etc. and  $U_f < Q_f$

since the evaporation proceeds in steps from excitation energy  $U_0$  to  $U_a$  to  $U_b \dots$ . Let  $P(r, \Delta)$  denote the probability of a neutron excess  $\Delta$  at stage  $r$ , then

$$P(r+1, \Delta) = P(r, \Delta+1)P_n + P(r, \Delta-1)P_p + P(r, \Delta)P_d + P(r, \Delta+1)P_t + P(r, \Delta-1)P_t + P(r, \Delta)P_\alpha \dots (5.6)$$

and thus the moments of  $\Delta$  satisfy

$$\Sigma \Delta P(r+1, \Delta) = \Sigma P(r, \Delta)[(\Delta-1)(P_n + P_t) + (\Delta+1)(P_p + P_t) + \Delta(P_d + P_\alpha)],$$

$$\text{or} \quad \bar{\Delta}_{r+1} = \bar{\Delta}_r - \Sigma P(r, \Delta)(P_n + P_t - P_p - P_t) \dots (5.7)$$

and

$$\overline{\Delta_{r+1}^2} = \overline{\Delta_r^2} - 2\Sigma \Delta P(r, \Delta)(P_n + P_t - P_p - P_t) + \Sigma P(r, \Delta)(P_n + P_p + P_t + P_t) \dots (5.8)$$

and therefore the development of the variance is given by

$$\{\bar{\Delta}^2 - (\bar{\Delta})^2\}_{r+1} = \{\bar{\Delta}^2 - (\bar{\Delta})^2\}_r - (\bar{\Delta}_{r+1} - \bar{\Delta}_r)^2 - 2\Sigma(\Delta - \bar{\Delta})P(r, \Delta)(P_n + P_t - P_p - P_t) + \Sigma P(r, \Delta)(P_n + P_t + P_p + P_t). \dots (5.9)$$

These equations involve

$$P_n + P_p + P_t + P_t = 1 - P_d - P_\alpha = a \dots (5.10)$$

say. The approximation

$$P_n - P_p + P_t - P_t = a \tanh 2\beta(\Delta - \Delta^*)/\tau A$$

where

$$\Delta^* = \Delta_e - \{V_p' - (\delta - 1)^{-1} 4\gamma \Delta R/A^2\} A/4\beta \dots (5.11)$$

which was used in I, § 3.5 is exact at low temperatures and within 5% at high temperatures. Then at the high temperatures which prevail until the last stage of the evaporation, the equations reduce to

$$\bar{\Delta}_{r+1} - \bar{\Delta}_r = -a \tanh 2\beta(\bar{\Delta}_r - \Delta^*)/\tau A \dots (5.12)$$

$$\sigma_{r+1}^2(\Delta) - \sigma_r^2(\Delta) = a - (\bar{\Delta}_{r+1} - \bar{\Delta}_r)^2 - \sigma_r^2 \frac{4\beta a}{\tau A} \operatorname{sech}^2 \frac{2\beta}{\tau A} (\bar{\Delta}_r - \Delta^*). \dots (5.13)$$

Equation (5.12) is equivalent to I (70) or I (73) for  $\theta = \Delta/A$  which was solved in I. To test the validity of the approximations, the fundamental equations (5.6) were solved numerically in the special case

$$H_0 = (10 + 2\tau_a) \text{ Mev}, \quad \tau = (\frac{1}{8}U)^{1/2} \text{ or } \epsilon/A = \frac{1}{8} \text{ Mev and } 4\beta/A = 1 \text{ Mev} \dots (5.14)$$

with initial nucleus  $^{79}_{35}\text{Br}$  at excitation energy 112 Mev. The small  $\alpha$ -particle and deuteron emission was neglected. It is convenient to reckon  $\Delta$  from the initial value  $\Delta_0 = 9$  and the calculation yields the values in table 1.

Table 1

Stage	0	1	2	3	4	5	6	7
$U$ (Mev)	112	94	77	60	45	30	17	5
$\tau A/2\beta$	8.0	7.2	6.3	5.5	4.6	3.4	2.0	—
$\bar{\Delta}^* - \Delta_0$	-2	-2.3	-2.6	-2.9	-3.2	-3.5	-3.8	-4.1
$\bar{\Delta} - \Delta_0$ exact	0	-0.250	-0.522	-0.887	-1.18	-1.55	-2.01	-2.62
$\bar{\Delta} - \Delta_0$ approx (5.12)	0	-0.245	-0.522	-0.840	-1.23	-1.64	-2.13	-2.81
$\sigma^2(\Delta)$ exact	0	0.94	1.63	1.98	2.30	2.38	2.23	1.78
$\sigma^2(\Delta)$ approx (5.13)	0	0.94	1.60	2.05	2.25	2.30	1.97	1.46

The numerical values show that  $\Delta_{r+1} - \Delta_r$  is always small so fair approximations to (5.12) and (5.13) are

$$\left. \begin{aligned} \frac{d}{dr} (\bar{\Delta} - \Delta^*) &= -a \frac{2\beta}{\tau A} (\bar{\Delta} - \Delta^*) - \frac{d\Delta^*}{dr}, \\ \frac{d\sigma^2(\Delta)}{dr} &= a \left( 1 - \frac{4\beta}{\tau A} \sigma^2(\Delta) \right) \operatorname{sech}^2 \frac{2\beta}{\tau A} (\bar{\Delta} - \Delta^*) \end{aligned} \right\} \dots\dots (5.15)$$

with solutions

$$(\bar{\Delta} - \Delta^*)_f = (\bar{\Delta} - \Delta^*)_o \exp \left( - \int_o^f \frac{2\beta a}{\tau A} dr \right) - \int_o^f \frac{d\Delta^*}{dr} dr \exp \left( - \int_r^f \frac{2\beta}{\tau A} a dr \right) \dots\dots (5.16)$$

and

$$\sigma_f^2(\Delta) = \int_o^f a \operatorname{sech}^2 \frac{2\beta}{\tau A} (\bar{\Delta} - \Delta^*) dr \exp \left( - \int_r^f \frac{4\beta}{\tau A} a \operatorname{sech}^2 \frac{2\beta}{\tau A} (\bar{\Delta} - \Delta^*) dr \right), \dots\dots (5.17)$$

where o and f denote initial and final values. As in I (§ 3.5), one can write

$$dr = -dU/H = -\delta A(\tau/\epsilon)^{\delta-1} d\tau/H, \dots\dots (5.18)$$

so that

$$\int_r^f \frac{2\beta}{\tau A} a dr = \frac{2\delta\beta a}{(\delta-1)H} \left( \frac{\tau}{\epsilon} \right)^{\delta-1} = \frac{2\beta a S}{HA}, \dots\dots (5.19)$$

by (5.2). A mean value of the slowly varying quantity  $a/H$  is to be taken. Further integration yields

$$\begin{aligned} \int_o^f dr \exp \left[ - \frac{2\delta\beta a}{(\delta-1)H} \left( \frac{\tau}{\epsilon} \right)^{\delta-1} \right] &= \int \frac{\delta}{\delta-1} \frac{\epsilon A}{H} y^{1/(\delta-1)} dy \exp \left( \frac{-2\delta\beta a y}{\delta-1} \right) \\ &= \frac{\epsilon A}{2\beta a} \left( \frac{(\delta-1)H}{2\delta\beta a} \right)^{1/(\delta-1)} \Gamma \left( \frac{\delta}{\delta-1} \right) \dots\dots (5.20) \end{aligned}$$

for large  $U_o$ . The values of  $H$  and  $a$  should be taken at  $\tau = \epsilon[(\delta-1)H_f/2\delta\beta]^{1/(\delta-1)}$  where the integrand is a maximum. For high initial energy,  $S > \frac{1}{2}A$  say, the first term in (5.16) is negligible and the final value of the mean neutron excess tends to

$$(\bar{\Delta} - \Delta^*)_f = \left| \frac{d\Delta^*}{dr} \right| \frac{\epsilon A}{2\beta a} \begin{cases} \frac{1}{4}(H/\beta a) & \text{for } \delta = 2 \\ \frac{1}{2}(\pi H/3\beta a)^{1/2} & \text{for } \delta = 3 \end{cases} \dots\dots (5.21)$$

where  $\Delta_f^* = (\Delta_o - AV'/4\beta)_f$  and  $H$  is evaluated at

$$\tau = \epsilon(H_f/4\beta) \text{ for } \delta = 2 \text{ or } \tau = \epsilon(H_f/3\beta)^{1/2} \text{ for } \delta = 3. \dots\dots (5.22)$$

This result is in agreement with I (76), though more simply expressed.

To calculate the variance  $\sigma_f^2(\Delta)$ , one may replace  $\bar{\Delta} - \Delta^*$  in (5.17) by its final value since the  $\operatorname{sech}^2$  differs from unity only at the end of the disintegration when the temperature is low. Below some temperature  $\tau'$  the  $\operatorname{sech}^2$  is negligibly small and the approximation

$$\begin{aligned} \int_o^\tau \frac{4\delta\beta a \tau^{\delta-2}}{H\epsilon^{\delta-1}} d\tau \operatorname{sech}^2 \frac{2\beta}{\tau A} (\bar{\Delta} - \Delta^*)_f &= \frac{4\delta}{\delta-1} \left[ \frac{a\beta}{H} \left( \frac{\tau}{\epsilon} \right)^{\delta-1} \right]_\tau^\tau \\ &= 0 \text{ for } \tau < \tau', \end{aligned} \dots\dots (5.23)$$

where  $\tau' = 4\beta(\bar{\Delta} - \Delta^*)_f/A$  for  $\delta = 2$  or  $4 \cdot 4\beta(\bar{\Delta} - \Delta^*)_f/A$  for  $\delta = 3$ , may be derived



by evaluation of  $\int y^{\delta-2} dy \operatorname{sech}^2 1/y$  and leads to

$$\begin{aligned}\sigma_f^2(\Delta) &= \left[ 1 + \frac{4\delta}{\delta-1} \frac{\beta}{H_f} \left( \frac{\tau'}{\epsilon} \right)^{\delta-1} \right] \frac{\epsilon A}{4\beta} \left( \frac{\delta-1}{4\delta} \frac{H}{\beta a} \right)^{1/(\delta-1)} \Gamma \left( \frac{\delta}{\delta-1} \right) - \frac{A\tau'^\delta}{H\epsilon^{\delta-1}} \\ &= \left( 1 + \frac{8\beta}{H_f} \frac{\tau'}{\epsilon} \right) \frac{\epsilon A}{4\beta} \frac{H}{8\beta a} - \frac{A\tau'^2}{H\epsilon} \text{ for } \delta=2 \\ &= \left[ 1 + \frac{6\beta}{H} \left( \frac{\tau'}{\epsilon} \right)^2 \right] \frac{\epsilon A}{8\beta} \left( \frac{\pi H}{6\beta a} \right)^{1/2} - \frac{A\tau'^3}{H\epsilon^2} \text{ for } \delta=3, \quad \dots\dots(5.24)\end{aligned}$$

with  $H$  and  $a$  calculated at

$$\tau = \epsilon(H_f/8\beta) \text{ for } \delta=2 \text{ or } \tau = \epsilon(H_f/6\beta)^{1/2} \text{ for } \delta=3. \quad \dots\dots(5.25)$$

The accuracy of these simple formulae is adequate. In the example (5.14)  $|\partial\Delta^*/\partial r| = 0.3$ ,  $a = 1$ ,  $\epsilon A/8\beta^2 = \frac{1}{3}$ , and so (5.21) gives  $(\Delta - \Delta^*)_f = 0.3 \times \frac{1}{3} \times 13.3 = 1.33$  or  $\bar{\Delta} - \Delta_0 = -4.1 + 1.33 = -2.77$ , in excellent agreement with the accurate results of table 1. Similarly for  $\sigma^2(\Delta)$  one finds  $\tau' = 1.33$  mev from (5.23) and (5.24) gives  $\sigma_f^2 = (1 + 1.6) \times \frac{1}{4} \times \frac{1}{3} \times 11.7 - 6 \times 1.77/10 = 2.6 - 1.06 = 1.5$ , which is also rather accurate.

## § 6. THE NEUTRON EMISSION

The total number of prongs (charged particles) emitted is

$$N_c = n_p + n_d + n_t + n_\alpha \quad \dots\dots(6.1)$$

and the total number of particles emitted is

$$r = N_c + n_n. \quad \dots\dots(6.2)$$

The final value of the neutron excess differs from its equilibrium value by

$$\begin{aligned}n_p + n_t - n_n - n_\alpha + \frac{\partial \Delta_e}{\partial A} (n_p + n_n + 2n_d + 3n_t + 3n_\alpha + 4n_\alpha) \\ = (\Delta - \Delta_e)_f = (\bar{\Delta} - \Delta_e)_f \pm \sigma_f(\Delta), \quad \dots\dots(6.3)\end{aligned}$$

which was calculated in § 5. If, for simplicity of writing, the numerical values

$$\partial \Delta_e / \partial A = 0.2 \quad \text{or} \quad \partial N_c / \partial Z_e = 1.5 \quad \dots\dots(6.4)$$

used in I are assumed, eqn. (6.3) fixes the neutron emission as

$$n_n = 1.5n_p + n_\alpha + 0.5n_d - 0.5n_t + 2n_\alpha + 1.25\{\Delta_e - \bar{\Delta} \pm \sigma(\Delta)\}_f. \quad \dots\dots(6.5)$$

In many experiments the charged particles are not distinguished from each other, and then (6.5) must be expressed in terms of the total number of prongs  $N_c$  and the corresponding expected numbers  $\bar{n}_p$  of protons, etc. (which for silver bromide may be taken from I, fig. 2). The resulting expression for the neutron emission of an  $N_c$ -prong star is

$$\begin{aligned}n_n = 1.5N_c - 0.5\bar{n}_\alpha - \bar{n}_d - 2\bar{n}_t + 0.5\bar{n}_\alpha + 1.25(\Delta_e - \bar{\Delta})_f \\ \pm \{1.56\sigma_f^2(\Delta) + \frac{1}{4}\bar{n}_\alpha + \bar{n}_d + 4\bar{n}_t + \frac{1}{4}\bar{n}_\alpha\}^{1/2}, \quad \dots\dots(6.6)\end{aligned}$$

the standard deviation being obtained by adding to the variance  $1.56 \sigma_f^2(\Delta)$  in (6.5) the contribution from the statistical fluctuations found in (3.13) of the relative numbers of  $\alpha$ -particles, etc. amongst the  $N_c$  prongs. For silver bromide this formula for the standard deviation gives approximately

$$\sigma(n_n, \text{ given } N_c) = 2.8^{1/2} \text{ for } N_c \leq 2, \{2.8 + 0.7(N_c - 2)\}^{1/2} \text{ for } N_c > 2, \quad \dots\dots(6.7)$$

if the numerical results of § 5 and of I, fig. 2 are used.

## § 7. THE PRONG DISTRIBUTION

The prong distribution of an evaporation star with given initial energy  $U$  can be derived from §§ 4 and 6. If  $\bar{H}_n$  and  $\bar{H}_c$  are the average energies removed from the nucleus by neutrons and charged particles respectively, the fluctuations of the number of particles emitted are subject to

$$\bar{H}_c N_c + \bar{H}_n n_n = U - \frac{1}{2}Q = \bar{H}(\bar{N}_c + \bar{n}_n) = \bar{H}\bar{r} \quad \dots\dots(7.1)$$

which, in conjunction with (6.6) gives

$$\bar{N}_c = [\bar{r} - 1.25(\Delta_e - \bar{\Delta})_f]/c, \quad \dots\dots(7.2)$$

$$\sigma^2(N_c) = [\sigma^2(r) + (\bar{H}_n/\bar{H})^2(1.56\sigma_f^2(\Delta) + \frac{1}{4}\bar{n}_\alpha + \bar{n}_d + 4\bar{n}_t + \frac{1}{4}\bar{n}_e)]/c^2, \quad \dots\dots(7.3)$$

where

$$c = 2.5 - (0.5\bar{n}_\alpha + \bar{n}_d + 2\bar{n}_t - 0.5\bar{n}_e)/\bar{N}_c \quad \dots\dots(7.4)$$

and of course  $\bar{H}_n/\bar{H} \simeq 1 - \frac{1}{2}\bar{V}'/\bar{H}$ , where  $\bar{V}'$  is the mean potential barrier for protons.

Equation (7.2) for the mean number of prongs has the merit of simplicity and should be useful for the analysis of experiments, in which case the value of  $c$  can be taken directly from the experiments. Numerical integration as in I should yield more accurate values for the mean emission but is much more laborious.

The main result of the calculation is the explicit formula (7.3) for the variance of the number of prongs in terms of the known mean emission and of the variance of  $r$ , which was calculated in § 4 with sufficient accuracy for the present purpose.

The main results of this paper are simple to use. As an example, table 2 shows the full calculation for silver bromide stars, assuming the mean of the energy-temperature relationships d, e of I, § 4. Thus  $\epsilon = 12.4$  mev or  $\tau = (12.4U/A)^{1/2} \simeq (U/6.7)^{1/2}$  if the average value 83 for  $A$  is used. Also  $H = Q + 2\tau$  is used with  $Q = 10$  mev.

Table 2\*  
(parameters d, e)

$U$ (mev)	50	100	200	400	600	900	
$\tau_m$ (mev)	2.44	3.66	5.33	7.60	9.40	11.6	eqn. (4.3)
$s = 2\tau_m/Q$	0.488	0.732	1.066	1.52	1.88	2.32	
$\bar{r}$	3.4	6.45	11.7	20.5	28.0	36.8	fig. 2
$c$	2.5	2.3	2.2	2.1	2.1	2	eqn. (7.4)
$\bar{N}_c$	0.4	1.8	4.3	8.8	12.3	17.4	eqn. (7.2)
$\sigma^2(r)$	0.22	0.46	1.09	2.4	3.8	6.1	fig. 2
$\sigma^2(n_n, \text{ given } N_c)$	2.8	2.8	4.4	7.5	10	13.6	eqn. (6.6)
$\sigma^2(N_c, \text{ given } U)$	0.4	0.52	1.0	2.0	2.8	4.7	eqn. (7.3)
$\sigma^2(T, \text{ given } U) (\text{mev}^2)$	7	16	33	66	100	151	fig. 2

§ 8. SPECTRUM OF EXCITATION ENERGIES FOR GIVEN STAR SIZE  $N_c$ 

The spread  $\sigma(n_n)$  of neutron emission implies a spread of amount  $\bar{H}_n\sigma(n_n, \text{ given } N_c) \simeq Q\sigma/X$  in the total excitation energy  $U$ ; the approximation is a slight overestimate of  $\bar{H}_n$ . Also the thermal fluctuations cause a variance

\* For  $U < 400$  mev these values of  $N_c$  agree perfectly with those plotted in I, fig. 2, which assumes the same parameters. At higher energies there is a small error in I, attributed to the use in this energy range of an approximate path of integration in the  $(N, Z)$  plane.

$r\sigma^2(T)$  in the total kinetic energy of the emitted particles. Since different particles have different binding energies  $Q$  and barriers  $V'$ , the spectrum (2.6) implies that with  $N_c$  fixed the statistical fluctuation in the relative numbers of protons,  $\alpha$ -particles, etc. gives a further contribution

$$(Q_p + V_p' - \bar{Q}_c)^2 \bar{n}_p + (Q_\alpha + V_\alpha' - \bar{Q}_c)^2 \bar{n}_\alpha + \dots \equiv N_c \sigma^2(Q_c + V_c')$$

to the variance of  $U$ , where  $\bar{Q}_c$  is the mean value of  $Q + V'$  for the charged particles. This contribution is much smaller than the others. Thus the variance of  $U$  given  $N_c$  is

$$\sigma^2(U, \text{given } N_c) = (\bar{H}_n)^2 \sigma^2(n_n, \text{given } N_c) + \bar{r} \sigma^2(T) + N_c \sigma^2(Q_c + V_c'). \quad \dots (8.1)$$

It follows that  $\tau_m$  is distributed about the mean  $\bar{\tau}_m = \tau(\bar{U} - \frac{1}{2}Q)$  with standard deviation  $\sigma(\tau_m) = \sigma(U) d\tau/dU$ .

If, as is usual, measurements from a large sample of stars with given  $N_c$  are combined together to derive say a proton energy spectrum, this will be wider than that calculated in §4 for the mean energy  $\bar{U}$  and temperature  $\bar{\tau}_m$  corresponding to  $N_c$ . In the sample the average value of  $\Sigma(T - V')^2$  is, according to (4.9), proportional to  $\bar{\tau}_m^2 = (\bar{\tau}_m)^2 + \sigma^2(\tau_m)$  and so the fluctuation of  $U$  increases the variance of the kinetic energy of the protons in the sample to

$$\sigma^2(T, \text{given } N_c) = \sigma^2(T, U = \bar{U}) + \frac{6\delta}{\delta + 2} \sigma^2(\tau_m, \text{given } N_c), \quad \dots (8.2)$$

$\delta$  being the exponent introduced in (4.1) and (5.1).

However, the values in table 3 show that the effect is very small.

Table 3

Nuclear constants are as in table 2, from which the first two lines are taken.

$N_c$ (prongs)	0.4	1.8	4.3	8.8	12.3	17.4
$\bar{U}$ (MeV)	50	100	200	400	600	900
$(\bar{H}_n)^2 \sigma^2(n_n)$ (MeV <sup>2</sup> )	478	605	1220	2270	4505	8100
$\bar{r} \sigma^2(T)$ (MeV <sup>2</sup> )	24	101	382	1350	2800	5550
$N_c \sigma^2(Q_c + V_c')$ (MeV <sup>2</sup> )	1	4	30	135	240	430
$\sigma^2(U, \text{given } N_c)$ (MeV <sup>2</sup> )	503	710	1622	3755	7545	14080
$\sigma(U, \text{given } N_c)$ (MeV)	22.4	26.6	40.4	61.3	86.9	118
$\sigma(\tau_m, \text{given } N_c)$ (MeV)	0.55	0.49	0.53	0.58	0.68	0.76

$\sigma(\tau_m)$  is so small that the difference (8.2) between  $\sigma(T, \text{given } U)$  and  $\sigma(T, \text{given } N_c)$  is always negligible; the former, which may be taken directly from fig. 2 or table 2 is easier to work with. So far experiments have always been analysed by comparing experimental spectra of given  $N_c$  with theoretical spectra of given  $U$ ; the above numerical results show that this procedure is quite legitimate.

The values of  $\sigma(U, \text{given } N_c)$  should be useful for the interpretation of experiments in which star size distributions are observed. Note that the uncertainty in neutron emission is the largest contribution to  $\sigma(U)$ . According to the results of §6 this contribution would be much smaller if the different charged particles were identified and in this case for stars of more than eight prongs the temperature fluctuations would give the main contribution to  $\sigma(U)$ .



## 8.1. Note on very large Cosmic-Ray Stars

The previous calculations have assumed that the evaporation starts from a nucleus, normally stable, which has been highly excited so that initially  $N - Z \equiv \Delta$  has the equilibrium value  $\Delta_e$ . In large cosmic-ray stars this may not be the case.

Suppose that  $n_s$  charged mesons are emitted from the stable target nucleus by the primary collision. Positive and negative mesons are equally likely, so the charge removed from the nucleus has average 0 and standard deviation  $\sqrt{n_s}$ . Since  $N + Z$  is unchanged this implies a standard deviation  $2\sqrt{n_s}$  of  $\Delta$ .

A number  $R$  of fast recoil nucleons with energy above the limit of the evaporation spectrum are also emitted. Of these  $N_g \simeq R\partial Z_e/\partial A$  will be protons, observed as 'grey' tracks, and  $R - N_g \simeq R\partial N_e/\partial A$  will be neutrons. This process contributes  $2N_g$  to the variance of  $\Delta$ .

Therefore after emission of mesons and fast nucleons in the primary collision processes, there is left a highly excited nucleus with neutron excess  $\Delta$  close to the equilibrium value  $\Delta_e$  appropriate to its mass, but with standard deviation  $\sigma_o(\Delta) = \sqrt{(4n_s + 2N_g)}$ .

In calculating the neutron evaporation as in § 6, the variance  $\sigma_o^2(\Delta)$  must be added to  $\sigma_f^2(\Delta)$ , the variance of the final neutron excess.

Experimental statistics suggest the following average numbers of grey and shower tracks for a given number  $N_e$  of evaporation prongs:

$N_e$	( $\leq 5$ )	8	13
$N_g(\text{average})$	0	3	8
$N_s(\text{average})$	0	1	3
$\sigma_o^2(\Delta)$	0	10	28

which inserted in table 3 would lead to the values in table 4.

Table 4

$N_e$	0.4	1.8	4.3	8.8	12.3	17.4
$\sigma(U, \text{ given } N_e) \text{ (mev)}$	22.4	26.6	40.4	90	167	260
$\sigma(\tau_m, \text{ given } N_e) \text{ (mev)}$	0.55	0.49	0.54	0.85	1.31	1.68

As in § 8 these small values of  $\sigma(\tau_m)$  do not give a significant contribution to  $\sigma(T, \text{ given } N_e)$ .

§ 9. NOTE ON  $\pi$ -MESON INDUCED DISINTEGRATIONS

The disintegration of silver and bromine nuclei by capture of slow negative  $\pi$ -mesons has been studied experimentally by Menon, Muirhead and Rochat (1950) who find  $\bar{N}_e = 1.1$ ,  $\sigma(N) = 1.1$  for the mean and standard deviation of the number of prongs. According to table 2, this corresponds to a mean excitation energy of 75 mev. This is probably an underestimate because of the peculiar method of nuclear excitation, which is discussed by Menon *et al.* The  $\pi$ -meson is probably absorbed in a primary process like  $\pi^- + P \rightarrow N + P$  or  $\pi^- + P + N \rightarrow N + N$  and it is likely that one fast neutron is emitted before thermal equilibrium is reached and only the balance of energy remains to excite the nucleus which reaches stability by evaporation. On this assumption, the excited nucleus starts with a neutron surplus of about  $\frac{1}{2}$ , since its charge was reduced by one by capture of the meson and  $\partial N_e/\partial Z_e = 1.5$ . Since the total neutron evaporation is fixed by the final value of the neutron excess, the neutron emission must exceed that

calculated in §6, by this amount. This requires a correspondingly greater excitation energy, so that the *mean* value may be estimated as approximately 80 Mev.

The variance 1.2 of the observed prong distribution is much greater than the value 0.5\* given by table 2 for the mean excitation energy. A spread of excitation energy must be assumed with standard deviation  $\sigma(U)$  such that  $\{\sigma(U)\partial N_c/\partial U\}^2 + 0.5 = 1.2$ , which gives  $\sigma(U) = 30$  Mev so that the distribution of excitation energy is  $U = 80 \pm 30$  Mev. This wide spread of  $U$  is quite in accordance with what would be expected from the method of nuclear excitation, for the fast primary particles may sometimes escape immediately from the nucleus and sometimes traverse a nuclear diameter with large loss of energy which appears as nuclear excitation.

#### § 10. RESULTS FOR THE CUBE LAW $U = A\tau^3/\epsilon^{-2}$

Numerical results have also been calculated for  $\delta = 3$ , that is for

$$U = A\tau^3/\epsilon^2, \quad \tau = (\epsilon^2 U/A)^{1/3}, \quad \dots (10.1)$$

which Miss Lang's results suggest as a reasonable connection between nuclear temperatures at  $U \simeq 20$  Mev and the temperatures found in large stars. Two numerical values were considered:

$$\begin{aligned} f \quad & \epsilon = 8.2 \text{ Mev, giving } \tau = (67U/A)^{1/3}, \\ g \quad & \epsilon = 6.8 \text{ Mev, giving } \tau = (46U/A)^{1/3}. \end{aligned}$$

The values  $f$  were chosen to give the same temperature at  $U = 200$  Mev as the square law  $U \propto \tau^2$  which was used in I and in tables 2 and 3. As explained in the introduction, the choice ensures reasonable agreement with most of the available data from cosmic-ray stars. The values  $g$  were considered for comparison.

With these temperature laws and  $\beta$ ,  $\partial \Delta^*/\partial r$  as in § 5, eqns. (5.21) and (5.24) give

$$\begin{aligned} f \quad & (\bar{\Delta} - \Delta^*)_f = 2.25, \quad (\bar{\Delta} - \Delta_e)_f = -1.75, \quad \sigma_f^2(\Delta) = 3.9 \\ g \quad & (\bar{\Delta} - \Delta^*)_g = 1.8, \quad (\bar{\Delta} - \Delta_e)_g = -2.2, \quad \sigma_g^2(\Delta) = 3. \end{aligned}$$

The final variance of  $\sigma(\Delta)$  is higher than was calculated with the square law because of the higher nuclear temperatures during the last stages of evaporation.

For comparison with the square law (tables 2, 3), the numerical values for law (g) with  $H = Q + 2\tau$ ,  $Q = 10$  Mev are given in table 5.

Table 5. (Parameters g)

$U$ (MeV)	50	100	200	400	600	900
$\tau_m$ (MeV)	2.9	3.7	4.7	6.0	6.9	7.94
$\bar{r}$	3.1	6.2	11.5	20.9	29.7	42
$\bar{N}_c$	0.3	1.7	4.2	9.0	13.1	20
$\sigma^2(r)$	0.27	0.51	1.07	2.4	3.8	5.7
$\sigma^2(N_n, \text{ given } N_c)$	4.7	4.7	6.2	9.6	12.5	17.3
$\sigma^2(N_c, \text{ given } U)$	0.7	0.9	1.4	2.5	3.5	5.4
$\sigma^2(T, \text{ given } U) \text{ (MeV)}^2$	11	18.3	29	47	62	82
$\sigma(U, \text{ given } N_c) \text{ (MeV)}$	31.6	34.9	45.9	66.4	82.7	106.3
$\sigma(\tau_m, \text{ given } N_c) \text{ (MeV)}$	0.61	0.43	0.36	0.33	0.32	0.31

The values of  $c$  used were the same as in table 2. The differences between the square and cube laws arise because at low excitation energies the cube law gives

\* The numerical integration of § 5 applies directly to this case so the estimate of variance should be accurate.

the higher temperature and at high excitation energies the square law gives the higher temperature. As in §8 the increase of  $\sigma(T, \text{ given } N_c)$  over  $\sigma(T, \text{ given } U)$  is negligible.

### § 11. COMPARISON WITH OBSERVED SPECTRA

Experimental energy spectra of protons emitted from silver and bromine stars of several sizes are given by Harding *et al.* (1949) in their fig. 1\*. The interpretation is not quite straightforward; one has to estimate where the evaporation spectrum ends and the tail of 'knock-on' or Heisenberg protons begins. Two methods of analysis have been used: (a) The mean  $\bar{T}$  and mean square deviation  $\sigma^2(T)$  were calculated for the proton tracks of kinetic energy  $T < \bar{V} + 3\tau_0$  and the number of evaporated particles was taken to be the number of prongs in this energy range, for large stars about 85% of the total number recorded. This is thought to be an underestimate of  $\bar{T}$  and  $\sigma^2(T)$  because the theoretical spectrum (4.12) predicts that 5% of the particles are evaporated with a kinetic energy above this limit. The experimental points are plotted as — in fig. 3. (b) All proton tracks with  $T < \bar{V} + 4\tau_0$  were analysed as in (a). These experimental points are plotted as + in fig. 3 and may be overestimates of  $\bar{T}$  and  $\sigma^2(T)$ , because in the evaporation spectrum (4.12) 98% of the particles have lower kinetic energy and so some 'knock-on' particles must be included amongst those analysed. For small stars of 1 or 2 prongs formed by  $\pi^-$  capture, the energy spectrum of Menon *et al.* (1950, fig. 3) is available. This has been analysed as above.

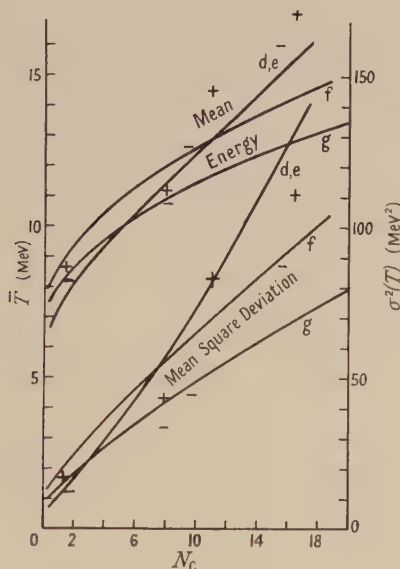


Fig. 3. Upper + and lower — experimental estimates of the mean  $\bar{T}$  and mean square deviation  $\sigma^2(T)$  of the kinetic energy of protons evaporated from silver and bromine stars with  $N_c$  evaporation prongs. The curves are theoretical estimates for the parameters  $d, e$  with  $U \propto \tau^2$  and  $f, g$  with  $U \propto \tau^3$ .

Theoretical values of  $\bar{T}$  and  $\sigma^2(T)$  for the three sets of parameters,  $d, e$  (square law) and  $f, g$  (cube law), considered in this paper are plotted in fig. 3. The

\* The total excitation energies there quoted are too low: revised values are given in figs. 19, 21 of the review of Camerini *et al.* (1952).



potential barrier is the same as in  $d, e$  of I, § 4, but as explained in § 4.1 above in the present analysis it is more easily represented by  $V' = V_f' - \frac{1}{3}\tau$  and so the mean proton kinetic energy was taken as  $T = \bar{V}' + 2\tau = 4 + 5\tau/3$  MeV. The slight reduction (about 6% for  $\delta=2$ , 4% for  $\delta=3$ ) of  $\sigma^2(T)$  given by (4.15) for  $k = \frac{1}{3}$  was ignored; it would be partly compensated by the increase given by (8.2).

Because of the scatter of the experimental points a very large range of star sizes must be considered if any conclusion is to be drawn. It must be remembered that the curves of mean energy but not of variance can be slightly displaced by making different assumptions about the potential barrier. All the curves lie close together and to the experimental points for stars of less than 12 prongs. The square law predicts a somewhat greater variance  $\sigma^2(T)$  for large stars than is found experimentally for stars of 15–22 prongs and, if taken seriously, this would be evidence in favour of the cube law or a similar law. However, the discrepancy, which is hardly significant, may arise because in such large stars thermal equilibrium is not set up until the energy has been reduced by emission of many particles.

## § 12. DISCUSSION

The main sources of fluctuation in nuclear evaporation have been analysed and evaluated numerically; the results for  $\sigma(n_n, \text{ given } N_c)$ ,  $\sigma(N_c, \text{ given } U)$  and  $(\sigma U, \text{ given } N_c)$  should be of some practical use.

In all the problems considered the fluctuations have little effect on the mean number of particles emitted or on their energy spectra. This justifies the procedure of I in which the very complicated equations of the actual physical problem were integrated for mean values only, ignoring fluctuations. It is out of the question to solve the cascade equations of § 2 exactly for the actual physical problem.

It is known that mean value integrations are not adequate to solve the problem of the electron–photon cascade in cosmic-ray theory for which a refined treatment of fluctuations (Jánosy 1950) is required. The reason is that the process is multiplicative so that any excess of electrons or photons produced by fluctuation at the start of the cascade gives birth to further particles and the fluctuations tend to grow as in other population problems (Kendall 1949). There is no such effect in the evaporation problem, where the equations of motion are such as to damp out fluctuations, as has been discussed in detail for the neutron–proton fluctuation. A similar, but very much smaller, effect exists for the fluctuation in the total number of particles emitted.

It has never been established how far temperature laws other than the Fermi gas,  $U \propto \tau^2$ , can explain cosmic-ray stars. The results of § 11 suggest that a law  $U = A\tau^\delta \epsilon^{1-\delta}$  with  $\delta$  between 2 and 3, and  $\epsilon$  chosen as in  $f$  of § 10 to fit the known temperature at 200 MeV, would do, although only the square law has actually been shown to be consistent with the observed emission frequencies of  $\alpha$ -particles, deuterons, fragments, etc. The different possibilities lead to very different average spacings  $D$  between nuclear levels at low energies. For  $A=93$ ,  $U=8$  MeV the results are

$d, e$	$\delta=2$	$\epsilon=12.4$ MeV	$D=6.5$ eV
	$\delta=7/3$	$\epsilon=10.7$ MeV	$D=240$ eV
	$\delta=5/2$	$\epsilon=9.4$ MeV	$D=1300$ eV
	$\delta=3$	$\epsilon=6.8$ MeV	$D=8700$ eV

and according to measurements of Selove (1951) the first is very reasonable. On this evidence the Fermi gas law is the best adapted to span large ranges of energy. Its failure to follow the variation of  $D$  with  $A$  at very low excitation energies is probably due to the complexities of nuclear shell structures.

*Note added in Proof.* Some predictions of this paper can now be checked against experimental results.

(1) V. C. Tongiorgi and D. Edwards (private communication), using the Cornell Synchrotron as a meson source, studied the neutrons emitted when negative  $\pi$ -mesons are captured in Pb, Sn, Al, C. If these results are interpolated to mass 100, which is a mean for AgBr, one finds  $\bar{n}_n = 5.5 \pm 0.5$ ,  $\sigma(\bar{n}_n) = 1.9$  for the mean and standard deviation of the number of neutrons emitted with energy below 10 mev. The considerations of § 9 indicated a distribution  $u = 80 \pm 30$  mev of the thermal excitation energy following  $\pi^-$  capture, which leads to a neutron evaporation with average 4.5 and standard deviation

$$\sigma(n_n) = \left\{ \left( \frac{30}{80} \times 4.5 \right)^2 + 0.4 \right\}^{1/2} = 1.9,$$

which agree surprisingly well with the observations.

(2) Figure 1 of Bernardini, Booth and Lindenbaum (1952, *Phys. Rev.*, **85**, 828) shows the distribution of numbers of black prongs in stars induced by 400 mev protons. The number of events decreases steadily from 3 to 6 prong stars, but has a tail extending to 8 prongs. It seems likely that the steep part of the curve represents a distribution of excitation energy resulting from the primary collisions, and that the tail represents the fluctuation  $\sigma(N_c)$  of the charged particle evaporation. Table 2 gives  $\sigma(N_c) = 1.2$  for  $\bar{N}_c = 7$ , which is consistent with this interpretation of the distribution.

#### REFERENCES

- BAGGE, E., 1941, *Ann. Phys., Lpz.*, **39**, 370.  
 BARTLETT, M. S., and KENDALL, D. G., 1951, *Proc. Camb. Phil. Soc.*, **47**, 65.  
 BARTON, J. C., GEORGE, E. P., and JASON, A. C., 1951, *Proc. Phys. Soc. A*, **64**, 175.  
 BERNARDINI, G., GORTONI, G., and MANFREDINI, A., 1950, *Phys. Rev.*, **79**, 952.  
 CAMERINI, U., LOCK, W. O., and PERKINS, D. H., 1952, *Progress in Cosmic Ray Physics* (Amsterdam: North-Holland).  
 FUJIMOTO, Y., and YAMAGUCHI, Y., 1949, *Prog. Theor. Phys.*, **4**, 468; 1950, *Ibid.*, **5**, 787.  
 HARDING, J. B., LATTIMORE, S. A., and PERKINS, D. H., 1949, *Proc. Roy. Soc. A*, **196**, 325.  
 HODGSON, P. E., 1951, *Phil. Mag.*, **42**, 207; 1952, *Ibid.*, **43**, 190.  
 JÁNOSSY, L., 1950, *Proc. Phys. Soc. A*, **63**, 241.  
 KENDALL, D. G., 1949, *J. R. Statist. Soc. B*, **11**, 230.  
 LE COUTEUR, K. J., 1950, *Proc. Phys. Soc. A*, **63**, 259; *Ibid.*, **63**, 498.  
 MENON, M. G. K., MUIRHEAD, H., and ROCHAT, O., 1950, *Phil. Mag.*, **41**, 583.  
 ROCHESTER, G. D., and ROSSER, W. G. V., 1951, *Rep. Prog. Phys.*, **14**, 227 (London: Physical Society).  
 SELOVE, W., 1951, *Phys. Rev.*, **84**, 869.  
 WEISSKOPF, V., 1937, *Phys. Rev.*, **52**, 295.  
 YAMAGUCHI, Y., 1950, *Prog. Theor. Phys.*, **5**, 439.

## Deuteron Production in the Collision of High Energy Neutrons with Nuclei

By B. H. BRANSDEN\*

Physics Department, University College, London

*Communicated by H. S. W. Massey; MS. received 17th January 1952, and in amended form 2nd April 1952*

**ABSTRACT.** The production of deuterons in high-energy collisions of neutrons with nuclei has been explained in terms of a direct 'pick-up' process by Chew and Goldberger and by Heidmann, the reaction being of the form nucleus  $A + \text{neutron} \rightarrow \text{nucleus } B + \text{deuteron}$ . Here it is shown that an alternative reaction, in which the incident neutron interacts with a nucleon in the target nucleus, which in turn 'picks up' a second nucleon to form a deuteron, is more important at incident energies greater than approximately 200 mev (nucleus  $A + \text{neutron} \rightarrow \text{neutron} + \text{nucleus } B + \text{deuteron}$ ).

The total cross section for deuteron production is calculated numerically for energies of the incident neutron in the range 100–300 mev and comparison is made with the results of the direct 'pick-up' theory.

### § 1. INTRODUCTION

**A**MONG the products of high-energy collisions between nucleons and nuclei a large percentage of deuterons (of energies of the order of 50–100 mev) have been observed. Detailed experiments on the deuterons produced by 90 Mev neutrons incident on carbon, copper and lead (first reported by Brueckner and Powell 1949) have been made by York (1949). Serber and his collaborators (Serber 1947, Serber, Fernback and Taylor 1949, see also Goldberger 1948) have shown that high-energy collisions take place in two stages. During the first stage the incident nucleon traverses the nucleus, which at these energies is partially 'transparent', in a time of the order of  $10^{-22}$  sec, interacting with and possibly ejecting a small number of the target nucleons; the nucleus is left in an excited state and its subsequent break-up, occurring a relatively long time after the primary events, may be described by an 'evaporation' or 'compound nucleus' model. The deuterons observed in these experiments are produced at high energies mainly in the direction of incidence, during the first stage of the reaction. The experimental results have been explained, in the main, in terms of a direct 'pick-up' process (Chew and Goldberger 1950, Heidmann 1950), whereby an incident neutron associates with a proton of a suitable momentum in the target nucleus to form a deuteron, the interaction of the incident neutron with other nucleons in the nucleus being neglected (the incident energy being sufficiently high). The process is thus, in some sense, the converse of the 'stripping' of deuterons to form neutrons.

At even higher energies (from 500–1 000 mev) the primary products of cosmic-ray 'stars' (that is before 'evaporation' takes place) also include a large number of deuterons. At first sight it is difficult to account for these deuterons, as the direct 'pick-up' cross section although large at 100 mev falls off with energy as  $E^{-6}$  (Heidmann 1950). However, at least two alternatives exist, either or both of which may be responsible for the production of these deuterons: (a) incident neutrons may react with neutrons in the nucleus producing deuterons and  $\pi$ -mesons (the reaction  $p + p \rightarrow d + \pi^+$  has been observed); (b) deuterons may be formed as the result of a second-order process in which a nucleon of relatively small momentum (produced by the collision of the incident neutron with a

\* Now at Queen's University, Belfast, Northern Ireland.



nucleon in the target nucleus) 'picks up' a second nucleon in the target nucleus, to form a deuteron. This is the process described below, and will be referred to as the indirect 'pick-up' process.

This indirect process (neutron + nucleus  $A \rightarrow$  deuteron + neutron + nucleus  $B$ ) will favour the production of deuterons of lower energies than those produced by direct 'pick-up', and it is possible that this accounts for the result of Chew and Goldberger (1950) that at 100 mev, rather more low-energy deuterons are produced than is consistent with the direct pick-up energy.

To facilitate comparison, the calculation has been made using, as far as possible, the same constants and methods similar to those of Heidmann, the main points of interest being the relative magnitude of the cross sections at 100 mev and their variation with the energy of the incident neutron.

## § 2. GENERAL THEORY

It is supposed that the energy of the incident neutron 0 is such that it interacts, effectively, with only one nucleus 1 in the target nucleus, the interaction of the nucleon 1 with another 2 in the target nucleus leading to the formation of a deuteron in the final state. To calculate the cross section of this reaction Born's approximation is used, with  $V_{01}$  the interaction between nucleons 0 and 1 as perturbation energy.

The target and residual nuclei are described by the Fermi model, but (following Heidmann 1950) the nucleons 1 and 2 are described by a wave function, generated by their mutual interaction  $V_{12}$ , which differs from a plane wave. The interaction  $V_{12}$  is not introduced explicitly.

The cross section for ejection of deuterons, wave vector  $\mathbf{K}_1$ , from nucleus  $A$  when nucleons 1 and 2 are in a state described by wave vectors  $\mathbf{k}_1, \mathbf{k}_2$  is

$$\sigma(\mathbf{K}_1, \mathbf{k}_0) d\mathbf{K}_1 = \frac{2\pi V}{\hbar v_0} \int d\mathbf{k}_n \delta(E_i - E_f) \rho(k_n, K_1) d\mathbf{K}_1 \\ \times w \{ |(\mathbf{k}_0, \mathbf{k}_1, \mathbf{k}_2 | R^{np} | \mathbf{K}_1, \mathbf{k}_n)|^2 + |(\mathbf{k}_0, \mathbf{k}_1, \mathbf{k}_2 | R^{nn} | \mathbf{K}_1, \mathbf{k}_n)|^2 \} \\ \dots\dots(1)$$

where  $v_0$  is the velocity of the incoming neutron,  $\mathbf{k}_n$  the wave vector of the scattered neutron,  $E_f, E_i$  are the energies of final and initial states,  $\rho(k_n, K_1)$  the density of final states, and the wave functions are normalized to a box of volume  $V$ .

$R^{np}$  is the matrix element for the transition when nucleon 1 is a proton and  $R^{nn}$  is the matrix element when 1 is a neutron.  $w$  is the number of neutron-proton pairs in the nucleus which are in even triplet states; then  $w = \frac{3}{8}(A - Z)Z$ . (It is assumed that the probability of the reaction occurring is small if 1 and 2 are in a singlet state and further that the exchange properties of the nuclear interaction are of the Serber type.) In eqn. (1) the use of the incoherent superposition  $\{|R^{np}|^2 + |R^{nn}|^2\}$  rather than the coherent expression  $\{|R^{np} + R^{nn}|^2\}$  follows from the initial assumption that the energy of the incident neutron 0 is such that it interacts, effectively, with only one nucleon 1 in the nucleus—either a neutron or a proton—the subsequent interaction of nucleon 1 with some other nucleon 2 in the target nucleus forming the deuteron. The coherent expression  $\{|R^{np} + R^{nn}|^2\}$  would occur only for a true three-body collision.

To obtain the cross section irrespective of the initial states of 1 and 2 in the nucleus  $A$ , the expression (1) is multiplied by the probability of finding 1 and 2 in a state described by  $\mathbf{k}_1, \mathbf{k}_2$  (denoted by  $P(\mathbf{k}_1, \mathbf{k}_2) d\mathbf{k}_1 d\mathbf{k}_2$ ) and integrated over all  $k_1, k_2$  such that  $|\mathbf{k}_1|, |\mathbf{k}_2| < L$ ,  $L$  being the radius of the Fermi momentum sphere.

To evaluate the matrix elements  $R^{np}$  (or the similar matrix elements  $R^{nn}$ ) an approximation suggested by Chew (1948) is used. The matrix elements are computed, using Born's approximation, for an imaginary situation, in which particles 0, 1 and 2 are unlike and have no spin. The matrix elements for the reaction then prove to be the product of two terms, one of which,  $G$ , is a function of the momentum lost by the incident neutron ( $\mathbf{k}_0 - \mathbf{k}_n$ ) and the difference ( $\mathbf{k}_1 - \mathbf{k}_2$ ), only. The second term  $F(\mathbf{k}_0 - \mathbf{k}_n)$  turns out to be identical with the matrix element for a free collision (with the same assumptions) of particles 0 and 1 having the relative momentum ( $\mathbf{k}_0 - \mathbf{k}_n$ ).  $F(\mathbf{k}_0 - \mathbf{k}_n)$  contains the potential  $V_{01}$ , while  $G$  does not. The function  $F$  is expressed in terms of the differential cross section for free scattering of particle 0 by particle 1, for which numerical experimental n-p scattering data are substituted.

This procedure avoids the explicit introduction of the imperfectly known potential  $V_{01}$ . Assumptions about the form of potential have to be made when choosing the deuteron ground state wave function and for the wave function describing nucleons 1 and 2, but the exact form of these wave functions does not influence the result critically.

If the momentum of the scattered or ejected particles lies within the occupied Fermi sphere of the residual nucleus, the cross section will be much reduced by the exclusion principle. As the method used does not allow for exchange effects between nucleons (except that the scattering of 1 by 0 is described by experimental data and hence includes exchange effects correctly), the final integrations over the momenta of the scattered and ejected particles have been carried out excluding the occupied Fermi sphere.

To this approximation  $R^{np} = \int \Psi_f^* V_{01}^{np} \Psi_i d\tau$  where  $\Psi_i$  the wave function for the unperturbed system is

$$\Psi_i = V^{-1/2} \psi_A \exp(i\mathbf{k}_0 \cdot \mathbf{r}_0) \quad \dots\dots(2)$$

$\psi_A$  being the wave function of the target nucleus A,  $\Psi_f$  the wave function describing the final state of the system is

$$\Psi_f = V^{-1/2} \psi_B \psi_D(\mathbf{r}_1 - \mathbf{r}_2) \exp(i\mathbf{k}_n \cdot \mathbf{r}_0) \times V^{-1/2} \exp\{i\mathbf{K}_1 \cdot (\mathbf{r}_1 + \mathbf{r}_2)/2\} \quad \dots\dots(3)$$

$\psi_B$  being the wave function of the residual nucleus B and  $\psi_D$  that of the ejected deuteron.

Following Heidmann (1950), the nuclei A, B will be described by a Fermi plane wave model, with the exception of nucleons 1 and 2. Then if  $\eta$  is the volume of nucleus A

$$\psi_A(1 \dots A) = \eta^{-1/2} \phi(3 \dots A) \psi_{\mathbf{k}_3}(\mathbf{r}_1 - \mathbf{r}_2) \exp\{2i\mathbf{K}_3 \cdot (\mathbf{r}_1 + \mathbf{r}_2)/2\} \quad \dots\dots(4)$$

where  $\psi_{\mathbf{k}_3}(\mathbf{r}_1 - \mathbf{r}_2)$  is the wave function describing the relative motion of 1 and 2 in the nucleus and differs from a plane wave by the action of the potential between 1 and 2,  $\mathbf{k}_3$ ,  $\mathbf{K}_3$  being defined by  $\mathbf{k}_3 = \frac{1}{2}(\mathbf{k}_1 - \mathbf{k}_2)$ ,  $\mathbf{K}_3 = \frac{1}{2}(\mathbf{k}_1 + \mathbf{k}_2)$ . If nucleus B and the remainder of nucleus A are described by a plane wave model then the integration over the coordinates of nucleons 3 ... A gives unity.

$$\int \phi(3 \dots A) \psi_B^*(3 \dots A) d\tau_{3 \dots A} = 1. \quad \dots\dots(5)$$

With  $\mathbf{x} = \mathbf{r}_0 - \mathbf{r}_1$ ,  $\mathbf{y} = \mathbf{r}_1 - \mathbf{r}_2$  and  $\mathbf{z} = \frac{1}{2}(\mathbf{r}_1 + \mathbf{r}_2)$  one obtains for  $R^{np}$

$$R^{np} = V^{-3/2} \eta^{-1/2} \int \exp(i\mathbf{K}_2 \cdot \mathbf{x}) V^{np}(\mathbf{x}) d\mathbf{x} \times \int_{\text{nucleus}} \psi_{\mathbf{k}_3}(\mathbf{y}) \psi_D^*(\mathbf{y}) \exp(i\mathbf{K}_2 \cdot \mathbf{y}/2) d\mathbf{y} \\ \times \int_{\text{nucleus}} \exp\{-i(\mathbf{K}_1 - 2\mathbf{K}_3 - \mathbf{K}_2) \cdot \mathbf{z}\} d\mathbf{z} \quad \dots\dots(6)$$

where  $\mathbf{K}_2 = \mathbf{k}_0 - \mathbf{k}_n$ .

The integration over  $\mathbf{z}$ , the position vector of the centre of mass of 1 and 2, is limited by the nuclear boundary and gives therefore a factor  $\eta$  and  $2\mathbf{K}_3 \simeq \mathbf{K}_1 - \mathbf{K}_2$  hence

$$R^{\text{np}} = V^{-3/2} G(\mathbf{K}_2, \mathbf{k}_3) F^{\text{np}}(\mathbf{K}_2)$$

where  $G(\mathbf{K}_2, \mathbf{k}_3) = \eta^{-1/2} \int_{\text{nucleus}} \psi_{\mathbf{k}_3}(\mathbf{y}) \psi_D^*(\mathbf{y}) \exp(i\mathbf{K}_2 \cdot \mathbf{y}/2) d\mathbf{y}$

$$F^{\text{np}}(\mathbf{K}_2) = \int V^{\text{np}}(\mathbf{x}) \exp(i\mathbf{K}_2 \cdot \mathbf{x}) d\mathbf{x}. \quad \dots\dots(7)$$

Since  $\rho(K_1, k_n) = (2\pi)^{-6} V^2$  and  $P(\mathbf{k}_3, \mathbf{K}_3) d\mathbf{k}_3 d\mathbf{K}_3 = (9/2\pi^2 L^6) d\mathbf{k}_3 d\mathbf{K}_3$  (changing from  $\mathbf{k}_1, \mathbf{k}_2$  to  $\mathbf{k}_3, \mathbf{K}_3$  and normalizing so that  $\int P(\mathbf{k}_3, \mathbf{K}_3) d\mathbf{k}_3 d\mathbf{K}_3 = 1$  the integrations being over all  $\mathbf{k}_3, \mathbf{K}_3$  such that  $|\mathbf{k}_1|, |\mathbf{k}_2| \leq L$ , the cross section  $\sigma(\mathbf{k}_6, \mathbf{K}_1)$  may be written finally as

$$\sigma(\mathbf{k}_0, \mathbf{K}_1) = (9/64\pi^7) (w/\hbar v_0 L^6) \int \{ |F^{\text{np}}(\mathbf{K}_2)|^2 + |F^{\text{nn}}(\mathbf{K}_2)|^2 \} \times G^2(\mathbf{k}_3, \mathbf{K}_2) \delta(E_i - E_f) \delta(2\mathbf{K}_3 - \mathbf{K}_1 - \mathbf{K}_2) d\mathbf{K}_2 d\mathbf{k}_3 d\mathbf{K}_3. \quad \dots\dots(8)$$

### (i) The Function $G(\mathbf{k}_3, \mathbf{K}_2)$

If a Yukawa potential is assumed, a very good approximation to the deuteron wave function  $\psi_D$ , which occurs in  $G$  is the Hulthén expression

$$\psi_D = A_D y^{-1} \{ \exp(-\alpha_1 y) - \exp(-\alpha_2 y) \}. \quad \dots\dots(9)$$

Following Heidmann (1950), the wave function  $\psi_{\mathbf{k}_3}(\mathbf{y})$  is taken to be a Hulthén S wave function, for a Yukawa potential. The normalizing constant is adjusted so that in limit  $\delta \rightarrow 0$ ,  $\psi_{\mathbf{k}_3}(\mathbf{y})$  is asymptotic to the S part of a plane wave, normalized to the nuclear dimensions.

$$\psi_{\mathbf{k}_3}(\mathbf{y}) = \eta^{-1/2} y^{-1} (\alpha^2 + k_3^2)^{-1/2} \left[ \frac{\sin(k_3 y + \delta)}{\sin \delta} - e^{-\mu y} \right] \sim \eta^{-1/2} \sin(k_3 y) / k_3 y \text{ when } \delta \rightarrow 0 \quad \dots\dots(10)$$

where  $\cot \delta \simeq -\alpha/k_3$ ,  $\alpha^{-1}$  being the triplet scattering length and  $\mu^{-1}$  the range of the nuclear force for a Yukawa shape.

The integration over the nucleus may be extended over all space without loss of accuracy as  $\psi_D(y)$  decreases sufficiently rapidly with  $y$ , and hence  $G(\mathbf{k}_3, \mathbf{K}_2)$  may be computed by standard methods:

$$G(\mathbf{k}_3, \mathbf{K}_2) = 8\pi A_D K_2^{-1} (\alpha^2 + k_3^2)^{-1/2} \left[ \frac{1}{4} \cot \delta \log \frac{(\alpha_1^2 + q_1^2)(\alpha_2^2 + q_2^2)}{(\alpha_1^2 + q_2^2)(\alpha_2^2 + q_1^2)} + \frac{1}{2} \tan^{-1} \frac{(q_1 + q_2)(\alpha_2 - \alpha_1)(\alpha_1 \alpha_2 + q_1 q_2)}{(\alpha_1^2 - q_1 q_2)(\alpha_2^2 - q_1 q_2) + (q_1 + q_2)^2 \alpha_1 \alpha_2} + \frac{1}{2} \tan^{-1} \frac{2(q_1 + q_2)(\alpha_1 - \alpha_2)}{4(\mu + \alpha_1)(\mu + \alpha_2) + (q_1 + q_2)^2} \right] \quad \dots\dots(11)$$

with  $q_1 = \frac{1}{2} K_2 + k_3$ ,  $q_2 = \frac{1}{2} K_2 - k_3$ .

### (ii) The Functions $F^{\text{np}}(\mathbf{K}_2)$ and $F^{\text{nn}}(\mathbf{K}_2)$

If  $\sigma(\mathbf{K}_2)$  is the differential cross section in the centre-of-mass system for a free collision (in Born's approximation) between unlike particles of relative momentum  $\mathbf{K}_2$ , then

$$\sigma(\mathbf{K}_2) d\Omega = (\mathbf{m}/4\pi\hbar^2)^2 \left| \int V(x) \exp\{-i\mathbf{K}_2 \cdot \mathbf{x}\} d\mathbf{x} \right|^2 = (\mathbf{m}/4\pi\hbar^2)^2 |F(\mathbf{K}_2)|^2.$$

In accordance with the remarks above  $|F^{\text{np}}(\mathbf{K}_2)|^2$  is replaced by  $16\pi^2(\hbar^2/\mathbf{m})^2 \times$  (the experimental cross section for n-p scattering at the appropriate energy) and



$|F^{\text{nn}}(\mathbf{K}_2)|^2$  is replaced by  $16\pi^2(\hbar^2/m)^2 \times$  (the experimental p-p scattering cross section), in default of direct information about the n-n collision.

### (iii) The Energy Relations

The energy of the nucleus A,  $\epsilon_A$  differs from that of nucleus B,  $\epsilon_B$  by the potential and kinetic energies of nucleons 1 and 2 in A, so

$$\epsilon_A - \epsilon_B = (\hbar^2/2m)(k_1^2 + k_2^2) - 58 \text{ mev}$$

where nucleons 1 and 2 are assumed to be moving in a uniform potential well of depth 29 mev. Then, as

$$E_1 - E_f = \epsilon_A - \epsilon_B + (\hbar^2/2m)(k_0^2 - k_n^2) - (\hbar^2/4m)K_1^2 - \epsilon_d$$

where  $\epsilon_d$  is the binding energy of the deuteron, the energy conservation relation becomes

$$\hbar^2/2m(-\frac{1}{2}K_1^2 + 2\mathbf{k}_0 \cdot \mathbf{K}_2 - K_2^2 + 2k_3^2 + 2K_3^2 - B) = 0$$

where the variables have been changed from  $\mathbf{k}_n$ ,  $\mathbf{k}_1$ ,  $\mathbf{k}_2$  to  $\mathbf{K}_2$ ,  $\mathbf{k}_3$ ,  $\mathbf{K}_3$  and where  $B = 58 \text{ mev} + \epsilon_d \approx 56 \text{ mev}$  if the binding energy of the deuteron is taken as approximately 2 mev.

### (iv) Integrations over $\mathbf{K}_3$ , $\mathbf{k}_3$ , $\mathbf{K}_2$ and $\mathbf{K}_1$

To obtain the total cross section, expression (8) has to be integrated over all  $\mathbf{K}_3$ ,  $\mathbf{k}_3$  such that  $|\mathbf{k}_1|, |\mathbf{k}_2| \leq L$  and all  $\mathbf{k}_2$ ,  $\mathbf{K}_1$  such that  $|\mathbf{k}_n|, |\frac{1}{2}\mathbf{K}_1| \geq L$ . The integrations over  $\mathbf{K}_3$  and the angular variables of  $\mathbf{k}_3$ ,  $\mathbf{K}_2$  and  $\mathbf{K}_1$  may be performed analytically by standard methods, with the help of the conservation of momentum ( $2\mathbf{K}_3 = \mathbf{K}_1 - \mathbf{K}_2$ ) and energy relationships.

The total cross section  $\sigma_T(k_0)$  is then obtained by numerical integration over  $k_3$ ,  $K_2$  and  $K_1$ , the limits being

$$\begin{aligned} (a) \quad & 0 \leq k_3 \leq L - \frac{1}{4}|K_1 - K_2|^2 \\ (b) \quad & K_1 - 2L \leq K_2 \leq K_1 + 2L \\ (c) \quad & K_1 \geq 2L, \quad K_1^2 \leq 2\{k_0^2 + L^2 - (2m/\hbar^2)B\}. \end{aligned}$$

If  $\sigma^{\text{np}}$  and  $\sigma^{\text{pp}}$  are the experimental n-p and p-p scattering cross sections then

$$\sigma_T(k_0) = (72w/\pi^2 L^6) \int \{\sigma^{\text{np}}(K_2) + \sigma^{\text{pp}}(K_2)\} G^2(K_2, k_3) \phi(K_1, K_2, k_3) K_1, K_2, k_3^2 dK_1 dK_2 dk_3 \quad \dots (12)$$

where  $G$  is given by eqn. (11) and  $\phi(K_1, K_2, k_3)$  is a complicated factor arising from the angular integrations.

### § 3. NUMERICAL CONSTANTS

As mentioned above the same numerical values were used in computing from eqn. (12) as were used by Heidmann (1950).

(i) For the deuteron ground state wave function:  $A_D^2 = 0.0613 \times 10^{13} \text{ cm}^{-1}$ ,  $\alpha_1 = 0.237 \times 10^{13} \text{ cm}^{-1}$ ,  $\alpha_2 = 1.55 \times 10^{13} \text{ cm}^{-1}$ . For the initial wave function of nucleus 1 and 2  $\psi_{k_0}(y)$ ,  $\alpha^{-1} = 5.39 \times 10^{-13} \text{ cm}$ ,  $\mu = 0.847 \times 10^{13} \text{ cm}^{-1}$ .

(ii) For the Fermi nucleus: The nucleons were considered to move in a uniform potential well of depth 29 mev and the maximum of the Fermi sphere was taken as  $L = 1.0 \times 10^{13} \text{ cm}^{-1}$ .

(iii) For the functions  $F^{\text{np}}(K_2)$ ,  $F^{\text{pp}}(K_2)$ : As explained above, these functions were replaced by the differential cross sections  $\sigma^{\text{np}}$ ,  $\sigma^{\text{pp}}$  for neutron-proton and proton-proton scattering.

(a)  $\sigma^{pp}$  proton-proton scattering. The scattering was taken as isotropic in the centre-of-mass system the differential cross sections being of magnitude  $3.9 \times 10^{-26} \text{ cm}^2$  at 340 mev (Chamberlain *et al.* 1950, 1951),  $5.0 \times 10^{-26} \text{ cm}^2$  at 146 mev (Cassels *et al.* 1951),  $5.5 \times 10^{-26} \text{ cm}^2$  at 105 mev (Birge *et al.* 1951).

(b)  $\sigma^{np}$  neutron-proton scattering. The data of Hadley *et al.* (1950) at 260 mev and Hadley *et al.* (1949) at 90 mev was used. (The total n-p cross section of Hadley *et al.* is in good agreement with more recent measurements at 95 mev by De Juren and Knable (1950) and at 97 mev by Taylor *et al.* (1951)). The total cross sections are  $0.076 \times 10^{-24} \text{ cm}^2$  at 90 mev and  $0.035 \times 10^{-24} \text{ cm}^2$  at 260 mev.

The differential cross sections are roughly symmetrical about  $90^\circ$ . The forward direction only is of importance and the cross sections in this region are approximately of the form  $a/(b + K_2^2)$ .

(iv) The Number  $w = \frac{3}{8}(A - Z)A$ : If  $Z$  is taken as  $A/2$  then  $w = \frac{3}{16}A^2$ . As explained below, the number of nucleons effective in deuteron production is less than  $A$  and a correction has to be made.

#### §4. NUMERICAL RESULTS AND CONCLUSION

The total cross sections computed from eqn. (12) are shown in the table, compared with those of Heidmann, for energies of 100, 200 and 300 mev. As eqn. (12) describes a kind of double process, the cross section depends on  $A^2$ , in contrast with the direct pick-up cross section which is proportional to  $A$ .

Energy (mev)	100	200	300
Indirect cross section (from eqn. (12)) ( $10^{-28} \text{ cm}^2$ )	$3.6 A^2$	$5.5 A^2$	$4.5 A^2$
Direct cross section (Heidmann 1950) ( $10^{-28} \text{ cm}^2$ )	$194 A$	$37 A$	$10.5 A$

The asymptotic variation of the cross section with energy may be deduced from eqn. (12) and the expressions for  $G$  and  $\phi$ . If it is assumed that the variation with energy of the function  $F(K_2)$  is small above 300 mev, then the total cross section will decrease as  $E_0^{-1}$ . This is in marked contrast to the variation of the direct 'pick-up' cross section which Heidmann found to decrease with energy at  $E_0^{-6}$ .

In comparing theory with experiment certain difficulties arise. The Fermi model used cannot be expected to give good agreement for nuclei such as carbon (for which the most complete experiments have been made), and on the other hand, for heavier nuclei the incident neutrons may make several collisions in passing through the nucleus. Another difficulty is that if deuteron production occurs inside the nucleus the deuteron will have a large probability of disintegrating before it can escape. Heidmann supposed that deuteron production occurred in a layer of thickness  $r_0$  (the nuclear volume being  $4\pi r_0^3 A/3$ ) on the escape side of the nucleus, thus reducing the effective number of nucleons from  $A$  to  $\frac{3}{4}A^{2/3}$ . The theoretical total cross section for carbon given by Heidmann was  $8 \times 10^{-26} \text{ cm}^2$ , about three times the experimental value of  $2.6 \times 10^{-26}$ ; the discrepancy is probably due in part to overestimating the thickness of the deuteron producing layer. However, these considerations do not affect the ratio of the cross sections for the direct and indirect modes of deuteron production.

Figure 1 indicates the cross section as a function of energy for a carbon nucleus, where the deuteron producing layer is of thickness  $r_0$ . At 100 mev the cross section for the indirect process is 11% of the direct pick-up cross section.

This is satisfactory, as at this energy the experimental data may be explained in the main by the direct 'pick-up' process. At 300 mev, however, the indirect process is already twice as important as direct pick-up and at higher energies predominates.

It is characteristic of the indirect process that the production of deuterons of low energies is favoured, in marked contrast to the direct pick-up distribution where at high energies the deuterons are produced in a narrow band at  $8E_0/9$ . The energy distribution for  $E_0=300$  mev is shown in fig. 2. The production of deuterons below 41 mev is not considered, the cross section probably decreasing rapidly below this energy, as then the individual particles of the deuteron would have momenta less than the Fermi maximum.

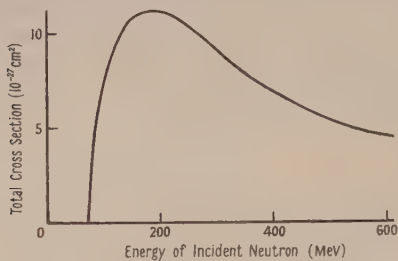


Fig. 1. Total cross section for the production of deuterons by neutron bombardment of a carbon nucleus (indirect process).

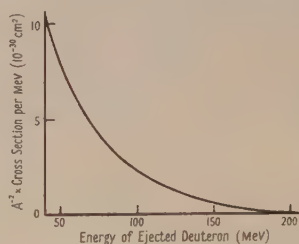


Fig. 2. The energy spectrum of deuterons ejected by neutrons of energy 300 mev.

To conclude, it may be said that while at the lower energies of the order of 100 mev, deuteron production can be understood in terms of a direct pick-up process, at higher energies, indirect processes play an increasingly important part. Although comparison of the magnitude of theoretical and experimental cross section is difficult, the mode of production may be distinguished easily by means of the energy distribution of the emerging deuterons.

#### ACKNOWLEDGMENT

I wish to thank Dr. E. H. S. Burhop for his advice and interest in the problem.

#### REFERENCES

- BIRGE, R. W., KRUSE, V. E., and RAMSEY, N. F., 1951, *Phys. Rev.*, **83**, 274.  
 BRUECKNER, K., and POWELL, W. M., 1949, *Phys. Rev.*, **75**, 1224.  
 CASSELS, J. M., STAFFORD, G. H., and PICKAVANCE, T. G., 1951, *Nature, Lond.*, **168**, 468.  
 CHAMBERLAIN, O., and WIEGAND, C., 1950, *Phys. Rev.*, **79**, 81.  
 CHAMBERLAIN, O., WIEGAND, C., and SEGRÈ, E., 1951, *Phys. Rev.*, **81**, 661.  
 CHEW, G. F., 1948, *Phys. Rev.*, **74**, 809.  
 CHEW, G. F., and GOLDBERGER, M. L., 1950, *Phys. Rev.*, **77**, 474.  
 DE JUREN, J., and KNABLE, N., 1950, *Phys. Rev.*, **77**, 606.  
 GOLDBERGER, M. L., 1948, *Phys. Rev.*, **74**, 1296.  
 HADLEY, J., KELLY, E., LEITH, C., SEGRÈ, E., WIEGAND, C., and YORK, H., 1949, *Phys. Rev.*, **75**, 351, and **76**, 38; 1950, *Ibid.*, **79**, 98.  
 HEIDMANN, J., 1950, *Phys. Rev.*, **80**, 171.  
 SERBER, R., 1947, *Phys. Rev.*, **72**, 1114.  
 SERBER, R., FERNBACH, S., and TAYLOR, T. B., 1949, *Phys. Rev.*, **75**, 1352.  
 TAYLOR, A. E., PICKAVANCE, T. G., CASSELS, J. M., and RANDLE, T. C., 1951, *Phil. Mag.*, **42**, 328.  
 YORK, H. F., 1949, *Phys. Rev.*, **75**, 1467.



# The Angular Distribution of Long-Range Alpha-Particles from the Bombardment of Boron-11 by Protons

BY D. M. THOMSON, A. V. COHEN, A. P. FRENCH  
AND G. W. HUTCHINSON

Cavendish Laboratory, University of Cambridge

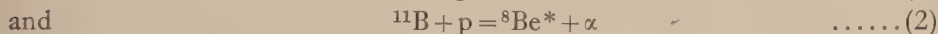
*Communicated by O. R. Frisch; MS. received 14th January 1952, and in amended form 10th March 1952*

**ABSTRACT.** The angular distribution of alpha-particles of long range from the reaction  $^{11}\text{B}(p, \alpha)^8\text{Be}$  has been studied over the range 130 to 280 kev proton energy. A strong anisotropy varying with energy is observed and can be explained in terms of an interference between states of opposite parity in  $^{12}\text{C}$ . The theoretical analysis gives the result that the well-known 16.11 mev level in  $^{12}\text{C}$  formed by resonant capture of 162 kev protons in  $^{11}\text{B}$  has spin 2 and even parity.

## § 1. INTRODUCTION

THE reaction of  $^{11}\text{B}$  with protons gives a high yield of alpha-particles at comparatively low bombarding energies and was one of the first nuclear reactions to be studied. Cockcroft and Lewis (1936) bombarding a thick target at 300 kev found a continuous distribution of alpha-particles with a maximum range in air of about 4 cm, and a much less intense homogeneous group of about 4.4 cm range.

Dee and Gilbert (1936) showed that the observed spectrum could be produced by the competing processes



followed in each case by break-up of the  $^8\text{Be}$  into two alpha-particles.

The present work is concerned only with the homogeneous group which leads to the ground state of  $^8\text{Be}$ . No measurements have been made on the continuum.

A resonance at about 160 kev bombarding energy in the yield of the long range group was discovered by Williams *et al.* (1937). The resonance has since been shown to be identical with that found for the  $^{11}\text{B}(p, \gamma)^{12}\text{C}$  reaction and has been studied repeatedly (Jacobs and Whitson 1941, Marvin 1945, Morrish 1949, Neuert 1937, 1939). Recent work by Tangen (1946) and Morrish (1949) has established the natural width of the level and the absolute voltage at which the resonance maximum occurs.

The angular distribution of the long range group has also been studied, but it proved difficult to make sure that none of the particles from the much more intense continuous distribution were being included. The present work has shown that the continuum overlaps the long range group rather more in the forward than in the backward direction. Mica absorbers—as employed in almost all the older measurements—may not be very reliable for separating the two components, in view of straggling, etc. In the work to be described here a fast pulse-height analyser (Hutchinson and Scarrott 1951) and proportional counter was used. This made it possible to observe the spectrum of alpha-particles while counting was in progress and to estimate the contribution of the continuum to the recorded count at each experimental point.

## § 2. EXPERIMENTAL TECHNIQUE

2.1. *General Arrangement*

The 1 mv High Tension apparatus of the Cavendish Laboratory was used to supply protons with energies between 100 and 300 kev. The targets were thin films of ordinary borax (of about 4 kev thickness for protons) evaporated on to thin aluminium foil and supported on a wire frame at the centre of an evacuated cylindrical tank. The beam of protons was limited to a diameter of  $\frac{1}{8}$  in. by a molybdenum stop at the entrance to the tank. Two proportional counters, to detect the alpha-particles, were mounted on arms which could be rotated (using standard oil seals and Gaco rings) about an axis through the centre of the tank. Kovar-glass seals were used to bring in the counter leads, and the coupling condensers and pre-amplifiers were supported immediately outside. The counter cases were maintained at earth potential. Figure 1 shows the general arrangement.

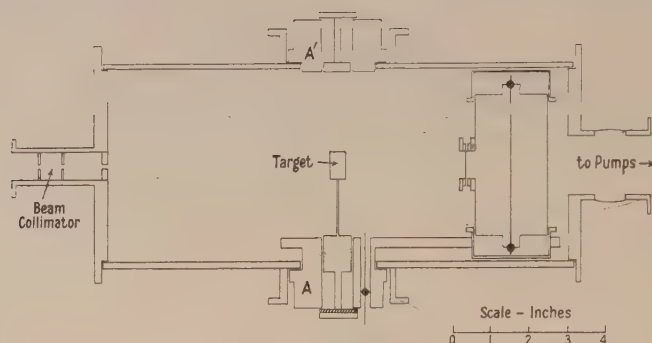


Fig. 1. Diagrammatic view of apparatus. The cylindrical block A carries the counter shown. A' carries the second counter, which is omitted for clarity.

2.2. *Counters and Target*

The counters were made from brass tubing of 2 in. internal diameter and their overall length was about  $3\frac{1}{2}$  in. The wire, 0.002 in. diameter tungsten, was supported along the counter axis by two Kovar seals. A mica window of about 2 cm air equivalent with a circular aperture of about  $\frac{3}{4}$  in. diameter was mounted on the side of each counter by sealing the mica between two brass rings with Araldite; no supporting grid was then needed.

The counters were filled with slightly purified tank argon at 60 cm pressure, sufficient to stop all the alpha-particles from the  $^{11}\text{B}(\text{p}, \alpha)^8\text{Be}$  reaction, and were normally used at 800 volts, giving a gas amplification of about 10. With no special precautions it was found that the counters gave peaks of about 200 kev width at half height for 5 mev alpha-particles.

Monitoring was done by keeping one of the counters at a fixed angle, usually  $150^\circ$  to the beam. The other counter was moved round to plot out the angular distributions.

When thin foil targets were used there was no trouble from the deposition of carbon layers on the target surface, though solid backed targets did collect such layers.

2.3. *Counting Procedure*

The output of the amplifier associated with the moving counter was connected in parallel to the inputs of an ordinary discriminator and of the pulse-height

analyser. The visual display of this instrument showed the peak due to the long-range group at the end of a continuous distribution from the other processes. The bias of the discriminator was related to the channel number of the pulse height analyser by injecting a standard test pulse into the pre-amplifier, and in an actual measurement the bias was set at a voltage corresponding approximately to the valley between the continuum and the group in the pulse-height distribution. Pulses of a height greater than this were counted on a scale of 100. It was felt necessary to adopt this procedure rather than to rely on the readings of the pulse height analyser directly, because in some of the measurements the average interval between pulses was shorter than the maximum dead time (1.2 msec) of the analyser.

It will be seen from the plot of a typical spectrum (fig. 2) that it was not possible in practice to resolve the long-range group completely from the continuum. This was probably due to a combination of poor resolution in the counter and a genuine overlap in energy (caused in part by straggling in the mica window). In order to estimate the number of particles in the long-range group the spectrum was plotted on semi-log paper and the upper end of the continuum

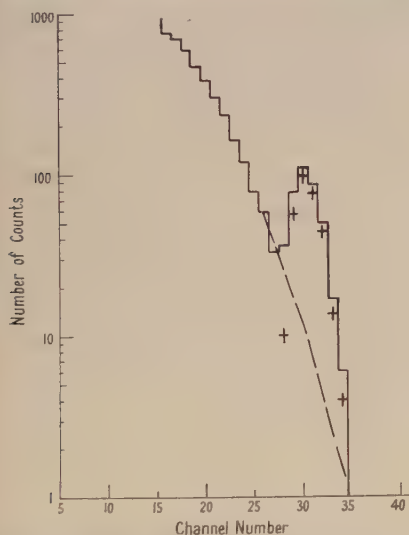


Fig. 2. Pulse height spectrum observed at 230 keV,  $30^\circ$  to beam. The crosses represent yield in homogeneous group after subtraction of continuum.

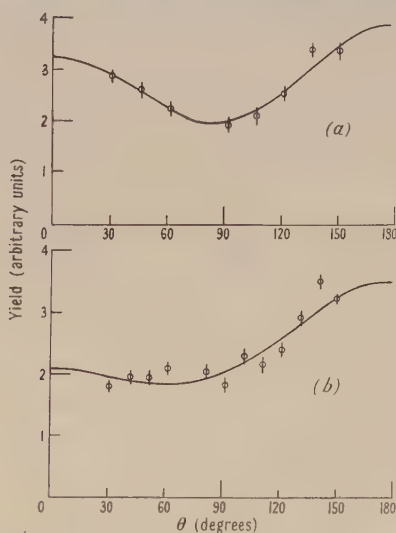


Fig. 3. Angular distributions near resonance. Values of coefficients are:  
(a) 162 keV:  $a = -0.15$ ,  $b = +0.78$ .  
(b) 172 keV:  $a = -0.36$ ,  $b = +0.39$ .

extrapolated. The background thus obtained was subtracted from the total count recorded by the pulse-height analyser in the channels above the voltage level defined by the discriminator. The result was used to correct the count registered by the scaler. (Plotting on semi-log paper allowed an almost linear extrapolation to be made.) The background to be subtracted in this way amounted usually to 20% or less of the total count, and no substantial error is thought to have arisen from the process. A test showed that it produced a symmetrical peak for the long-range group even under quite unfavourable conditions, namely for a spectrum observed at a forward angle (see fig. 2).

Readings were taken at angles between  $30^\circ$  and  $150^\circ$  to the proton beam. (The limits were set by the size of the counters.) The forward and backward



readings were taken with the target at  $90^\circ$  to the beam. In order to obtain points between  $120^\circ$  and  $70^\circ$  the target was rotated to  $45^\circ$  and the two distributions were normalized to fit at  $150^\circ$  and  $120^\circ$ .

The angular symmetry of the tank was checked by mounting on the target holder a  $\text{ThC} + \text{C}'$  alpha-particle source of the same size as the target spot. No departure from isotropy was found greater than 1% and no correction has been made.

### § 3. RESULTS

Preliminary runs with a solid target backing confirmed the general result of Neuert (1937, 1939) that the angular distribution is markedly more anisotropic near the resonance than at higher energies. It was also found that the distribution appeared to contain a term in  $\cos \theta$ , and this was confirmed when foil targets were used, allowing measurements as far forward as  $30^\circ$ . Detailed angular distributions were taken at the resonance and at about 10 kev higher bombarding energy. The results, corrected for centre-of-mass motion, are shown in fig. 3. The solid curves have been fitted using the method of least squares, and the numerical values of the constants in expressions of the form  $I(\theta) = 1 + a \cos \theta + b \cos^2 \theta$  are shown below each curve. Corrections to take account of the finite angle subtended by the counter window were found to be always less than 1% and have therefore been ignored.

Following the discovery of this definite evidence for the existence of a  $\cos \theta$  term in the distribution, the magnitude of which varies with the bombarding energy, the technique of Devons and Hine (1949) was then adopted and the ratio of the yields at  $150^\circ$  and  $30^\circ$  measured over a range of voltage from 130 kv to 300 kv. The results corrected for centre-of-gravity motion are shown in fig. 4 together with an excitation curve. It was not possible to obtain reliable results below 130 kv because of the instability of the h.t. set and the extremely low yield; above 300 kv the long-range group becomes almost swamped by the continuum at the forward angle and the subtraction process becomes unreliable. It will be seen that the curve has a form very similar to that obtained by Devons and Hine near the 440 kev resonance in the  ${}^7\text{Li}(p, \gamma){}^8\text{Be}$  reaction, though the voltage scale is less extensive.

An uncertainty in all the readings has been in the absolute value of the bombarding voltage. The h.t. set uses a high voltage (30 kv) discharge tube ion source for which the initial energy of the beam depends on the rate of gas inflow. It was found that this caused the apparent resonance voltage, as read on the high voltage meter, to vary by as much as 10 kv from day to day. It does appear, however, to have remained constant over the period of any one run, and each day's readings have been adjusted to give the resonance voltage the same nominal value.

### § 4. THEORY

#### 4.1. Preliminary Discussion

The anisotropy of the alpha-particles at resonance implies that protons of  $l=1$  or higher must be effective in forming this sharp state. Considerations of barrier penetrability at such low energies make it likely that  $l=1$  is in fact the correct choice, as the yield observed by Bowersox (1939) appears too large to

admit of  $l=2$  or more. The variation of angular distribution with energy (fig. 4) points to the interference of two states of opposite parity. We therefore suppose the broad state to be formed by protons with  $l=0$ .

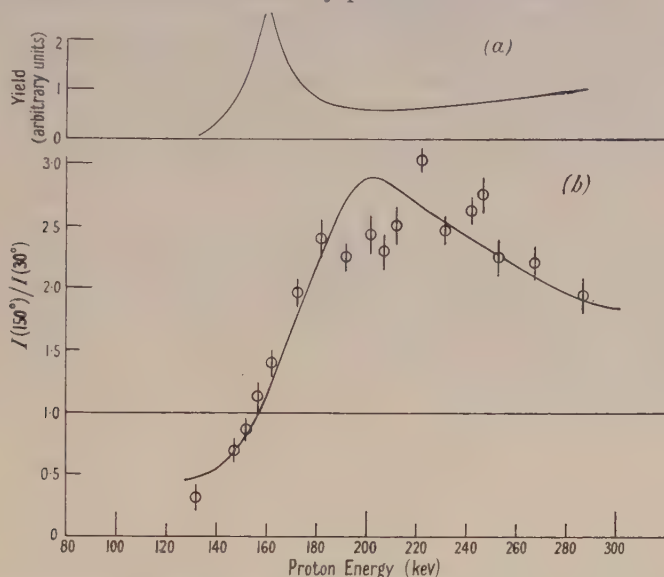


Fig. 4. (a) Observed thin target excitation curve at  $150^\circ$ . (b) Variation of  $I(150^\circ)/I(30^\circ)$  with energy (same energy scale as (a)). The full curve is obtained from the theoretical analysis.

We shall assume that  $^{11}\text{B}$  has spin  $3/2$  and odd parity. This is in accord with experiment (Gordy *et al.* 1948) and with the predictions of the shell model. With these assignments of spin and orbital momentum, we arrive at the following possible designations of the interfering states in  $^{12}\text{C}^*$ :

Resonant state ( $l=1$ ):  $(0, +)$ ,  $(1, +)$ ,  $(2, +)$ ,  $(3, +)$

Broad state ( $l=0$ ):  $(1, -)$ ,  $(2, -)$ .

Both the resonant and the broad states undergo a branched  $\alpha$ -decay to the ground state or to the first excited state of  $^8\text{Be}$ . Both of the  $^8\text{Be}$  states break up into two  $\alpha$ -particles, and therefore have even spin and even parity. Moreover, it seems probable that one or other of these  $^8\text{Be}$  states has zero spin, and the formation of a  $(0, +)$  state of  $^8\text{Be}$  by  $\alpha$ -particle emission from  $^{12}\text{C}^*$  can occur only if the latter has spin and parity denoted by  $(0, +)$ ,  $(1, -)$ ,  $(2, +)$ ,  $(3, -)$ , etc. We can thus infer that the broad compound state of  $^{12}\text{C}$  is  $(1, -)$  and that the resonant state is  $(2, +)$ . Zero spin is of course excluded, since it would lead to an isotropic angular distribution at resonance.

If the spin of the  $^{12}\text{C}$  resonant state is indeed 2, it seems likely that the ground state of  $^8\text{Be}$  has zero spin, and that the excited state has spin 2. The evidence pointing to this in the present reaction is of two kinds.

(a) The transition from the  $^{12}\text{C}$  resonant state to the ground state of  $^8\text{Be}$  is much less probable ( $\sim \frac{1}{100}$ ) than the competing transition to the first excited level. If we assign zero spin to the ground state, and spin 2 to the excited state, transitions to the former could occur only by d-wave  $\alpha$ -particle emission, whereas s-wave as well as d-wave  $\alpha$ -particles would be effective in the latter case.

(b) The strong anisotropy of the long-range alpha-particles at resonance would be surprising if the ground state of  $^8\text{Be}$  has spin 2, since in this case one would expect that emission of s-wave alpha-particles would render the angular distribution predominantly isotropic.

It must be admitted that neither of these arguments is very substantial, for the coulomb and angular momentum barriers do little to discourage d-waves as against s-waves in the alpha-particle emission. Our assignment is, however, favoured on theoretical grounds and also finds support in some recent work on the reaction  $^{12}\text{C}(\gamma, \alpha)$  (Telegdi 1951).

#### 4.2. Detailed Analysis

We now make use of the above conclusions to obtain the exact form of the angular distributions. The spins of  $^{11}\text{B}$  and a proton can combine to give a resultant  $j$  equal to 1 or 2. Only  $j=1$  can be effective in forming the broad state, but both spin combinations can take part in forming the resonant state. The differential cross section at a given energy  $E$  can thus be written in the form:

$$\sigma(\theta, E) \sim \sum_{m,=0,\pm 1} \left| \langle 1, m; 1, 0 | 2, m \rangle \frac{A e^{i\alpha}}{(E-E_r) + \frac{1}{2}i\Gamma} Y_2^m(\theta, \phi) + pB e^{i\beta} e^{i\pi} Y_1^m(\theta, \phi) \right|^2 \\ + \sum_{m,=0,\pm 1,\pm 2} f \left| \langle 2, m; 1, 0 | 2, m \rangle \frac{A e^{i\alpha}}{(E-E_r) + \frac{1}{2}i\Gamma} Y_2^m(\theta, \phi) \right|^2.$$

Here  $p = \{P_0(E)/P_1(E)\}^{1/2}$  where  $P_0(E)$  and  $P_1(E)$  are the barrier penetrabilities at energy  $E$  for s and p proton waves respectively (Christy and Latter 1948).  $(A, \alpha)$  and  $(B, \beta)$  relate the amplitude and phase for the resonant state to that for the broad state after allowance has been made for resonance factors and the size of the barrier penetration factor. The additional phase  $\pi$  that we have introduced for the broad state comes from our assumption that it has a resonance at a much higher energy.  $f$  is the relative probability that the resonant state should be formed from the initial spin configuration  $j=2$ . Inserting the appropriate values of transformation coefficients  $\langle j, m; l, 0 | J, m \rangle$  (Condon and Shortley 1935, 1951) and spherical harmonics, we find

$$\sigma(\theta, E) \sim \frac{5}{4} \frac{1}{R^2} \left\{ \left( \frac{1}{3} + f \right) + (1-f) \cos^2 \theta \right\} + \frac{3}{2} a^2 p^2 + \sqrt{10} a p \frac{1}{R} \cos(\alpha - \beta - \delta - \pi) \cos \theta.$$

In this expression we have used the following abbreviations:

$$R(E) = \{E - E_r\}^2 + \frac{1}{4}\Gamma^2\}^{1/2}, \quad a = B/A, \quad \delta(E) = \tan^{-1} \{\Gamma/2(E - E_r)\}.$$

The values of  $E_r$  and  $\Gamma$  are known from the work of Morrish (1949) and Tangen (1946). The other parameters at our disposal in fitting the experimental results are  $f$ ,  $(\alpha - \beta)$  and  $a$ . All these may be energy dependent, although we have fitted the results assuming them constant. It is reasonable to suppose that their variations are small, provided that we are far from any resonance for the broad state. The change with energy of long-range alpha-particle yield between 200 and 500 kev (von Ubisch 1942) can in fact be explained in terms of barrier penetration alone.

#### § 5. COMPARISON WITH EXPERIMENT

The value of  $f$  in the expression for the differential cross section was found from the coefficient of  $\cos^2 \theta$  at resonance, where the influence of the broad state is very small, and the term in  $a^2$  can be ignored. The coefficient of  $\cos^2 \theta$  at resonance is then  $(1-f)/(\frac{1}{3}+f)$ . The mean of several determinations at resonance gave  $f = 0.42 \pm 0.02$ .



The ratio of the differential cross sections at  $150^\circ$  and  $30^\circ$  is then easily found to be

$$Z(E) = \frac{1 + a^2 p^2 R^2 - 1.84 a p R \cos \phi}{1 + a^2 p^2 R^2 + 1.84 a p R \cos \phi}$$

where  $\phi(E) = \alpha - \beta - \delta - \pi$ .

At a fair distance from resonance, such that  $(E - E_r) > 5\Gamma$ , we can assume that to the order of accuracy of the experiment  $R$  can be written as  $(E - E_r)$  and  $\phi$  remains constant. In fact, the error in  $R$  thus introduced, even at  $(E - E_r) = 5\Gamma$ , is only 1%, and  $\phi$  changes by as little as  $6^\circ$  in going from  $(E - E_r) = 5\Gamma$  to  $(E - E_r) = \infty$ .

It is convenient to consider the function  $(Z+1)/(Z-1)$  in this region; using this function, a method of least squares may be devised to find the values of  $a$  and  $\cos \phi$  which agree best with the experimental points.

By taking a suitable mean value of  $\delta$  in this region, we find  $a = 0.022 \pm 0.002$ ,  $\alpha - \beta = 60^\circ \pm 7^\circ$ .

With these values for the parameters the exact expression for  $Z(E)$  was calculated for the whole range of energies, from 120 kv to 300 kv, and the result is shown as the full curve in fig. 4(b). Its close agreement with the observed values may be taken as to some extent confirming the constancy of  $a$ .

It is interesting to note that modern dispersion theory (Wigner and Eisenbud 1947) predicts a definite value for  $\alpha - \beta$ . It is determined by the phase angles of the complex penetration factors for incoming protons and outgoing alpha-particles. We have calculated this angle, using the tabulation of coulomb functions by Bloch *et al.* (1951), and find it to be about  $-60^\circ$  (with little dependence on the assumed value of nuclear radius). The curve obtained with the theoretical phase would resemble that of fig. 4(b), except that the  $\cos \theta$  term in the angular distribution would vanish a few kilovolts above resonance, instead of below as the experimental results suggest. The discrepancy appears to be genuine, but the following points should be considered: (i) The definition of proton energy in the experiment was not very good, and an observed angular distribution represents an average over several times the width of the 162 keV resonance. Computation shows that this does not markedly affect the observed value of the phase; it could shift the curve of  $I(150^\circ)/I(30^\circ)$  in the desired direction, but only by about 2 kv. (ii) The outgoing alpha-particle energy is near the top of the potential barrier, and the theoretical phase shift may be very sensitive to the assumed shape of potential near the nuclear boundary. Bloch *et al.* (1951) give the phase retardations for a pure coulomb potential since it is usual, though perhaps not very realistic, to assume such a shape right down to the nuclear radius. One could thus argue that a comparison with theory is not profitable in experiments of this kind unless both ingoing and outgoing particles have energies well below their respective barrier heights.

The shape of the curve of fig. 4(b) is determined in the main by  $a$  and  $\alpha - \beta$ , and the value of  $\Gamma$  only affects the curve in the region of the resonance peak. The experimental results cannot, therefore, be used to obtain an accurate value for  $\Gamma$ , the resonance width.

## § 6. CONCLUSION

The main feature of the experiments described here is undoubtedly the demonstration of interference effects between states of opposite parity. It is difficult to draw any quantitative conclusions from the fitting of a theoretical

curve to the experimental points. It does, however, seem clearly established that the resonant state in  $^{12}\text{C}$  formed at 162 kev proton energy has spin 2 and even parity. Although our analysis gives a fairly good fit to the measurements, its assumption that the interfering background is due to a single state of spin one and odd parity is not demanded by the results, and further measurements of the excitation function above 300 kv would be desirable.

#### ACKNOWLEDGMENTS

We are grateful to Mr. A. M. Lane, of Selwyn College, Cambridge, for an illuminating discussion of modern dispersion theory as it applies to these experiments.

Two of us (D. M. T. and A. V. C.) wish to thank Trinity College, Cambridge, for scholarships, and the Department of Scientific and Industrial Research for grants while this work was being done.

One of us (G. W. H.) wishes to thank the administrators of the University of Cambridge Clerk Maxwell Scholarship Fund for financial support during the course of the work.

We would like to thank Mr. M. B. Turner and Mr. R. G. Hawkins for much technical assistance.

#### REFERENCES

- BLOCH, I., *et al.*, 1951, *Rev. Mod. Phys.*, **23**, 147.  
 BOWERSOX, R. B., 1939, *Phys. Rev.*, **55**, 323.  
 CHRISTY, R. F., and LATTE, R., 1948, *Rev. Mod. Phys.*, **20**, 185.  
 COCKCROFT, J. D., and LEWIS, W. B., 1936, *Proc. Roy. Soc. A*, **154**, 246.  
 CONDON, E. U., and SHORTLEY, G. H., 1935 and 1951, *The Theory of Atomic Spectra* (Cambridge: University Press).  
 DEE, P. I., and GILBERT, C. W., 1936, *Proc. Roy. Soc. A*, **154**, 279.  
 DEVONS, S., and HINE, M. G. N., 1949, *Proc. Roy. Soc. A*, **199**, 56 and 73.  
 GORDY, W., RING, H., and BURG, A. B., 1948, *Phys. Rev.*, **74**, 1191.  
 HUTCHINSON, G. W., and SCARROTT, G. G., 1951, *Phil. Mag.*, **42**, 792.  
 JACOBS, J. A., and WHITSON, W. L., 1941, *Phys. Rev.*, **59**, 108.  
 MARVIN, J. F., 1945, *Phys. Rev.*, **68**, 228.  
 MORRISH, A. H., 1949, *Phys. Rev.*, **76**, 1651.  
 NEUERT, H., 1937, *Phys. Z.*, **38**, 621; 1939, *Ann. Phys., Lpz.*, **36**, 437.  
 TANGEN, R., 1946, *K. Norske Vidensk. Selsk. Skr.*, **19**, No. 1.  
 TELEGI, V. L., 1951, *Phys. Rev.*, **84**, 600.  
 VON UBISCH, H., 1942, *K. Norske Vidensk. Selsk. Skr.*, **15**, No. 9.  
 WIGNER, E. P., and EISENBUD, L., 1947, *Phys. Rev.*, **72**, 29.  
 WILLIAMS, J. H., *et al.*, 1937, *Phys. Rev.*, **51**, 434.

## Angular Distributions of Particle Groups from Deuteron Bombardment of Neon

BY R. MIDDLETON AND C. T. TAI  
 Nuclear Physics Laboratory, University of Liverpool

*Communicated by H. W. B. Skinner; MS. received 8th February 1952*

**ABSTRACT.** The angular distributions of nine proton groups, the elastically scattered deuteron group and an inelastically scattered deuteron group from the 8 mev deuteron bombardment of neon have been investigated using the photographic plate technique. The absolute differential cross sections for the production of the various groups have been calculated and the spins and parities of some of the states of the residual nucleus  $^{21}\text{Ne}$  determined.

## § 1. INTRODUCTION

IN a previous communication (Middleton and Tai 1951) the technique used to investigate the charged particles emitted when neon of normal isotopic constitution was bombarded by 8 Mev deuterons was described. Also presented were the measured  $Q$ -values of the reactions  $^{20}\text{Ne}(d, p)^{21}\text{Ne}$ ,  $^{20}\text{Ne}(d, d')^{20}\text{Ne}$  and  $^{20}\text{Ne}(d, \alpha)^{18}\text{F}$ . In this communication the angular distributions of the protons, elastically scattered deuterons and inelastically scattered deuterons are presented.

## § 2. PROCEDURE

From the measurement of the total number of tracks belonging to a particular particle group in a well-defined area of emulsion and the known geometry of the scattering chamber (Chadwick *et al.* 1944, Rotblat *et al.* 1951) the relative cross sections of the various particle groups at different angles can be calculated. Since the intensities of most of the particle groups, particularly the elastically scattered deuterons, show a pronounced maximum at small angles it is necessary to make more than one exposure of different intensities to obtain a convenient track density at all angles. For our purpose two exposures were made, one with neon at a pressure of 18.6 cm Hg and a total beam intensity of 0.62 microcoulomb, the other, intended for measurement at small angles, with neon at a pressure of 10.0 cm Hg and a beam intensity of 0.25 microcoulomb. Comparison between the two exposures was made by measuring the numbers of elastically scattered deuterons within the same area at angle  $30^\circ$ . The ratio of the exposures thus obtained differs by  $7 \pm 3\%$  from the value computed from the above exposure data. The weaker exposure was used for measurement of angles  $20^\circ$  and  $25^\circ$  and the mean value of the ratios of the two exposures was used to correlate the data with that of the other angles.

Measurements have been made at fourteen angles, for each of which some 3000 proton and deuteron tracks were measured within an area of about  $10\text{ mm}^2$ . Due to the excessive intensity of the elastically scattered deuterons at angles less than  $30^\circ$ , the major portion of the measurements were made neglecting tracks within the range limits of the elastically scattered deuterons. The number of tracks contained in groups which were not entirely resolved was obtained by fitting each group with a gaussian distribution.

Since the emulsions used were of thickness  $100\text{ }\mu$ , there was a tendency for some of the long range tracks to escape either into the glass or out of the surface. To minimize this effect the positions of measurement were chosen so that the angle of incidence of the particles with respect to the emulsion lay between  $4^\circ$  and  $8^\circ$ . The number and range of all tracks escaping were also recorded. These tracks were then assigned to the longer range groups in proportion to the number of tracks already contained in these groups. This simple method of correction was adopted since corrections based on statistical considerations of scattering phenomena are both complicated and not justifiable for the small number of observed escape tracks. The uncertainty in this correction for the four long range proton groups is believed to be less than 6% of the total number of particles in the groups and for the remaining groups to be negligible.

## § 3. RESULTS

The results of the measurements of the angular distributions have been converted into the centre-of-mass system and in figs. 1 and 2 are shown those



obtained for the elastically and inelastically scattered deuteron groups. In figs. 3 and 4 are shown the distributions of the proton groups  $P_0$  and  $P_1$  corresponding to the formation of  $^{21}\text{Ne}$  in the ground and first excited states respectively. The unit of relative intensity is the same for all groups and corresponds to a differential cross section of 0.74 millibarn/steradian (see §4).

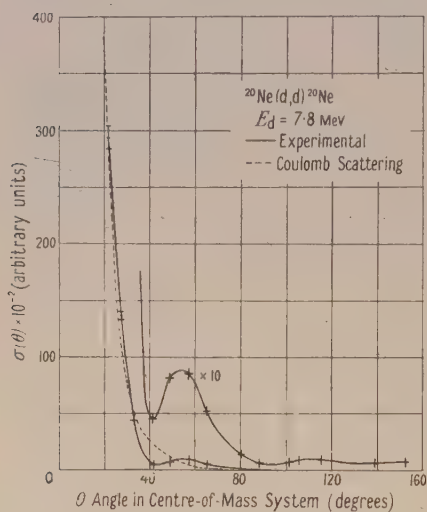


Fig. 1.

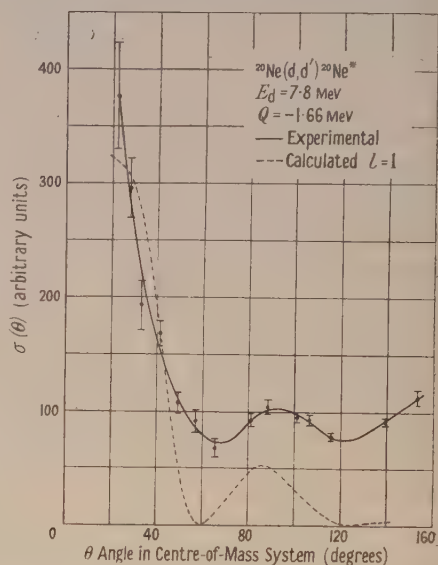


Fig. 2.

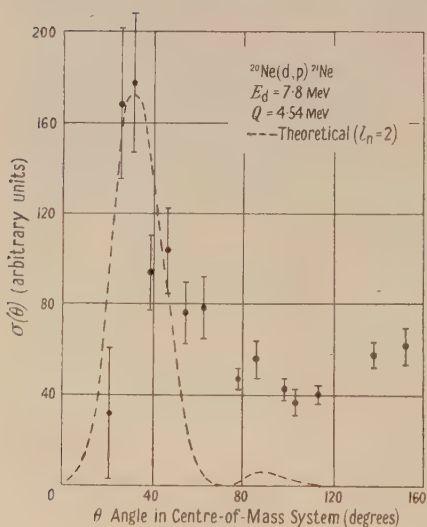


Fig. 3.

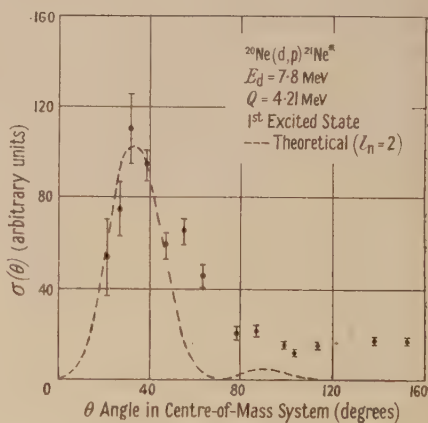


Fig. 4.

The probable errors shown are those of a statistical nature only. Other possible errors may arise from (i) the uncertainty in the ratio of the intensities of the two exposures which may affect the  $20^\circ$  and  $25^\circ$  data by about 3% and (ii) the uncertainty in the escape correction which is about 5% for the proton groups  $P_0$ ,  $P_1$ ,  $P_2$  and  $P_3$ .

## § 4. DISCUSSION

(i) *Elastically Scattered Deuteron Group*

The general behaviour of the angular distribution of the elastically scattered deuterons (fig. 1) is similar to those observed for 6.3 mev deuterons scattered by oxygen and nitrogen (Guggenheimer *et al.* 1947) except for a slight shift in the position of the secondary maximum. It therefore appears likely that our angular distribution can also be explained by using the one-body theory of elastic scattering (Bethe 1937). The shift in the position of the secondary maximum to a smaller angle and the low intensity at large angles is probably due to the wavelength associated with the collision being less than those associated with the collisions of 6.3 mev deuterons with nitrogen and oxygen, and also the larger nuclear radius of neon.

If we assume that the intensity of the scattered deuterons below  $30^\circ$  is due to coulomb scattering alone then, by comparing our arbitrary unit of intensity with the calculated coulomb scattering cross section, we can obtain a conversion factor to correlate our unit with the absolute unit. In this manner we have determined one unit of relative intensity to be equivalent to 0.68 millibarn/steradian. For the particle groups, arising from the bombardment of  $^{20}\text{Ne}$ , the above conversion factor has to be corrected for the contribution of about ten per cent of  $^{22}\text{Ne}$  to the elastically scattered deuteron group and is 0.74 millibarn/steradian per unit of relative intensity.

(ii) *Proton Groups*

The experimental angular distributions of nine proton groups from the reaction  $^{20}\text{Ne}(d, p)^{21}\text{Ne}$  have been determined and those corresponding to the formation of  $^{21}\text{Ne}$  in the ground and first excited states are shown in figs. 3 and 4. All groups show a marked increase in intensity at small angles. From the measured angular distributions and the conversion factor obtained we have calculated the approximate total cross sections for each group and the results are given in table 1. The cross section of the remaining proton groups not listed in this table is estimated to be about one quarter of the sum of the listed total cross sections. This corresponds to a total cross section for all the proton groups of about 0.5 barn.

Table 1

Particle group	$P_0$	$P_1$	$P_2$	$P_3$	$P_4$	$P_5$	$P_6$	$P_7$	$P_8$	D	inelastic
Total cross section (millibarn)	13	21	14	50	21	97	38	41	54	98	

The theoretical angular distribution curves of the proton groups from the reaction  $^{20}\text{Ne}(d, p)^{21}\text{Ne}$  have been calculated by Huby and Newns using a stripping theory which gives results nearly identical with those of the published theory of Butler (1950 a, b). Comparison at small angles of the observed and calculated distributions gives for the states corresponding to proton groups  $P_0$ ,  $P_1$  and  $P_3$  a unique assignment of the angular momentum  $l_n$  transferred by the neutron to the corresponding state of  $^{21}\text{Ne}$ . The angular distributions of the remaining six proton groups can each equally well be fitted by two theoretical curves corresponding to different values of  $l_n$ . This ambiguity arises as a result of the poor statistics of the observations at small angles coupled with the fact that it was impossible to extend measurements below  $20^\circ$  due to the high intensity of the elastically scattered deuterons. Since  $^{20}\text{Ne}$  has zero spin and even

parity, the corresponding state of  $^{21}\text{Ne}$  has spin  $l_n \pm \frac{1}{2}$  and even or odd parity according to whether  $l_n$  is even or odd. The results thus obtained are listed in table 2.

Table 2. Spins and Parities of  $^{21}\text{Ne}$  Energy Levels. (Where two sets of values are given, the one without the parenthesis fits experimental data better than the other.)

Particle group	P <sub>0</sub>	P <sub>1</sub>	P <sub>2</sub>	P <sub>3</sub>	P <sub>4</sub>	P <sub>5</sub>	P <sub>6</sub>	P <sub>7</sub>	P <sub>8</sub>
Energy (MeV)	—	0.33	1.68	2.79	3.73	4.71	5.44	5.74	7.30
$l_n$	2	2	0 or 1	0	2 or 1	1 or (2)	1 or (2)	2 or (1)	1 or (2)
Spin of $^{21}\text{Ne}$ : $I_f$	$\frac{5}{2}$ or $\frac{3}{2}$	$\frac{5}{2}$ or $\frac{3}{2}$	$\frac{1}{2}$ $\frac{1}{2}$ or $\frac{3}{2}$	$\frac{1}{2}$	$\frac{5}{2}$ or $\frac{3}{2}$ $\frac{3}{2}$ or $\frac{1}{2}$	$\frac{3}{2}$ or $\frac{1}{2}$ $(\frac{1}{2}$ or $\frac{3}{2})$	$\frac{3}{2}$ or $\frac{1}{2}$ $(\frac{1}{2}$ or $\frac{3}{2})$	$\frac{5}{2}$ or $\frac{3}{2}$ $(\frac{3}{2}$ or $\frac{1}{2})$	$\frac{3}{2}$ or $\frac{1}{2}$ $(\frac{1}{2}$ or $\frac{3}{2})$
Parity	+	+	+ or -	+	+ or -	-(or +)	-(or +)	+(or -)	-(or +)

The salient feature of these results is that for all the measured distributions the value of  $l_n$  is less than or equal to 2. This indicates the absence of states of  $^{21}\text{Ne}$  of spin larger than  $5/2$  below an excitation energy of 7.3 MeV (corresponding to group P<sub>9</sub>) or if such states do exist they are not significantly formed by 7.8 MeV deuteron bombardment.

It will be observed from figs. 3 and 4 that at large angles the theoretical differential cross sections fall off to much lower values than are measured. Similar behaviour has been observed in the cases of (d, n) reactions at 8 MeV bombarding energy (El-Bedewi, Middleton and Tai 1951 a, b). This is probably due either to an inadequacy in the stripping theory or to the reaction proceeding predominantly via a compound nucleus interaction at large angles of particle emission. The former possibility arises from the fact that the present stripping theory cannot be expected to predict the correct differential cross section for the particles emitted as a result of deuterons of low incident angular momentum. Such nearly head-on encounters would be expected to cause the emergence of particles at large angles, but would not contribute significantly to small-angle particle emission. Similar conclusions seem indicated by the work of Cohen and Falk (1951).

It is interesting to note that both the ground and the first excited state of  $^{21}\text{Ne}$  have the same value of  $l_n (=2)$  for the absorbed neutron and may therefore form a spin doublet of  $^2D_{5/2; 3/2}$  states. It follows from the stripping theory of Bhatia *et al.* (1952) that for two states for which the wave functions are believed to be similar the total cross sections are roughly in the ratio of the statistical weights. Applying to the present case, we find, from table 1, that the ratio of cross sections of P<sub>0</sub> to P<sub>1</sub> is 13/21 which is very near the ratio 4/6 of the statistical weights of  $D_{3/2}$  and  $D_{5/2}$  states. Therefore we are justified in concluding that the ground state of  $^{21}\text{Ne}$  has a spin  $3/2$  and the first excited state a spin  $5/2$ . This is in agreement with the value  $3/2$  given for the spin of the ground state by observations of hyperfine structure (Koch and Rasmussen 1949). It disagrees with the prediction of a  $D_{5/2}$  state for the ground state of  $^{21}\text{Ne}$  from the Mayer's shell model. A similar disagreement has been reported in the case of  $^{23}\text{Na}$  (Mayer 1950) which contains an equal number of particles in the outer shell. This may be explained by assuming that three particles in a state  $D_{5/2}$  can couple to give a spin  $3/2$ , rather than  $5/2$ , which is the value on the principle, suggested by Mayer, that the spin of even numbers of particles in a shell balance out, leaving simply the spin of the odd particle.



(iii) *Inelastically Scattered Deuteron Group*

The angular distribution of the inelastically scattered deuteron group from  $^{20}\text{Ne}$  (fig. 2) shows a resemblance to that from  $^{24}\text{Mg}$  as observed by Holt and Young (1949). The total cross section for the process is calculated to be about 98 millibarns. The similarity between the appearances of the angular distributions and the order of magnitude of cross sections for the inelastically scattered deuteron group and for the proton groups suggests the interaction concerned to be of a similar nature. Theoretical calculations similar to those for the (d, p) reactions have been carried out by Huby and Newns (1951). Comparison shows the measured distribution to be consistent with the calculated one when the incident deuteron is assumed to impart one unit of angular momentum to the  $^{20}\text{Ne}$  nucleus. Since the ground state of  $^{20}\text{Ne}$  has spin zero and even parity, the excited state of 1.66 mev would therefore be of spin 0, 1, or 2 and of odd parity. Since there is a  $\gamma$ -ray transition from that state to the ground state (Jelley 1950) the possibility of spin 0 is eliminated.

It is also interesting to note that the appearance of the angular distribution for inelastically scattered protons from  $^{20}\text{Ne}$  at an energy of 4.2 mev (Heitler *et al.* 1947) shows similar features to that of the inelastically scattered deuterons observed in the present work.

## ACKNOWLEDGMENTS

The authors wish to acknowledge their indebtedness to Professor H. W. B. Skinner for his continuous interest and helpful advice and to Professor J. Rotblat and Dr. J. R. Holt for some useful discussions. We also thank Dr. R. Huby and Mr. H. Newns for making the results of their calculations available to us and Miss B. Anderson for assistance in observations.

## REFERENCES

- BETHE, H. A., 1937, *Rev. Mod. Phys.*, **9**, 179.  
 BHATIA, A. B., HUANG, K., HUBY, R., and NEWNS, H. C., 1952, *Phil. Mag.*, **43**, 485.  
 BUTLER, S. T., 1950 a, *Harwell Conference Report*; 1950 b, *Phys. Rev.*, **80**, 1095.  
 CHADWICK, J., MAY, A. N., PICKAVANCE, T. G., and POWELL, C. F., 1944, *Proc. Roy. Soc. A*, **183**, 1.  
 COHEN, B. L., and FALK, C. E., 1951, *Phys. Rev.*, **84**, 173.  
 EL-BEDEWI, F. A., MIDDLETON, R., and TAI, C. T., 1951 a, *Proc. Phys. Soc. A*, **64**, 756 ; 1951 b, *Ibid.*, **64**, 1055.  
 GUGGENHEIMER, K. M., HEITLER, H., and POWELL, C. F., 1947, *Proc. Roy. Soc. A*, **190**, 196.  
 HEITLER, H., MAY, A. N., and POWELL, C. F., 1947, *Proc. Roy. Soc. A*, **190**, 180.  
 HOLT, J. R., and YOUNG, C. T., 1949, *Nature, Lond.*, **164**, 1000.  
 HUBY, R., and NEWNS, H. C., 1951, *Phil. Mag.*, **42**, 1442.  
 JELLEY, J. V., 1950, *Proc. Phys. Soc. A*, **63**, 538.  
 KOCH, J., and RASMUSSEN, E., 1949, *Phys. Rev.*, **76**, 1417.  
 MAYER, M. G., 1950, *Phys. Rev.*, **78**, 16.  
 MIDDLETON, R., and TAI, C. T., 1951, *Proc. Phys. Soc. A*, **64**, 801.  
 ROTBLAT, J., BURROWS, H. B., and POWELL, C. F., 1951, *Proc. Roy. Soc. A*, **209**, 461.

## LETTERS TO THE EDITOR

## Local Penetrating Showers from Water and Carbon

A cloud chamber of diameter 30 cm and illuminated depth 15 cm with a 2.5 cm Pb plate across the middle was operated for  $4\frac{1}{2}$  months under a layer of water 90 cm thick. The bottom of the water was 20 cm above the top of the cloud chamber. The cloud chamber was operated by two counter trays (each of area  $750\text{ cm}^2$ ), one immediately beneath the water and the other in a lead pile beneath the cloud chamber. At least a two-fold coincidence from each of the trays was required. Extensive showers were detected by a tray of area  $750\text{ cm}^2$  placed 1.5 m from the cloud chamber. At the end of the run a second run was made for an equal time with an amount of carbon equivalent in mass and geometry to the oxygen in the water substituted for the water.

An event was classified as a local penetrating shower if it had either (a) at least two penetrating particles visible in the cloud chamber, or (b) at least one penetrating particle plus at least one nuclear reaction visible in the cloud chamber. Events in which the extended tray was discharged were disregarded.

The number of events in which various multiplicities of penetrating particles occurred are as follows:

No. of penetrating particles	1	2	3	4	5	6	7	8	13	Total
No. of showers from water	42	56	23	9	6	—	1	—	—	137
No. of showers from carbon	52	45	21	5	3	2	1	2	1	132

The average multiplicity of penetrating particles from carbon is  $2.25 \pm 0.13$  and that for showers from water is  $2.16 \pm 0.13$ . If we assume geometric cross section for interaction for carbon, oxygen and hydrogen and that the multiplicity from the oxygen of the water is equal to that from the carbon, this gives an average multiplicity for showers from hydrogen of  $1.88 \pm 0.68$ .

The average multiplicity of the showers from carbon is in good agreement with the results of Salant *et al.* (1950) working with photographic plates and primaries of similar energy; it also agrees well with the results of Chang and Del Castillo (1951) working with a cloud chamber; it is however only about half the value of the average multiplicity for events from carbon obtained by Walker, Duller and Sorrels (1952). It seems very likely that this is due to differences in geometry and selection. On the other hand the low multiplicity for the events from hydrogen is in good agreement with the conclusion of these workers that showers from hydrogen are of low multiplicity. This disagrees with the conclusion of Bertolino *et al.* (1952) that the average multiplicity in nucleon-proton collisions is of the order of 10. However it seems likely that this last result was due either to the simultaneous arrival of several nucleons as part of an extensive air shower or to the cascading of secondary particles in the lead shielding.

Dublin Institute for Advanced Studies.  
23rd June 1952.

C. B. A. McCUSKER.  
D. D. MILLAR.\*

BERTOLINO, G., CINI, M., COLOMBINO, P., WATAGHIN, G., 1952, *Nuovo Cim.*, **9**, No. 5, 407.  
CHANG, W. Y., and DEL CASTILLO, G., 1951, *Phys. Rev.*, **84**, 504.  
SALANT, E. O., HORNOSTEL, J., FISK, C. B., and SMITH, J. E., 1950, *Phys. Rev.*, **79**, 184.  
WALKER, W. D., DULLER, N. M., and SORRELS, J. D., 1952, *Phys. Rev.*, in the press.

\* Now at University of Manchester.

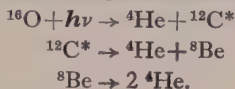
## Resonance Effects in the Photo-Disintegration of $^{16}\text{O}$ Nuclei into four $\alpha$ -Particles

The disintegration of  $^{16}\text{O}$  nuclei into four  $\alpha$ -particles by high-energy  $\gamma$ -rays has been studied by several workers. The reaction is



and the data relate to  $\gamma$ -ray energies up to 23 meV. In this energy region, stars were found with an average total  $\alpha$ -particle energy of about 7.5 meV, corresponding to  $\gamma$ -rays of 22 meV

energy. It was also reported that about half of these stars were apparently produced by the disintegration in flight of  $^8\text{Be}$  nuclei in the ground state. Goward and Wilkins (1950) suggested that these  $^8\text{Be}$  nuclei were formed from an excited level in the  $^{12}\text{C}$  nucleus at 9.7 mev, so that the entire reaction may be represented as three processes in rapid succession



We have undertaken further experiments to investigate first, the nature of the excitation function of reaction (1), and second, the detailed mechanism of the disintegration and the possible excited levels of intermediate  $^8\text{Be}$  and  $^{12}\text{C}$  nuclei.

Ilford C2 nuclear plates of 100  $\mu$  emulsion thickness were irradiated in a synchrotron beam of maximum energy *c.* 32 mev (University Department of Radiotherapeutics, Cambridge).

The results obtained refer to 83 stars and the histogram (fig. 1) shows the number of stars plotted against the  $\gamma$ -ray energy. Although the number of stars is not high and although the histogram is not corrected for the spectral distribution of  $\gamma$ -rays from the target, the results strongly suggest that the stars fall into various energy groups. The first of these corresponds to the distribution reported by Goward and Wilkins. The shaded histogram, showing stars apparently involving  $^8\text{Be}$  nuclei in the ground state, agrees with previous results, in that 21 out of 54 stars in this low-energy region fall into this category. A more sharply defined group of stars occurs close to a  $\gamma$ -ray energy of 25 mev and there is some evidence of a further group at 29 mev but this is near the maximum energy of the  $\gamma$ -rays used. In this respect the reaction shows significantly different properties from those other photo-reactions of the  $(\gamma, p)$  and  $(\gamma, n)$  types which have already been investigated. Up to the present, the results already published on oxygen  $\alpha$ -stars show no group structure such as we have found. In some cases this certainly is due to the fact that the maximum energy of the photons was too low (e.g. Goward and Wilkins 1950, Millar and Cameron 1950).

The occurrence of  $^8\text{Be}$  in the ground state seems to be confined to the low-energy group near 22 mev  $\gamma$ -ray energy. In a study of stars of this kind it is easy to recognize the two  $\alpha$ -particles coming from the ground state  $^8\text{Be}$ . The other two  $\alpha$ -particle tracks may then be used to calculate possible values for the excitation energy of a  $^{12}\text{C}$  nucleus as parent to the  $^8\text{Be}$ . Only one half of these results can be significant; therefore fig. 2, which shows the

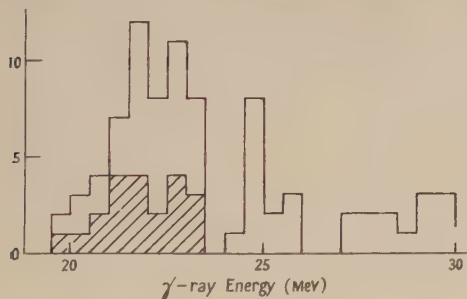


Fig. 1. Yield curve.



Fig. 2. Possible excitation energies of  $^{12}\text{C}$  producing  $^8\text{Be}$  in ground state.

numbers plotted against excitation energy of  $^{12}\text{C}$  nucleus, should exhibit a background continuum with significant peaks superposed, if the reaction proceeds via an intermediate  $^{12}\text{C}$  nucleus. Interpretation of these results is rendered difficult by the experimental errors in determining ranges and angles of very short  $\alpha$ -particle tracks. Nevertheless it is clear that, although 10 out of the 21 stars can be interpreted in terms of a level at 9.7 mev, the remaining stars cannot be explained in this way. An alternative level near 11.3 mev would account for the other stars. This deduction is confirmed by theoretical calculations predicting the appearance of stars of this kind. If we take a star produced via a 9.7 mev level in  $^{12}\text{C}$  by a 22 mev  $\gamma$ -ray it will in general have one long  $\alpha$ -particle track of energy 3.9 mev, and three shorter tracks with energies totalling 3.6 mev. Such stars are in fact observed; but in others the two  $\alpha$ -particle tracks, not derived from the  $^8\text{Be}$  in the ground state, are of comparable length, and these may be explained in terms of a  $^{12}\text{C}$  level near



11.3 mev. The other stars in the low-energy group, not involving  $^8\text{Be}$  in the ground state, are apparently produced from the 3 mev level in  $^8\text{Be}$ .

An analysis of that group of stars produced by  $\gamma$ -rays of energy about 25 mev shows that it is improbable that the disintegration goes via an excited state of  $^{12}\text{C}$  but there is evidence that an excited state in  $^8\text{Be}$  at 4.3 mev is involved. In the high-energy group the number of stars is too small for any detailed analysis to be significant.

If these deductions are confirmed, it would seem that the photo-disintegration of  $^{16}\text{O}$  into four  $\alpha$ -particles is, at least partly, a resonance process for  $\gamma$ -rays below 30 mev, and that in the lowest energy group there are alternative modes of disintegration via  $^8\text{Be}$ .

Oundle School,  
Northants.  
Department of Radiotherapeutics,  
University of Cambridge.  
7th May 1952.

D. L. LIVESY.

C. L. SMITH.

GOWARD, F. K., and WILKINS, J. J., 1950, *Proc. Phys. Soc. A*, **63**, 1171.  
MILLAR, C. H., and CAMERON, A. G. W., 1950, *Phys. Rev.*, **78**, 78.

## The Nuclear Electric Quadrupole Moment of Erbium 167

Recently Bleaney and Scovil (1951) reported paramagnetic resonance measurements on erbium ethyl sulphate diluted with lanthanum ethyl sulphate in the ratio  $\text{Er} : \text{La} \approx 1 : 200$ . Their observations were made at 1.2 cm wavelength and at temperatures down to  $13^\circ \text{K}$ ; at this temperature, where the line width resulted predominantly from the short spin-lattice relaxation time, the hyperfine structure was just resolved perpendicular to the hexagonal axis of the crystal and only partially resolved parallel to the axis. The spectrum was analysed in terms of the usual Hamiltonian

$$\mathcal{H} = -\beta\{g_{\parallel}H_zS_z + g_{\perp}(H_xS_x + H_yS_y)\} + AS_zI_z + B(S_xI_x + S_yI_y) + P\{I_z^2 - \frac{1}{3}I(I+1)\}$$

and values were given for the first four parameters and an upper limit assigned to  $P$ . This upper limit was based on measurements of the spacings between transitions of the type  $(M, m) \rightarrow (-M, m)$ .

We have extended the experiments to  $4^\circ \text{K}$  at 3 cm wavelength. Because of the longer spin-lattice relaxation time at this temperature we have been able to resolve the spectrum completely in all directions. As a consequence it is possible to give more accurate values for  $A$  and  $B$  as follows:  $|A| = 0.0052 \pm 0.0001 \text{ cm}^{-1}$ ;  $|B| = 0.0314 \pm 0.0001 \text{ cm}^{-1}$ .

A nuclear electric quadrupole term can be found from anomalies in the spacings of the  $\Delta m = 0$  transitions (Bleaney 1951). This effect not only requires very precise measurements of the hyperfine structure, which is not always possible because of the line widths, but can be masked by higher order terms resulting from the nuclear magnetic moment. A second method of finding a quadrupole term is to observe the otherwise forbidden transitions corresponding to the selection rules  $\Delta m = \pm 1$  and  $\pm 2$  for the nuclear quantum number. According to Bleaney these transitions are split into doublets by a nuclear quadrupole term; he gives formulae for this splitting and for the intensity of the lines.

We have observed the lines of both types. The great anisotropy in this crystal means that the accuracy of observations based on the  $\Delta m = \pm 1$  transitions is entirely limited by the precision with which the crystal can be aligned with its axis parallel to the magnetic field. There is no such limitation for the  $\Delta m = \pm 2$  lines, which have greatest intensity perpendicular to the axis, because irrespective of the mounting it is always possible to rotate the crystal through the perpendicular plane and this direction can easily be found from the position of the maximum  $g$  value.

From measurements of the doublet splitting of the  $\Delta m = \pm 2$  lines we find that  $|P| = (30 \pm 3) \times 10^{-4} \text{ cm}^{-1}$ . Insertion of this value in the intensity formulae gives a value which agrees with the measured intensity within the experimental error of 20%, thereby providing a rough check on the result.

Elliott and Stevens (1951) have estimated the gradient of the electric field and  $1/r^3$ . They gave two possible ground states for the ion; but since then the uncertainty has been removed (Elliott and Stevens, in course of publication) in favour of

$\cos \theta | \pm 7/2 \rangle + \sin \theta | \mp 5/2 \rangle$  with  $\theta \simeq 45^\circ$ . Using these results we can give the nuclear electric quadrupole moment  $Q$  as defined (Mack 1950) by  $Q = \int \rho_I (3z^2 - r^2) d\tau$  where  $\rho_I$  denotes the charge density for  $m_I = I$ . We find  $|Q| = (10.2 \pm 3) \times 10^{-24} \text{ cm}^2$ .

We wish to make grateful acknowledgment to Dr. A. H. Cooke for his co-operation during these experiments. One of us (H.J.D.) is indebted to the National Research Council of Canada for financial support.

Clarendon Laboratory,  
Oxford.

24th June 1952.

G. S. BOGLE.

H. J. DUFFUS.

H. E. D. SCOVIL.

BLEANEY, B., 1951, *Phil. Mag.*, **42**, 441.

BLEANEY, B., and SCOVIL, H. E. D., 1951, *Proc. Phys. Soc. A*, **64**, 204.

ELLIOTT, R. J., and STEVENS, K. W. H., 1951, *Proc. Phys. Soc. A*, **64**, 205.

MACK, J. E., 1950, *Rev. Mod. Phys.*, **22**, 607.

## Pile Neutron Absorption Cross Sections of Lead 206 and 207

At the request of B. B. Kinsey (Atomic Energy of Canada Ltd., Chalk River, Ontario, Canada) we have measured the pile neutron absorption cross sections of two lead samples which he supplied. One was a sample of natural lead and the other a sample of radio lead; both were measured on the G.L.E.E.P. oscillator by comparing them with boron, the thermal neutron absorption cross section of which was assumed to be 710 barns. The results obtained were  $\sigma(\text{natural lead}) = 162 \pm 5 \text{ mbarns}$ ,  $\sigma(\text{radio lead}) = 84 \pm 3 \text{ mbarns}$ .

Neither of the samples was analysed for chemical impurities, and therefore these cross sections come into the category B of Colmer and Littler (1950).

The value obtained for the cross section of natural lead is very different from the one obtained by Colmer and Littler, namely  $280 \pm 10 \text{ mbarns}$ . The sample used by them was remeasured, and the value of 280 mbarns was again obtained. A spectroscopic analysis was therefore made on the sample, and the presence of cadmium was detected. Mr. A. A. Smales then determined the cadmium content by a radio-activation method to be  $30 \pm 10$  parts per million. This involves a correction of  $134 \pm 45 \text{ mbarns}$  to the cross section, thus bringing it into agreement with the present measurement on natural lead.

Mass spectrometer analyses have been made of the isotopic abundances in the two kinds of lead. The analyses were made using a solid-source method with lead iodide as the source material. The results obtained were

Isotope	204	206	207	208
% abundance natural lead	$1.46 \pm 0.04$	$23.94 \pm 0.06$	$22.32 \pm 0.06$	$52.27 \pm 0.06$
% abundance radio lead	—	$88.19 \pm 0.02$	$8.86 \pm 0.02$	$2.95 \pm 0.01$

We have not been able to find any published value for the activation cross section of lead 204, and have assumed that it has not been measured to date because it has a very low value. The activation cross section of lead 208 to produce 3.3 hour lead 209 has been measured by J. S. Levinger and is quoted by Way and Haines (1948); the value obtained was 0.45 mbarns.

Therefore, taking  $\sigma(\text{Pb } 204) = 0$ ,  $\sigma(\text{Pb } 208) = 0.45 \text{ mbarns}$ , we derive

$$\sigma(\text{Pb } 206) = 25 \pm 5 \text{ mbarns,}$$

$$\sigma(\text{Pb } 207) = 698 \pm 25 \text{ mbarns.}$$

The values obtained for the cross sections of lead 206 and 207 are not very sensitive to the values assumed for lead 204 and 208; in fact, the activation cross section of lead 204 could be as high as 300 mbarns without changing the values for lead 206 and 207 by more than one standard error.

The mass spectrometer analyses were made by Aitken and Palmer, and the cross section measurements by Littler and Lockett.

Atomic Energy Research Establishment,  
Harwell, Berks.

30th June 1952.

K. L. AITKEN.

D. J. LITTLER.

E. E. LOCKETT.

G. H. PALMER.

COLMER, F. C. W., and LITTLER, D. J., 1950, *Proc. Phys. Soc. A*, **63**, 1175.

WAY, K., and HAINES, G., 1948, U.S. Atomic Energy Commission, Declassified Document (A.E.C.D. 2274).

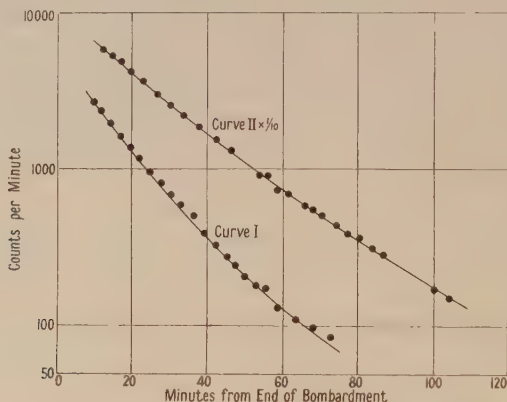
## Artificial Activity Induced in Carbon by Fast $^3\text{He}$ Ions

Natural helium 3 was discovered by Alvarez and Cornog (1939) by using the Berkeley 60 in. cyclotron as a mass spectrograph. Using a beam of  $^3\text{He}$  ions, they were able to produce some  $2\frac{1}{2}$  minute  $^{30}\text{P}$  from silicon. Since these experiments some lower energy work has been done with  $^3\text{He}$ , but the only use of  $^3\text{He}$  as a bombarding particle in the cyclotron which appears to have been reported is a study of reactions of the  $(^3\text{He}, \alpha)$  type which were observed in nuclear emulsions by Lukirsky, Mescheryakov and Khrenina (1947) using  $^3\text{He}$  ions of 5.7 mev energy.

In similar experiments made recently with the 60 in. Nuffield cyclotron of the University of Birmingham (1952) ordinary atmospheric helium containing about 1.3 parts per million of  $^3\text{He}$  (Aldrich and Nier 1948) was fed into the ion source. The cyclotron was operating at its normal frequency (10.2 Mc/s) but at three-quarters of the normal magnetic field. The exact magnet-current required for resonance for  $^3\text{He}$  was found by means of a tube carrying a fluorescent screen and terminated by a Perspex window at the outer end. Using this it was found that at 20 mev the width of the resonance peak was about 25 gauss (in 10 000).

The identity of the particles accelerated was confirmed by the use of Ilford C2 plates placed successively at various radii inside the cyclotron tank, plenty of tracks being obtained in one-second's exposure with an arc current of about one-tenth of normal. The grain-density of the tracks showed that the particles were doubly charged and the ranges had the expected average values.

Carbon in the form of pure graphite was bombarded for 10 minutes with the  $^3\text{He}$  ions at a radius in the cyclotron corresponding to 20 mev. The decay curve of the resulting activity is shown in curve I, and can be interpreted as that due to a mixture of activities of 20 minute and 10 minute half-lives in nearly equal initial strength. These are the half-lives of  $^{11}\text{C}$  and  $^{13}\text{N}$  respectively, which could be produced by the reactions  $^{12}\text{C}(^3\text{He}, \alpha)^{11}\text{C} + 1.86 \text{ mev}$  and  $^{12}\text{C}(^3\text{He}, d)^{13}\text{N} - 3.55$  or  $^{13}\text{C}(^3\text{He}, ^3\text{H})^{13}\text{N} - 2.29$ .



Decay of activities produced in bombardments of carbon targets.

Curve I. 10 minutes. Nominal  $^3\text{He}$  energy 20 mev.

Curve II. 50 seconds. Enriched helium. Nominal  $^3\text{He}$  energy 18.5 mev.

The experiment was repeated, using in the ion source helium enriched to 1/1000  $^3\text{He}$ . The decay of the activity resulting from a bombardment of 50 seconds with 18.5 mev  $^3\text{He}$  ions is shown in curve II. Comparison of these results shows that an increase in amount of bombarding  $^3\text{He}$  by a factor of about 800 increased the  $^{13}\text{N}$  activity by a factor of 200 and the  $^{11}\text{C}$  by 600. The latter agrees with the enrichment factor within experimental error and indicates that the whole of the  $^{11}\text{C}$  activity is due to  $^3\text{He}$ . On the other hand, some  $^{13}\text{N}$  activity in the first experiment must arise from other particles accelerated in the cyclotron under  $^3\text{He}$  resonance conditions; these have been shown, by experiments to be described elsewhere, to be deuterons.

Bombardment of carbon with ordinary and enriched  $^3\text{He}$  at energies of about 4.2 mev showed that for this energy the only activity attributable to the  $^3\text{He}$  ions was that of  $^{11}\text{C}$ .



Roughly  $10\mu\text{C}$  of  $^{11}\text{C}$  was produced by  $1\mu\text{Asec}$  of  $18.5\text{ MeV } ^3\text{He}$  ions. The current could only be estimated from the  $\alpha$ -currents with similar source conditions, and might therefore easily be wrong by a factor of two or three.

If the  $^{13}\text{N}$  was produced from  $^{12}\text{C}$ , the integrated cross section for its production was about one-third of that for  $^{11}\text{C}$ , while if it was produced from  $^{13}\text{C}$  it must have been thirty times as great.

The author is grateful to Professor W. E. Burcham for many valuable suggestions and to Mr. K. E. A. Effat and Mr. G. L. Munday for their help with the counting. He is also grateful to Mr. W. Hardy for his help in finding the exact conditions for acceleration and for making the necessary bombardments.

Department of Physics,  
University of Birmingham.

J. H. FREMLIN.

7th December 1951; in final form 13th June 1952.

ALDRICH, L. T., and NIER, A. O., 1948, *Phys. Rev.*, **74**, 1590.

ALVAREZ, L. W., and CORNOG, R., 1939, *Phys. Rev.*, **56**, 379 and 613.

LUKIRSKY, P. I., MESCHERYAKOV, M. E., and KHRENINA, T. I., 1947, *C.R. Acad. Sci., U.R.S.S.*, **55**, 117.

University of Birmingham Cyclotron, 1952, *Nature, Lond.*, **169**, 476.

## The Deuteron Stripping Reaction with Aluminium

Theories giving the angular distribution of the particles emitted in the (d, p) and (d, n) reactions based on the capture of one of the particles in the deuteron in a single-stage or 'stripping' process have been given by Butler (1951) and by Bhatia *et al.* (1952). With a beam of deuterons of approximately 8 MeV energy and using a triple proportional counter as the detector of emitted protons, we have carried out angular distribution measurements extending to the forward direction for proton groups from a variety of elements. The isotopes which have so far been investigated are the following:  $^6\text{Li}$ ,  $^9\text{Be}$ ,  $^{24,25,26}\text{Mg}$ ,  $^{27}\text{Al}$ ,  $^{28}\text{Si}$ ,  $^{32}\text{S}$ ,  $^{40}\text{Ca}$  and  $^{88}\text{Sr}$ . We report here briefly the results obtained with the reaction  $^{27}\text{Al}(\text{d}, \text{p})^{28}\text{Al}$ .

We have measured the angular distributions of the proton groups ( $p_0$  and  $p_1$ ) relating to the ground state and the first excited state of  $^{28}\text{Al}$ . The measurements for the group  $p_0$  are shown in fig. 1. The curve is a theoretical one which could be derived from either

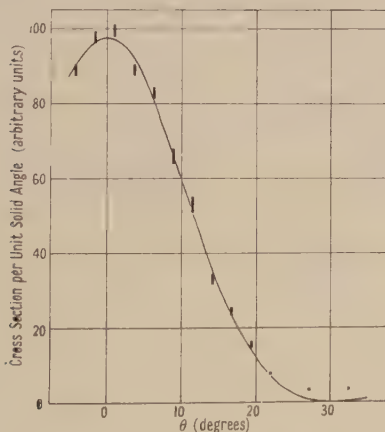


Fig. 1. Angular distribution of the proton group  $p_0$ .



Fig. 2. Angular distribution of the proton group  $p_1$ .

of the two theories mentioned above with suitable choice in each case of the parameter representing the radius at which the neutron is captured, and with the unambiguous value of zero for the orbital angular momentum  $l$  of the captured neutron. Thus neutrons are captured with zero orbital angular momentum to form one or both members of the

unresolved ground-state doublet of  $^{28}\text{Al}$  (Enge 1951). Since the spin of  $^{27}\text{Al}$  is  $5/2$  the spin of one or both members of the doublet must have either the value 2 or 3. According to the nuclear shell model, the lowest unfilled neutron orbit in  $^{27}\text{Al}$  is an s-orbit. Our results are consistent with a neutron being captured directly into an s-orbit to form the ground state of  $^{28}\text{Al}$ .

The experimental angular distribution for the proton group  $p_1$  (fig. 2) is unusual since it could be fitted only by adding together in suitable proportions two theoretical curves, one having  $l=0$  and the other having  $l=2$ . The curve drawn in fig. 2 was calculated on Butler's theory with the ratio of the peak values of the two component curves with  $l=0$  and  $l=2$  adjusted to be 1.85.

Such a double curve could, of course, be due to the energy level in question being an unresolved doublet. In the present case such an explanation is unlikely in view of the magnetic analysis of Enge. However, since the target nucleus has a spin greater than zero, the vector addition rules for angular momenta allow transitions to a final state of definite spin to take place with more than one value of  $l$ . In the present case, since the angular distribution shows that  $l$  can have the value zero, the first excited state of  $^{28}\text{Al}$  must have a spin of either 2 or 3. The transition from  $^{27}\text{Al}$  having spin  $5/2$  to a state of  $^{28}\text{Al}$  having spin 2 or 3 can take place with values of  $l$  of 0, 2 or 4. The  $p_1$  angular distribution shows the presence of the first two of these values. The component curve of this distribution having  $l=0$  has a peak value about 10% of that of the  $p_0$  distribution. The ratio of the peak value of the component curve of the  $p_1$  distribution having  $l=2$  to the peak value of the  $p_0$  distribution is in agreement with the ratio given by Butler assuming the same probability of capture of the neutron by the nucleus in both cases. Thus the first excited state of  $^{28}\text{Al}$  is formed by the capture of neutrons with zero orbital momentum with a probability about 10% of that for the capture of neutrons with two units of orbital momentum. If then we assume that the neutron is finally bound in the nucleus with the same orbital angular momentum with which it is captured, the results show that its final state in  $^{28}\text{Al}$  is not a pure d-state, but has a 10% admixture of s-state. Bethe and Butler (1952) have recently suggested a search for transitions with double  $l$ -values in order to examine the purity of nuclear states. Bohr and Mottelson (1952) on the basis of a modified form of the independent particle model of the nucleus, have predicted the existence of such mixed states. It would seem possible that our case of  $^{28}\text{Al}$  is an example.

Nuclear Physics Research Laboratory,  
University of Liverpool.  
30th June 1952.

J. R. HOLT.  
T. N. MARSHAM.

- BETHE, H. A., and BUTLER, S. T., 1952, *Phys. Rev.*, **85**, 1045.  
BHATIA, A. B., HUANG, KUN, HUBY, R., and NEWNS, H. C., 1952, *Phil. Mag.*, **43**, 485.  
BOHR, A., and MOTTELSON, B. R., 1952, Copenhagen Conference, June 1952.  
BUTLER, S. T., 1951, *Proc. Roy. Soc. A*, **208**, 559.  
ENGE, H. A., 1951, *Phys. Rev.*, **83**, 212 (A).

Note added in proof to paper entitled "Calculation of Scattering Amplitudes",  
by G. J. KYNCH.

Equations (2.9) and (2.10), using an integral representation for the wave function, are only true when  $f(k_1 : p)$  is the same for forward and backward scattering. In general, to correct these equations  $f(k_1 : p)$  should be replaced by  $f_0(k_1 : p) + (k/p)f_0(k_1 : p)$  when  $f_e$  and  $f_o$  contain even and odd angular momenta respectively.

Two other mistakes are that the factor  $(k^2/2\pi^2)$  should be replaced by  $(-1/4\pi^2)$  in these equations and that  $df/R^2dR$  in eqns. (2.7) to (2.10) should be multiplied by  $4\pi$  and not divided by it.

## REVIEWS OF BOOKS

*Physical Properties and Analysis of Heavy Water* (National Nuclear Energy Series, Vol. 4A, Division III), by I. KIRSHENBAUM. Edited by G. M. MURPHY and H. C. UREY. Pp. xv+438. (New York and London: McGraw-Hill, 1951.) \$ 5.25; 45s.

This volume is devoted to the experience obtained in the Manhattan Project of the complete isotopic analysis of water.

The earlier investigations of Joliot, Halban and Kowarski established the suitability of heavy water as a moderator for an atomic pile. One facet of the multilateral attack on the technical problems involved in the release of atomic energy, organized under the Manhattan District of the U.S. Corps of Engineers, was concerned with the industrial production of large quantities of deuterium oxide. The design, development and control of this plant required reliable, complete isotopic analyses of water. The project eventually accumulated a unique body of experience in this field, and, incidentally, critically appraised the existing data on the isotopically homogeneous varieties of water, redetermining some of the less satisfactorily established constants.

The first chapter deals with the physical data and includes a description of the new determinations of the specific gravity of deuterium oxide of normal oxygen content made by Kirshenbaum, Graff and Forstat and the confirmatory independent determinations of Voskuyl and Barach. The second chapter compares the experimental and calculated values of the equilibrium constants for the principal protium-deuterium exchange reactions.

The next two chapters, comprising nearly half the book, are devoted to the mass spectrometric analysis of water. After a brief description of the constructional details, including circuit diagrams, of the Nier types I and II 3:4 mass spectrometers and of the similar instrument designed for the carbon dioxide estimation of the oxygen isotopes, follows an excellent account of the difficulties that beset these determinations. Sufficient data are tabulated to substantiate estimates of the errors arising from a variety of causes. The precautions necessary when analysing samples of very low protium content are emphasized. These include the memory effect in the mass spectrometer, and the effect of handling this hygroscopic material in the ordinary atmosphere. Several techniques of preparation of the sample, both for hydrogen and oxygen estimations, are compared. Particular attention is paid to the method of equilibrating gaseous hydrogen with the liquid sample. Besides the mass spectrometric method, several densitometric procedures are discussed. These include pyconometric and the various float and falling drop methods, the latter being extended to cover low protium content waters. A very interesting continuous reading float gauge, suitable for recording the output from a deuterium separation plant, is described. Attention is drawn to the importance of careful pretreatment of the sample. The significance of some of the earlier densitometric estimations of deuterium is lost because of failure to normalize the  $^{18}\text{O}$  content of the samples. Normalization can be effected by equilibration of the water with excess sulphur dioxide.

Refractometric analysis is also described in detail and a method of complete isotopic analysis by the combination of refractive index and density determinations is mentioned. The data presented show that the mass spectrometric and densitometric procedures give equally consistent results for relative isotopic analysis of the hydrogen in water but that absolute determinations involve much greater errors. Although this book may confidently be expected to become the *vade mecum* of those making mass spectrometric or densitometric isotopic analyses of water there would still appear scope for the development of new procedures. It is surprising that the measurement of the freezing point is barely mentioned although certainly convenient for rough determinations of the isotopic analysis of waters containing comparable amounts of protium and deuterium. The large difference in the neutron scattering cross sections of protium and deuterium might form the basis of an analytical procedure for the protium content of the essentially pure deuterium oxide. Spectroscopic methods do not appear to have been exhausted.

The concluding chapter deals with new and existing data on the natural abundance of the oxygen and hydrogen isotopes in various materials. The distribution of the oxygen isotopes



is especially interesting since the nature of the principal fractionation mechanisms is not yet clearly established.

The book contains a mass of previously unpublished data culled from reports of the Manhattan Project. It has been most carefully edited, contains less typographical errors and is more homogeneous in treatment than previous volumes in this series. A. G. MADDOCK.

*X-ray Analysis of Crystals*, by J. M. BIJVOET, (the late) N. H. KOLKMEYER and C. H. MACGILLAVRY. Pp. xii+304. (London: Butterworths Scientific Publications, 1951.) 50s.

This book falls into three parts. Five chapters deal with methods, three with results, and these are followed by a set of appendices. Chapter 1 is introductory, dealing with diffraction by a single molecule and by a crystal, the plane groups and space groups. In Chapter 2 the derivation of the Laue and Bragg equations is followed by a brief description of the more important types of x-ray photographs. Here one reads: "The absence of a symmetry centre in a crystal can readily be established from the unequal development of plane and complementary plane, or from the presence of the piezoelectric effect etc." The reader is then referred to Chapter 4, where he reads: "Frequently, however, the macroscopic symmetry is not completely known. The decision whether or not a direction is polar is then often uncertain from crystallographic considerations, i.e. from the development of the faces, piezoelectric behaviour, etching patterns, etc." In Chapter 4 the space group  $Pm\bar{n}b$  is assigned to mercuric chloride without further comment because it forms bipyramidal crystals. There is no mention in the book of Wilson's work on this important subject.

Chapter 3 deals with the factors affecting the intensities of diffracted beams, the whole treatment being based on the powder photograph. Chapter 4 is devoted to the determination of structures by the 'trial' method. No less than ten pages are given to the determination of the structure of  $HgCl_2$  (carried out in 1934) from *rotation* photographs. Structure determination by Fourier methods is discussed in Chapter 5. The impression is given in these chapters that the older method (comparison of intensities) is a trial method whereas the Fourier method is in some ways more direct, an impression heightened by the emphasis placed on the use of pairs of isomorphous crystals. Not everyone would agree that "It is this method which now makes it possible to determine the structures of complicated organic compounds." Patterson techniques are only mentioned in Chapter 5, the reader being referred to Appendix 6.

Chapters 6, 7, and 8 contain a well-illustrated survey of the crystal structures of some inorganic and organic compounds, a survey useful for the general reader but obviously inadequate for the serious student of chemistry. Chapter 8 contains a number of minor blemishes such as the peculiar reference to the "spidery model of the molecule of cyanuric triazide  $(N_3CN)_3$  . . . which strikingly demonstrates the fragile structure of this explosive compound", the omission of the molecules of  $SO_2$  from Figure 146 c, and a thoroughly confusing discussion of bond lengths in certain aromatic molecules on page 198.

Nine Appendices account for about one-quarter of the book. They deal with the point groups, space groups, indexing of photographs, the formulae of Fourier and Patterson syntheses, the reciprocal lattice, and miscellaneous topics such as disorder in layer structures, electron and neutron diffraction, and finally Grimm's classification (1934) of structures in terms of bond type. The reciprocal lattice is first mentioned on page 248 in connection with the indexing of Weissenberg photographs (which is carried out with a special type of set-square, though it is mentioned that it is possible to use curves drawn on tracing-paper), but it is not discussed in detail until page 255. Two pages (244-5) are devoted to indexing a rotation photograph without use of a chart (none are illustrated in the book), and though the reference to the classical paper by Bernal is given no fewer than three times (twice incorrectly) there is no clear statement of the standard way of indexing oscillation photographs.

In the case of a book which is translated from the Dutch it is justifiable to ask whether it contains much information not readily available in English texts or a presentation of outstanding value for teaching purposes. This question is particularly relevant at the present time, for no expense has been spared in the production of this handsome book, a fact which is reflected in the price. It is claimed in the Preface (by W. H. Taylor) that this book will be valuable to students and stimulating to their teachers. Without doubting the truth of

the second statement the reviewer feels that a student will not find a clear statement of how crystal structures are determined at the present time, witness the large amount of space devoted to powder and *rotation* photographs as compared with Weissenberg photographs, and the archaic methods of indexing. There is also an undesirable lack of precision in many statements. For example, if the number of molecules in a unit cell does not calculate to exactly an integer "it is *mostly* due to errors in the gravimetric determination of density". Or, with reference to space group determination, "The further choice of the space group conforming to the crystal symmetry and the absences is *mostly* made with the help of auxiliary tables compiled for the use of x-ray crystallographers" (reviewer's italics). The reviewer suspects that this is unfortunately too often true and may account for many of the erroneous space groups to be found in the literature. A deeper understanding not only of space groups but also of the fundamental 'classical' crystallography would be preferable; this is only too obviously lacking in many of the 'x-ray crystallographers' produced today.

Although parts of this book might be suitable as general reading for certain classes of science students, it cannot be recommended to the serious student of x-ray crystallography; more detailed and more up-to-date treatments are already available in this country.

A. F. WELLS.

*Perturbation Methods in the Quantum Mechanics of n-electron Systems*, by E. M. CORSON. Pp. xii + 308. (London: Blackie, 1951.) 65s.

No one can get very far in the theory or application of quantum theory without meeting many-particle systems, and being at that moment introduced to plenty of difficulties and new ideas not encountered in the more familiar but simpler single-particle problems. For example, we can no longer hope for exact solutions of wave equations, but must seek methods of approximation which, while not too complex, yet do justice to the physical characteristics of our system. And we have to take into account the symmetry properties of wave functions, which result from the indistinguishability of our particles and the operation of the Pauli Exclusion Principle. Dr. Corson has set out to provide a theoretical account of some of the ways which are open to us. This is particularly necessary since no other such account is available in English. He has adopted the Dirac formalism rather than the Schrödinger one, with the result that matrices occur far more frequently than differential equations. There are certain advantages in this, for the vector model of Dirac and Van Vleck provides elegant answers to many problems which are dealt with much more clumsily by more conventional methods; and the density matrix is recognized at once to occupy the central role in all discussions of many-electron systems. The chief disadvantages are that, with our present knowledge, a good deal of preliminary analysis (about one third of the book) involving representation theory and group theory is necessary before any physical problems can be properly dealt with. But when the stage has been prepared, the play proceeds at a great pace, and perturbation theory, variation theory, Thomas-Fermi statistical theory, molecular valence theory, second quantization and S-matrix theory all fall into place.

As may be anticipated, the book does not make easy reading. The Dirac bra and ket notation does not lend itself to a neat appearance, and at times the argument seems a little abbreviated. But it is a scholarly book, worth serious reading and study by postgraduate workers. The absence of all but a few illustrative examples will appear to some as a great gain: to others, interested more in the relation between experimental results and their interpretation, it will appear as a minor deficiency. The book is extremely free from errors, and its approach is one which recognizes difficulties without glossing them over. Particularly in view of its unusual contents, it is a most welcome addition to the literature of quantum mechanics.

G. A. COULSON.

*Diélectriques solides*, by R. JOUAUST. Pp. 84. (Paris: Editions de la Revue d'Optique, 1949.) 500 fr.

This little book gives an elementary introduction to the physics of dielectrics. It is primarily written for engineers and does not presuppose any extensive knowledge of atomic physics. It starts with an introduction into the atomic and electronic structure of solids, which is followed by simple facts on polarization, conductivity and dielectric loss. Further chapters deal with the influence of surface layers, and with various types of dielectric breakdown. Naturally a book of this length can deal only superficially with such a large



subject. Thus, for instance, only seven pages could be allowed for dielectric loss, and the author has not found it possible to go much beyond the phenomenological theories. In other chapters, too, the explanation of the various properties in terms of atomic structure is only indicated.

As a whole, I think, the book will be valuable by showing to electrical engineers the importance of modern physics for the understanding of dielectric phenomena. H. FRÖHLICH.

*Isaac Newton*, by S. I. WAWILOW. Pp. viii + 214. 1st German Edition. (Berlin: Akademie-Verlag, 1951.) 8.90 DM.

This book is the authorized translation from Russian into German of a biography of Isaac Newton written by a Russian scientist who, at the time of his death early in 1951, was President of the Academy of Sciences of the U.S.S.R. His own interests, which lay predominantly in the optical realm, had led him to analyse and translate into Russian the *Opticks* of Newton, the tercentenary of whose birth subsequently called forth this wider survey of the philosopher's life and achievements. It was first published by the Russian Academy in 1943 as one of a series of scientific works apparently intended for the serious general reader; and this translation is based upon the second edition of 1945.

Following a brief sketch of Newton's boyhood and student years, six chapters (comprising nearly two-fifths of the book) are devoted to his researches on light, in which the author recognizes the germ of all Newton's subsequent discoveries and the mature expression of his characteristic philosophy of physics. It was from optics that Newton passed to gravitational theory by way of speculations on the role of the aether. Wawilow recognizes the contributions which lesser men such as Borelli and Hooke made to the Newtonian synthesis; and he explains the criticisms to which the underlying assumptions of the *Principia* have been subjected by Einstein. The later chapters deal more briefly with Newton's work in mathematics and his controversy with Leibniz, his researches in chemistry, his theological writings and public life. There is a short classified bibliography but no index. The plates include eight likenesses of Newton (several of admittedly doubtful authenticity).

Wawilow obviously took pains to acquaint himself with the unfamiliar historical setting of Newton's career. His book is soberly written, free from bias, and even from the expected 'social-economic' emphasis. The author has made considerable use of L. T. More's biography of 1934, but he has taken account of more recent amendments to the traditional story. In the course of translation and re-translation the versions of passages quoted here have become noticeably free; also some errors have crept into the text. On page 5 Bath should read Bate; the date of Römer's determination of the velocity of light (page 24) was 1676; the Royal Society list reproduced in fig. 13 relates to 1675, not 1671; something has gone wrong with the formulation of Kepler's third law on page 99, and *Meshemami* on page 152 should presumably read *Masham*.

A. ARMITAGE.

*Ultraviolet Spectra of Aromatic Compounds*, by R. A. FRIEDEL and M. ORCHIN. Pp. vi + 52 + 579 diags. (New York: Wiley; London: Chapman and Hall, 1951.) 80s.

This book consists mainly of a collection of solution spectra of nearly 600 benzenoid and heterocyclic compounds, partly taken from the literature and partly determined in the authors' laboratory. It is primarily intended for organic chemists, but will also constitute a valuable reference work for the growing number of mathematical physicists interested in the theory of the spectra of complex molecules. A diverse range of structures extending alphabetically from acenaphthene to xylenol are covered, and while many of the compounds included are probably too complicated chemically to be of much interest to physicists, the collection provides a convenient source of information on the ultra-violet and visible light absorption properties of most basic types of benzene derivatives which will be widely appreciated. The paucity of up-to-date reviews of reliable experimental data in this field has frequently been deplored in the past, and Friedel and Orchin's book represents a most welcome and timely addition to the literature of spectroscopy.

E. A. BRAUDE.



## CONTENTS FOR SECTION B

	PAGE
Dr. A. SCHALLAMACH. The Load Dependence of Rubber Friction . . . . .	657
Dr. K. V. SHOOTER and Dr. D. TABOR. The Frictional Properties of Plastics . . . . .	661
Dr. E. RABINOWICZ and Dr. K. V. SHOOTER. The Transfer of Metal to Plastics during Sliding . . . . .	671
Prof. L. S. PALMER. On the Dielectric Constant of the Water in Wet Clay . . . . .	674
Dr. R. STREET, Dr. J. C. WOOLLEY and Dr. P. B. SMITH. Magnetic Viscosity under Discontinuously and Continuously Variable Field Conditions . . . . .	679
Dr. N. L. ALLEN. The Threshold Gas Pressure Required to Sustain a Stable Arc in a Magnetic Field . . . . .	697
Dr. W. G. KANNULUIK and Mr. E. H. CARMAN. The Thermal Conductivity of Rare Gases . . . . .	701
Mr. L. D. BROWNLEE and Dr. E. W. J. MITCHELL. On the Variations of Lattice Parameters of some Semiconducting Oxides . . . . .	710
Mr. I. G. EDMUNDS and Mr. R. M. HINDE. The Formation of Order in the Alloy AuCu <sub>3</sub> . . . . .	716
Dr. W. WEINSTEIN. Iterative Ray-tracing . . . . .	731
 Letters to the Editor :	
Dr. E. H. PUTLEY. The Conductivity and Hall Coefficient of Sintered Lead Sulphide . . . . .	736
Mr. TOR H. TØNNESEN. On the Distribution of Transistor Action . . . . .	737
Dr. V. V. AGASHE. The Study of the Changes in Pressure Rise and Current in a Low-Frequency Discharge due to Irradiation . . . . .	740
Dr. J. FEINSTEIN. On the Nature of the Decay of a Meteor Trail . . . . .	741
Dr. R. J. UFFEN and Dr. A. D. MISENER. On the Thermal Properties of the Earth's Interior . . . . .	742
Corrigendum (SELÉNYI) . . . . .	742
Reviews of Books . . . . .	743
Contents for Section A . . . . .	750
Abstracts for Section A . . . . .	751

## ABSTRACTS FOR SECTION B

*The Load Dependence of Rubber Friction*, by A. SCHALLAMACH.

**ABSTRACT.** It is shown experimentally that the load dependence of rubber friction can be explained as being due to the load dependence of the true area of contact between rubber and track if the surface asperities of the rubber are assumed to be hemispherical.

*The Frictional Properties of Plastics*, by K. V. SHOOTER and D. TABOR.

**ABSTRACT.** The frictional properties of a group of linear polymers have been investigated at loads ranging from a few milligrams to several kilograms at slow speeds of sliding. At light loads the coefficient of friction tends to increase but at loads above 100 g the coefficient of friction is generally constant and is almost independent of the size and shape of the surfaces. From the results obtained at loads above 100 g a tentative theory to explain the origin and magnitude of the friction has been developed. The theory is similar to that of Bowden and Tabor for the friction of metals. When a plastic slides on a harder metal strong adhesion occurs between the surfaces and shearing takes place within the bulk of the plastic rather than at the interface. The frictional force is essentially equal to the product of the area of contact and the bulk shear strength of the plastic. The experiments also show that the area of contact is proportional to the applied load so that the plastic behaves as if it possesses an effective yield pressure which is constant. The coefficient of friction is thus primarily determined by the bulk properties of the plastic and is equal to the ratio of the shear strength to the effective yield pressure of the plastic. When a plastic slides on a softer metal shearing occurs within the metal and the friction is primarily determined by the bulk properties of the metal itself rather than those of the plastic. Examination of the surface damage produced during sliding shows marked transfer of the softer to the harder material.

The frictional behaviour of polytetrafluoroethylene differs from that of the other plastics in that the adhesion during sliding is small and shearing apparently takes place preferentially at the interface. However, when this plastic slides on a sufficiently soft metal marked adhesion and transfer of the metal to the plastic occurs.

*The Transfer of Metal to Plastics during Sliding*, by E. RABINOWICZ and K. V. SHOOTER.

**ABSTRACT.** Investigations have been carried out on the amount of metal transferred when a radioactive metal is slid over the surface of a plastic. It is found that in every case metal fragments are transferred to the plastic in amounts that are of the same order of magnitude for the various metals and plastics examined. The close similarity of the results with those obtained with sliding metals suggests that, by a process analogous to the welding that occurs between metal surfaces, strong local adhesion occurs when metal and plastic are pressed and slid together.

*On the Dielectric Constant of the Water in Wet Clay*, by L. S. PALMER.

**ABSTRACT.** Some recent experimental values of the variation of the dielectric constant of wet clay with moisture content cannot be explained on the assumption that the clay particles and water molecules form a simple mixture. The results can, however, be theoretically deduced by considering relatively dry clay to consist of closely packed water-coated clay particles in an air matrix and relatively wet clay to consist of clay particles uniformly distributed in a water matrix, the water associated with the clay having an effective dielectric constant which varies exponentially from that of 'bound' water (about 3) to that of 'free' water (about 80) as the percentage of water is gradually increased. The conclusion follows that water films have a very low dielectric constant compared with that of water in bulk.



*Magnetic Viscosity under Discontinuously and Continuously Variable Field Conditions*, by R. STREET, J. C. WOOLLEY and P. B. SMITH.

**ABSTRACT.** For a ferromagnetic specimen exhibiting magnetic viscosity, the intensity of magnetization increases continuously with time under steady external field conditions. An account is given here of investigations to determine the influence on magnetic viscosity of changes in the magnetic field applied to the specimen, two cases of discontinuous and continuous changes in field being considered. The latter case is of practical importance when direct measurements of magnetic viscosity are made using specimens with demagnetization coefficient other than zero, since the effective field acting in the specimen is then continuously variable in time. It is found that both cases can be adequately described by extending the previously proposed formal theory of magnetic viscosity in which it was supposed that the domain processes responsible for magnetization can be activated by thermal agitation.

The required extension of the theory consists in assuming that the activation energy of the domains is a function of the field. The experimental results show that the changes in domain activation energy are linearly proportional to the changes in field strength, if the latter are small. Denoting the constant of proportionality by  $q$ , and considering a possible domain model, it is shown that  $q$  is related to the elementary volume of the material in which thermal agitation leads to activation. Measurements on alnico show that the linear dimensions of this elementary volume are of the same magnitude as the width of a domain boundary wall. Results of the variation of  $q$  and other parameters characteristic of magnetic viscosity as functions of the temperature of the specimen are also presented and it is shown that the observed behaviour is consistent with the present views on the metallurgical structure of alnico.

*The Threshold Gas Pressure Required to Sustain a Stable Arc in a Magnetic Field*, by N. L. ALLEN.

**ABSTRACT.** Measurements of the minimum pressure required for the operation of stable, pulsed, high-current arcs in hydrogen and air, in strong longitudinal magnetic fields have been compared with earlier results obtained with helium. The values obtained are shown to be approximately those predicted by theoretical reasoning from the earlier work. Some relevant processes occurring in the discharge are discussed.

*The Thermal Conductivity of Rare Gases*, by W. G. KANNULUIK and E. H. CARMAN.

**ABSTRACT.** The thermal conductivity of the rare gases is determined in absolute measure by a 'hot wire' method at selected temperatures in the range  $-183^{\circ}\text{C}$  to  $306^{\circ}\text{C}$ . The experimental values of the thermal conductivity are shown to be in good agreement with the values calculated according to the recent theory of Hirschfelder, Bird and Spatz in the above range of temperature. The quantity  $\epsilon = K/\eta c_v$  is shown to be independent of the temperature, but the value of  $\epsilon$  increases slowly with the molecular weight from a value 2.43 for helium to a value 2.58 for xenon.

*On the Variations of Lattice Parameters of some Semiconducting Oxides*, by L. D. BROWNEE and E. W. J. MITCHELL.

**ABSTRACT.** Measurements have been made of the lattice parameters of the substitutional semiconductors  $\text{Ni}(\text{Li})\text{O}$ ,  $\text{Fe}_2(\text{Ti})\text{O}_3$  and also of reduced  $\text{Mg}_2\text{TiO}_4$ . The contraction of the nickel oxide lattice, which was briefly reported by Verwey *et al.* (1950), has been observed for a series of compositions. We have also observed the expansion of the  $\text{Fe}_2\text{O}_3$  lattice associated with the production of  $\text{Fe}^{2+}$  ions. Similarly, the expansion which accompanies the reduction of the spinel  $\text{Mg}_2\text{TiO}_4$  is attributed to the formation of  $\text{Ti}^{3+}$  ions. The lattice parameter of stoichiometric nickel oxide is believed to be  $4.1726 \pm 0.0002 \text{ kx}$  ( $4.1811 \text{ \AA}$ ) while that of unreduced magnesium titanate is found to be  $8.425 \pm 0.0005 \text{ kx}$  ( $8.442 \text{ \AA}$ ).



*The Formation of Order in the Alloy AuCu<sub>3</sub>*, by I. G. EDMUNDS and R. M. HINDE.

**ABSTRACT.** The approach to order in AuCu<sub>3</sub> has been studied by x-ray examination of single crystals. The distribution of intensity in the diffuse super-lattice reflections was measured from a series of photographs of a stationary crystal, and again from a moving-film photograph, the effect of instrumental broadening being eliminated by Stokes' method.

The intensity in the  $hkl$  reflection with  $(k+l)$  even is given as the Fourier summation

$$I(uvw) = \sum_x \sum_y \sum_z K \exp \{ -(\beta x^2 + \alpha y^2 + \alpha z^2) \} \exp 2\pi i(xu + yv + zw);$$

the constants  $\alpha$  and  $\beta$  tend to zero as complete order is approached. The experimental results of Strijk and MacGillavry conform to this expression, and a measure of agreement is obtained with Cowley's observations at a very early stage of ordering.

The discrepancy between the present observations and crystal models proposed by A. J. C. Wilson is discussed, and expressions are derived for order parameters at successive short ranges. It is suggested that the ordering process is similar at all stages, and depends on a tendency for gold atoms to avoid each other; ordered antiphase domains are formed as a consequence of this process.

*Iterative Ray-tracing*, by W. WEINSTEIN.

**ABSTRACT.** An iterative ray-tracing method described by T. Smith is shown to give a divergent sequence of approximations in certain cases; when it converges it has only first order convergence according to Hartree's classification of iterative processes. An iterative method which always gives second order convergence is described and the significance of the successive approximations in terms of higher order aberrations is discussed.